NOVA SCHOOL OF SCIENCE & TECHNOLOGY

CHEMICAL DEPARTMENT

BEATRIZ FILIPA CABRAL DIAS

BSc in Chemical and Biochemical Engineering

OPTIMIZATION OF LOSS IN WEIGHT FEEDING OF PHARMACEUTICAL POWDERS TO ENABLE CONTINUOUS DIRECT COMPRESSION

MSc IN CHEMICAL AND BIOCHEMICAL ENGINEERING

Universidade NOVA de Lisboa
December, 2021

NOVA SCHOOL OF SCIENCE & TECHNOLOGY

CHEMICAL DEPARTMENT

OPTIMIZATION OF LOSS IN WEIGHT FEEDING OF PHARMACEUTICAL POWDERS TO ENABLE CONTINUOUS DIRECT COMPRESSION

BEATRIZ FILIPA CABRAL DIAS

BSc in Chemical and Biochemical Engineering

Orientador: Nuno Filipe Martins Branco, Oral Drug Product Development Scientist, Hovione

MSc IN CHEMICAL AND BIOCHEMICAL ENGINEERING

Universidade NOVA de Lisboa
December, 2021

Optimization of Loss in Weight Feeding of Pharmaceutical Powders to enable Continuous Direct Compression

Dedicatory

I dedicate this Master Thesis to my grandfather Carlos, who's passed away recently.

Your biggest dream was to, one day, see me graduating but unfortunately there was not enough time for it. I know that besides the distance, you have always been so proud of all my achievements and by writing this words it means that I did it avô!

Acknowledgements

There are not enough words to thank to every person who directly or indirectly supported me throughout these last months.

I would like to thank Hovione for providing me this opportunity, where I had the chance to grow both personally and professionally. Also, I want to express my gratitude for both my mentors in this journey, Cláudia Moura and Nuno Branco, who provided me the tools to improve my sense of scientific and critical thinking and to the scientist Ricardo Sousa who helped me a lot with the programs' handling.

A huge thank you to Artur, Calixto and André that helped me directly throughout all my experimental challenges, it was a pleasure to share the laboratory and learn from you. A special mention to the other laboratory technicians who shared their experience, the know-how and the good manufacturing practices with me, Paula, Pedro, Ricardo, Eloy and Norberto. I would also like to thank to the Master Student Madalena for all the help during my laboratorial experiments.

To my university, FCT NOVA, namely to all the amazing professors from whom I had the opportunity to learn from and acquire the necessary knowledge to face this challenge.

The most special and truly thank you to all my family, I will never forget your support and continuous encouragement to never doubt on my capacities besides all the obstacles that we all have faced trough this year. A huge recognition to my sister for being my best friend and for always being there to help me during this period, without you it would have been much harder.

A massive thank you to my boyfriend, Ricardo, for the unconditional support, patience and love during this journey, you have always made me believe in myself and you never let me give up no matter how hard the situation was, I will never forget every effort that was made.

A super special thank you to my college friend, Sara it was a pleasure to share all my academic period with such an amazing person who has always inspired me, no doubts that there is no better pair of Chemical and Biochemical engineers.

I also have to thank my amazing friends Mariana, Ana Bia and Patricia for being so comprehensive of my absence during the last months. It is amazing that, no matter how long we stay without seeing each other, we know that when we meetup again, it will be like no days have passed since the last time together.

Last but not least, a super thank you to my rhythmic gymnastics friends, Carolina and Inês, for being such amazing friends and for all the infinite stories, travels and adventures that we had experienced together. As we say: until the 90's together!

Abstract

Over the last years the pharmaceutical industry has been gradually starting to adhere to the continuous production instead of the traditional batch production.

For the production of tablets through continuous direct compression (CDC) it is essential to ensure the control of all the equipment involved in the process, with special attention to the Loss-in-Weight (LIW) Feeders. This is due to the fact that even if there are small oscillations in the initial phase of the process, these will have big repercussions on the quality of the final product, making the drug getting out of the specification.

This work explore different materials with the goal of creating a methodology for the selection of the components (the tools) to be assembled on the feeder in order to optimise the process. Furthermore, the minimum and maximum limits of the feeders were tested to determine a stable range of operation for each analysed material.

Afterwards, a database with the different properties of the materials was developed with the goal of relating these properties with the components that would be necessary to integrate on the feeder and optimise its performance. To simplify the identification of similarities between the analysed materials, a principal component analysis (PCA) model was developed.

Following this, some alternatives to reduce the time and costs of the production process were identified. Thus, the development of partial least squares (PLS) models was essential to predict the feed factor (FF) values.

Lastly, the impact that the usage of the feeder had over the materials was analysed in order to find out if this equipment would cause any alterations in the properties of the materials to be used in the formulation.

Keywords: GEA Compact Feeder; Continuous Manufacturing; Excipients; Feed Factor; Particle Size; Flowability

Resumo

Nos últimos anos a indústria farmacêutica tem vindo gradualmente a aderir à produção em contínuo em detrimento da tradicional produção em *batch*.

Para a produção de comprimidos através de *continuous direct compression (CDC)* é essencial garantir o controlo de todos os equipamentos do processo, com especial atenção para *os Loss-in-Weight (LIW) Feeders*. Tal deve-se ao facto de que mesmo que sejam pequenas as oscilações na fase inicial do processo, estas terão grandes repercussões na qualidade do produto final, dando origem a um medicamento fora de especificação.

Durante este trabalho procurou-se testar diversos materiais com o objetivo de criar uma metodologia para a seleção dos componentes (peças) a serem integrados no *feeder* de forma a otimizar o seu funcionamento. Para além disso, foram também testados os limites mínimos e máximos de funcionamento do *feeder*, de forma a se determinar um intervalo de operação estável para cada material analisado.

Posteriormente, foi desenvolvida uma base de dados com as diversas propriedades dos materiais, cujo objetivo seria relacionar essas propriedades aos componentes que viriam a ser necessários integrar no *feeder* de forma a otimizar o seu funcionamento. Com o objetivo de facilitar a deteção das semelhanças entre os materiais analisados foi desenvolvido um modelo de *principal component analysis (PCA)*.

Em seguida, foram identificadas alternativas para reduzir o tempo e o custo dos processos de produção, para o que foi essencial o desenvolvimento de modelos de *partial least squares (PLS)* para prever os valores dos *feed factor (FF)*.

Por último, foi analisado o impacto que a utilização do *feeder* teve sobre os materiais, no sentido de se averiguar se a utilização deste equipamento provocaria alterações nas propriedades dos materiais a serem utilizados na formulação.

Palavras-chave: GEA *Compact Feeder*; Fabricação em Contínuo; Excipientes; *Feed Factor*; Tamanho das partículas; Escoamento

List of Contents

List of Figures

List of Tables

List of Acronyms

API	Active Pharmaceutical Ingredient
ASD	Amorphous Solid Dispersion
CDC	Continuous Direct Compression
CI	Carr's Index
CSD	Colloidal Anhydrous Silica
FDA	Food and Drug Administration
FF	Feed Factor
ffc	Flow Function Coefficient
HR	Hausner Ratio
LIW	Loss-in-Weight
MCC	Microcrystalline Cellulose
MPS	Major Principal Stress
NA	Not Available
NIR	Near Infrared
PAT	Process Analytical Technology
PCA	Principal Component Analysis
phiE	Bulk Friction Angle
PLS	Partial Least Squares
Q2	Goodness of prediction from cross validation
RMSEcv	Root Mean Square Error, computed from the selected cross validation round
RMSEE	Root Mean Square Error of the Estimation (the fit) for observations in the workset
RSD	Relative Standard Deviation
R2	Coefficient of Determination
R2X	Goodness of Fit
R2Y	Goodness of prediction from calibration
SD	Spray Drying
SEM	Scanning Electron Microscope
SMCC	Silicified Microcrystalline Cellulose
Stdev	Standard deviation
UYS	Unconfined Yield Strength
VIP	Variable Importance Plot
ρ_{bulk}	Bulk Density
ρ_{tap}	Tap Density

1. Introduction

1.1 The Emergency of Continuous Line Process & Motivation

Over the last two decades, substantial advances in science and engineering have made it possible to deploy continuous pharmaceutical manufacturing instead of the traditional batch.

The transition between the two processes has been facilitated by the adoption of the quality-by-design paradigm for pharmaceutical development and by the improvement of process analytical technology (PAT) for designing, analysing, and controlling the production [1]. Beyond that, the environmental, health, and safety legislations are encouraging the sector to develop processes that are more efficient [2]. Also, the advantages of the continuous manufacturing over the batch processing have been recognized by the pharmaceutical regulatory authorities [3].

Throughout the last few years, the prices of new products have been rising, as well as the time required to discover, develop and launch them into the market [2]. In order to give response to the demand, it is crucial to change the production processes for continuous so as to launch the new products into the market in the shortest time possible.

The Food and Drug Administration's (FDA) pharmaceutical quality expects that during the twenty-first century the pharmaceutical industry must be able to manufacture high-quality drugs without requiring extensive regulatory control and to reach that, continuous lines must be exceptionally optimised [4].

Tablets are the most popular option for delivering pharmaceutical products because they are simple to pack, store, transport, distribute, and ingest. Furthermore, if the formulation is managed properly, the dosage integrity (quality and quantity) is maintained in its intended form [5]. In order to secure that the continuous lines final products are within the guidelines, it is essential to carefully control the feeders (equipment responsible to feed into the process the right dosage of each material during time), because in case of their deviance the whole production is ruined.

Loss-in-weight (LIW) Feeders are subjected to perturbations, such as vibrations or filling phases during the continuous operation [6]. This perturbations are limiting their flowrate capacity, because small flowrates, typical from pharmaceutical processes (10–100 Kg/h), cause inaccuracies on the throughput mostly due to the powder cohesion and/or electrostatics [7].

To avoid feeding deviations, it is essential to perform a correct selection of the feeder's components that are most appropriate for each material. Currently, this tooling selection is performed

using trial-and-error which is an endless process considering the infinity of materials that can be used on continuous lines [7]. For this reason, this thesis focusses on developing a predictive analysis based on the experimental results to avoid this primitive and time spending trial-and-error “methodology” for further studies and productions.

1.2 Batch vs Continuous

Nowadays, some industries are starting to renew their processes into continuous lines. This changing of mindset is a great opportunity to improve the pharmaceutical productions because it becomes possible to use the same equipment for a complete project.

This was not even an option with the batch processes, because when the final product was ready, for the same project, it must be removed from the equipment and all the process need to be restarted [8]. This raises a large number of problems, namely the difficulty in reproducing homogeneous processing conditions because there are only two options: or the production is changed to a different equipment to continue the process, or all the equipment must be cleaned [9].

However, if the size of the batch is below a certain critical value, the batch processing is still a good process choice. If not, the cost of the batch manufacturing tends to be higher and the process less efficient than the alternative choice (continuous manufacturing) [2].

The following table (Table 1.1) provides a much clearer idea of the pros and cons between these two processes and also indicates a few challenges that must be overcome.

Table 1.1 – Main differences between batch and continuous manufacturing and also the challenges that continuous process still have to face [2] [5] [10] [11].

Batch	Continuous	
	Advantages	Challenges
Scale-up by volume	Scale-up by time	Not appropriate for small product loads
Quality-by-inspection	Quality-by-design	Less flexible regarding successive process steps
Long cycle times	Short residence time	Need for fast steady state
Size of operation	Modular manufacturing	Need for robust processes
Batch to batch variation	Variance reduction	Production changes for already licensed products
Lack of understanding	Continuous improvement	Regulatory uncertainty
Material contamination	Material containment	New mind-set needed for quality assurance
Weak in-process control	Online process control	------
Poor Yield	Better product quality assurance	------
Inflexibility	Ease of automation	------
Unsustainable	Reduced capital investment and labour costs	------
Drug shortages	Production of desired product amount	------
Intermediates	No transfer and storage of intermediate products	------
------	Shorter product development time and time-to-market	------
------	Less space and energy required	------
------	Less waste	------
------	Reduce the number of unit operations	------

Regarding Table 1.1, it is possible to conclude that continuous processes are much more advantageous than batch and fortunately the continuous' challenges are not that many. Furthermore, it must be noticed that most of the information present on the table relatively to batch process are problems which, by using continuous lines, can be avoided.

By using continuous processes, it is possible to spend less (money, resources and time), improve the product yield and quality while ensuring the replicability between different productions of the same product.

1.3 Continuous Direct Compression

Continuous direct compression (CDC) is a process where raw materials are transformed into finished products by continuously flowing through an integrated set of equipment, which is controlled to ensure the quality of the final product. Furthermore, it also enables the powder blend to be directly transformed into a tablet without any intermediate process steps of granulation, drying, and granule size reduction [11] [12].

The CDC-10 (GEA APC Pharma Solids, Wommelgem, Belgium) has a nominal massflow of 10 kg/h and a working limit between 1 – 25 kg/h. It is constituted by LIW Feeders, blenders, tablet press and a coater (Figure 1.1). Moreover, this continuous line has an in-line Near Infrared (NIR) spectroscopy integrated to monitor the blend uniformity in an integrated manufacturing system.

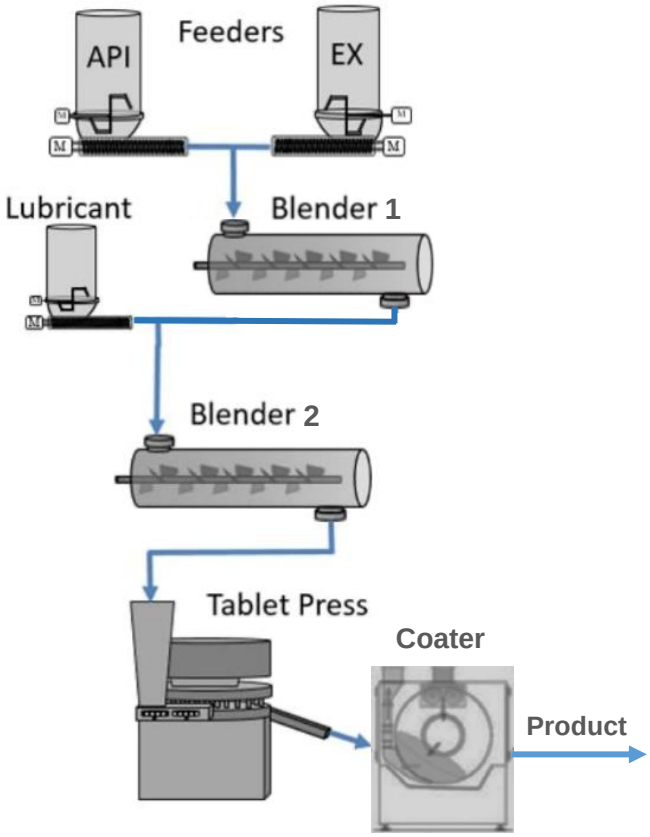

Figure 1.1 – Example of a CDC-10 system constituted by three feeders, two stage blenders, a tablet press and a coater.

Regarding Figure 1.1, the two first feeders, positioned before blender 1, feed active pharmaceutical ingredient (API) and excipient to the process. Afterwards, the lubricant is added and blended with the other materials on blender 2. After that, a homogeneous mixture is tableted and later coated. At the end, a final product is obtained.

On the GEA CDC System up to six compact twin screw feeders can be integrated. This feeders can be distributed through two different positions: at the inlet of the first and of the second blender which can have up to six and two feeders, respectively [13]. In cases where all the feeders are integrated before the first blender, there is no use for the second one, so it should be removed since the second blender is used when it is mandatory to add one or two lubricants to the process.

The following unit operations are typical on a continuous tableting line.

- **Feeder** – The number of feeders and their working feed rates depend a lot on each formulation's specifications (Figure 1.2). The LIW Feeders are able to release the material constantly per unit of time, which represents an advantage for continuous processes, mostly due to an improvement of the feed rate control system that minimizes the flow variability [14].

Figure 1.2 – Demonstration of a join of GEA Compact Feeders feeding into the continuous line [15].

- **Blender** – The blender is a horizontal cylinder with a bladed shaft circulating around its central axis. Its function is to uniform the materials mixture into a homogeneous blending as well as to continuously push the powder to the opposite end of the cylinder, out of the blender.

- **Tablet Press** – The tableting is the process of transforming powder into tablets. When the final mixture reaches the tablet press, it is compressed and ejected in accordance with the pre-defined shape and size.

- **Coater** – Finally, after tableting, the tablets are forwarded to a coater. In this process, a spray is spread on the tablets in order to gradually cover, uniformly, all tablets. This process is responsible for taste and odour masking, physical and chemical protection and it also protects the drug in the stomach, which enables the control of its releasing profile [16].

It is truly important to synchronize the yield of all the equipment in terms of mass balance, because the materials tend to accumulate if the continuous lines are not properly balanced, or it is even possible that one of the previously referred equipment runs out of material if it operates at a higher rate than the preceding unit [8].

Considering this, it is important to monitor and control the processes for an optimal production and that is the reason why the PAT tools are essential. Besides that, for a better control, these tools should run in-line. The most common spectroscopic methods are NIR and Raman [17].

1.4 State-of-the-art

Most of the publications referent to CDC perceive that feeding and blending are the most important steps in the production process, because they directly impact the consistency of the final product. In fact, the mixing efficiency is widely dependent on the feeding consistency, this means that in case of using, on the process, feeders with inconstant massflow rates, it might lead to undesirable blends with high composition variability [8] [18].

For this reason, the optimization of the LIW Feeders is important to guarantee the processes' quality. Furthermore, on pharmaceutical processes the usage of small massflow rates is mandatory, which makes the process more exposed to variations caused by powder cohesion or by electrostatic effects [7]. Moreover, it leads to low screw speeds which yields a slow response to perturbations induced by the hopper refill [3].

Considering this, it is definitely important to first test and optimise the LIW Feeders in terms of performance capabilities, with all the materials that are intended to be used in the formulation. This consistent powder feeding is particularly pertinent for APIs, since they cannot be selected by their suitability to the process as it happens during the excipients selection [19].

In order to optimise the feeding process recent work has been mainly focused on:

(i) Selection of the feeding equipment (feeder)

Due to the fact that on the pharmaceutical industry it is common to use low massflow rates, the majority of the companies demonstrated a preference for the GEA Compact Feeder and the Coperion K-Tron Feeders to feed their CDC lines and, amongst the huge diversity of Coperion K-Tron Feeders types, the KT20 Feeder is the most commonly chosen [20]-[24].

(ii) Design the feeding space

The operational range of LIW Feeders depends on the feeder size, tooling, and on the properties of the material being fed.

To fully understand how the materials behave during the feeding process, it is crucial to define the material's ideal range of feeding operation. In other words, to find for each material the maximum and the minimum values of stable massflow [25].

(iii) Selection of the feeder's components

Different studies were also made to identify the parameters that must be considered to perform the most appropriate feeder's components (the tools) selection in order to optimise the feeding process.

During the process of selecting the **screw** and **mesh** to be used, it is important to attend to the materials' properties, such as cohesion, adherence to the equipment, and diffusional problems, such as bridging [26]. Furthermore, the **gearbox** will depend on the screw speed required for a defined setpoint, which means that the screw and gearbox selection must be performed at the same time in order to achieve the most appropriate combination [27].

Developing a robust feeder refill strategy is critical to minimise perturbations when transitioning from volumetric to gravimetric feeding during the refill. Thus, the hopper fill level is the most significant factor. As so, it is necessary to find a compromise between lowering the amount of material that is dropped per refill (the **topup** volume), minimizing the deviations, and to only perform the necessary number of refills, to avoid that the system goes to volumetric mode too frequently. This is due to the fact that, when in volumetric mode, the equipment is essentially blind to changes in the screw filling [28].

(iv) Correlate LIW Feeders performance to materials' properties

Principal component analysis (PCA) models can be used to group materials by their similarities. Therefore, resorting to a materials' properties library, it is possible to predict the feeding behaviour of a new material never before tested on the feeder. In other words, if the new material has similar properties to one of the materials previously characterized on the model, it is a good prediction to initially run the feeder in the same conditions [22] [29].

Also, by using PCA and partial least squares (PLS) models it was concluded that the feeding performance is affected by both, the materials' properties and the feeder's configurations [27] [30]-[32]. Therefore, if similar materials use the same set of feeder's components it is expected that the feeding performance would be similar as well.

(v) Predict the feed factor

The feed factor (FF) profiles can be used to predict the gravimetric performance and the refill strategy of the feeders. It was also demonstrated that FF is strongly dependent on the materials' properties and on the screw type [27] [31]. Moreover, from all the materials' properties, density seems to be the parameter that affects FF the most. This was verified for both GEA Compact LIW Feeders [22] and for Coperion K-Tron KT20 LIW Feeders [25].

Some papers even refer alternatives to predict the FF profile, thus avoiding an initial run where a big amount of material and time are wasted [27] [30].

1.5 Thesis Outline

Given the preceding information about the trendiest researches, this dissertation focuses on six specific aims, which are summarized as follows:

- Optimise on GEA Compact Feeder as much materials as possible;
- Create a methodology to perform the selection of the feeder's components;
- Define the ideal design space for the materials tested on the feeder;
- Develop a database that considers the materials' properties as well as the most appropriate feeder's components for each material run on the feeder;
- Propose alternatives to avoid the first run, reducing production time and costs;

- Analyse the impact that the feeder has on the materials' properties.

This thesis is divided in four chapters.

The first chapter includes a theoretical background covering the main topics of CDC as well as the biggest areas of research about the theme. It also includes a GEA Compact Feeder description of functioning and tooling.

Chapter two covers all the selected materials and the methodology applied throughout this work.

Chapter three covers all the results and discussion grouped into four different sections:

Section 1: In the first section it is indicated the design space of the GEA Compact Feeder obtained during the experimental runs for all the materials tested. It is followed by a detailed analysis of the influence of the materials' characterization, the feeder's components and the feeder's parameters on the stability of the feeding process;

Section 2: In this section alternatives are elaborated to avoid the first run, in order to only perform the feeder calibration before the production process;

Section 3: Over this section the impact of the feeding performance on the materials' properties is studied;

Section 4: In this section the applicability of the obtained stable ranges of the feeder's design space on the selection of the production conditions and materials to be used is explained in detail;

Section 5: Finally, on the last section two case studies are presented:

- Case Study 1: An example of a formulation considering the experimental data;

- Case Study 2: Virtually simulate the feeder's response to each material that is intended to be added to the production process by resorting to the Digital Twin program.

The fourth chapter presents all the conclusions and future work that is considered important.

At the end of this thesis, there are appendixes attached with confidential information and with extra content to complement the work.

1.6 GEA Compact Feeder vs K-Tron KT20 Feeder

As previously indicated on Section 1.4, most of the pharmaceutical companies use either a GEA Compact Feeder or a Coperion K-Tron KT20 Feeder to feed their continuous lines. It is also important to refer that both are LIW Feeders.

The GEA Compact Feeder is ideal for dosing small amounts of powder with precision. This equipment has a 2.6L hopper that is filled through a horizontal impeller, equipped with a topup system. The hopper possesses a vertical agitator and a baffle to improve the screws filling and to avoid the powder's adherence to the equipment (Figure 1.3).

This feeder also includes a weight cell to measure the actual massflow and a speed controlled twin screw to regulate the powder dosage. Those screws are rotated through a servo motor that is controlled by a gearbox [33].

Figure 1.3 – GEA Compact Feeder's hopper with an asymmetric agitator and baffle set.

K-Tron KT20 (Coperion K-Tron Pitman, Inc. Sewell, NJ, USA) is a twin screw LIW Feeder, as GEA Compact Feeder, although there are some differences between the two equipment. KT20 Feeder's design consists of a modular twin-shaft feeder assembled on a weight bridge and it is constituted by three parts: the volumetric feeder, the weighing platform and a gravimetric controller [31].

The feeder is constituted by a cylindrical hopper of 20L that extends to the hemispherical hopper of 5L (25L combined) that connects to the twin screw conveying system [21]. The bottom of the 5L feeder's hopper contains a bowl with a horizontal agitator with two curved blades that match the profile of the bowl, which has the function of helping with the screws filling (Figure 1.4) [7].

Figure 1.4 – Horizontal agitator on KT20 Feeder's bowl [34].

For a better comparison between the two types of feeders it was decided to resume their specifications on Table 1.2.

Table 1.2 – Comparison between the GEA Compact Feeder [30] [33] and the K-Tron KT20 Feeder [21] [26] [34] [35].

Feeder	**GEA Compact**	**K-Tron KT20**
Image		
Hopper volume (L)	2.6 (working volume 2L)	25
Meshes	D1/ D2/ D8	FSqS/ MSqS/ CSqS
Twin Screws	Concave/ Auger – Coarse & Fine	Concave/ Auger / Spiral / Double Auger – Coarse & Fine
Material	Stainless Steel	Stainless Steel
Motor Speed (RPM)	0 – 9000	20 – 2000
Agitator Type	Vertical Symmetric/ Asymmetric	Horizontal
Topup volumes (L)	0.4/ 0.8/ 1.2/ 1.6	NA
Gearbox	63:1/ 235:1/ 455:1	A/ B/ C

One of the biggest differences is the feeders working volume. The GEA Compact Feeder has a much smaller hopper working volume (2L) than the K-Tron KT20 Feeder, although the first one has the advantage of being more stable operating between low to medium throughput, which is possible on a continuous process due to its topup system [21].

On the other hand, higher throughputs demand a too frequent refilling and, for those cases, K-Tron KT20 is the most appropriate feeder. This is due to the bigger hopper volume [21]. However, it would be worse for process stability, because the impact of the powder's weight will be noticed and it will be reflected on the process RPMs. In the beginning, when the feeder is full, the RPMs will be lower than at the end of the process, due to the less powder compressibility that will increase the RPMs and, as a consequence, provide a lower stability to the process [13].

The K-Tron KT20 Feeder has more types of screws than the GEA Compact Feeder that only has concave and auger screws. Concave screws, considered as the self-cleaning screws, are more appropriate for cohesive materials, because the powder sticks less on the screws during the process, which would avoid diffusional problems. On the other hand, auger screws are normally used for free flowing or compacting powders [36].

Another advantage of the GEA Compact Feeder is that it has two types of agitators, a symmetric and an asymmetric, while K-Tron KT20 Feeder only has one. The big advantage of the asymmetric agitator is the two C-anchor blades that are capable of removing the part of the material that adheres to the wall during the process.

Over the last years, researches were made with the aim of performing an automatic refill of the K-Tron KT20 by using "alternatives" such as: vacuum refilling apparatus (primitive version of GEA Compact Feeder refill mechanism) or utilizing another K-Tron to refill the K-Tron KT20 [28]. In fact, it has been noticed by the industry the need of having a refill system integrated and, for this reason, the GEA Compact Feeder was chosen as the more promising feeder.

1.7 Feeder's Components

On Figure 1.5 it is observed the GEA Compact Feeder fully assembled as well as the four main sections which it is divided.

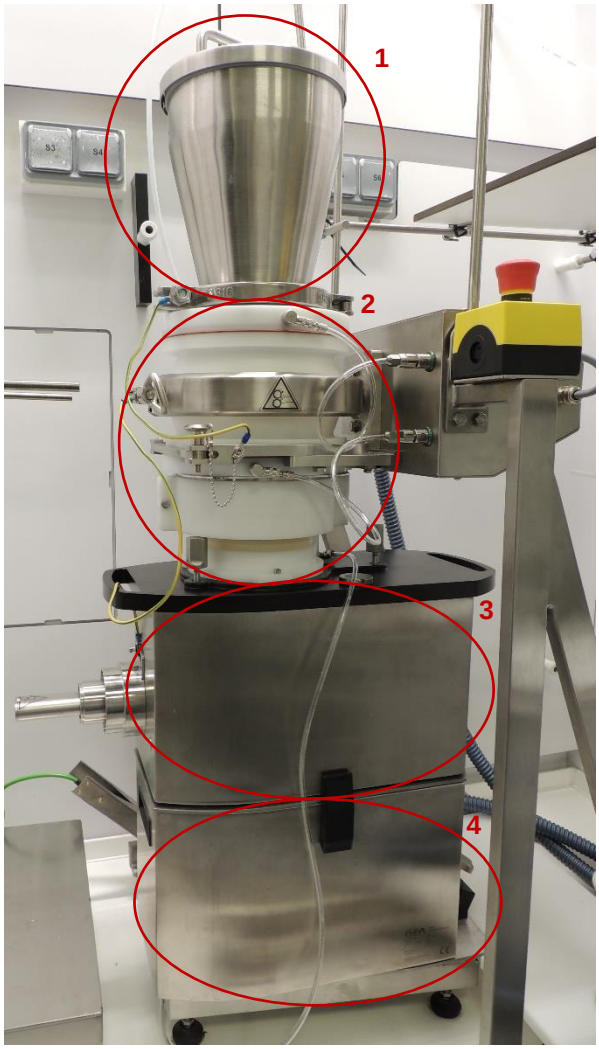

Figure 1.5 – GEA Compact Feeder fully assembled. 1 – External hopper; 2 – Topup system; 3 – Greenhouse; 4 – Weighing scale box.

1- **External Hopper –** The hopper with a volume of 5L is where the material to be run on the feeder is placed. It is important to refer that during a CDC production that hopper must be replaced by a structure prepared for being continually filled by a piping system.

2- **Topup System –** System composed by a variety of tools responsible for the refill, being the most important ones the **topup valve** (Figure 1.6 – A), which turns 180 º down and 180 º up by an electrical stimulus to perform the refill, and the **topup** itself (Figure 1.6 – B) that is a cup that is inside the topup valve and defines the volume of material that will drop inside the feeder for each refill.

Figure 1.6 – Most important components of the topup system; A – Topup valve; B – Topup.

Moreover, there is also a **silicon ring** which function is to connect the topup valve to the **inflatable seal**. Its purpose is to guarantee that all the powder gets into the hopper without any losses. Furthermore, at the same time that the topup turns down, the inflatable seal inflates in order to avoid the powder spilling to the greenhouse.

3- **Greenhouse –** The 2.6L hopper, that actually has 2L of working volume, is placed inside the greenhouse and within that hopper the **agitator**, **baffle** and **screw** are assembled. The agitator (Figure 1.7 – C) and the baffle (Figure 1.7 – D) work together to avoid the occurrence of diffusional problems. The screw (Figure 1.7 – E) is the component responsible for the feeding process, since it is the tool that transports the material from the inside to the outside of the feeder.

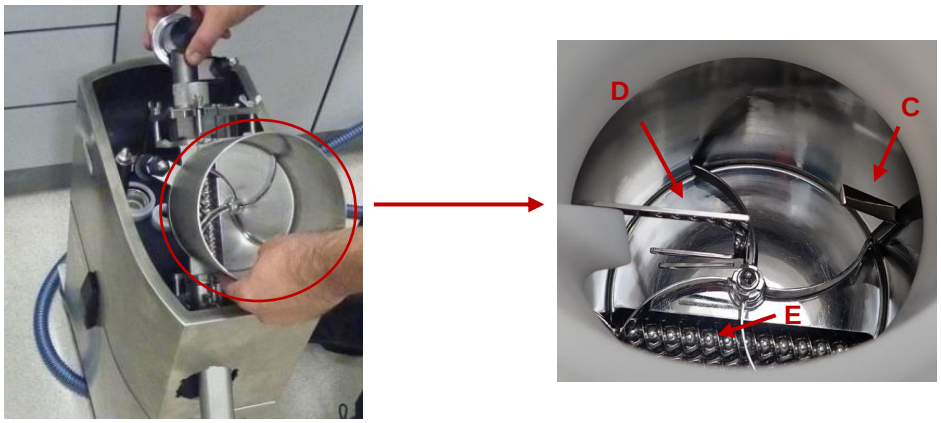

Figure 1.7 – Hopper being assembled inside the greenhouse [33]; C – Agitator; D – Baffle; E – Screw.

4- **Weighing Scale Box –** It is at the bottom of the feeder that the weighing cell and the gearbox (Figure 1.8 – F) are placed. Both are responsible for the feeding control process.

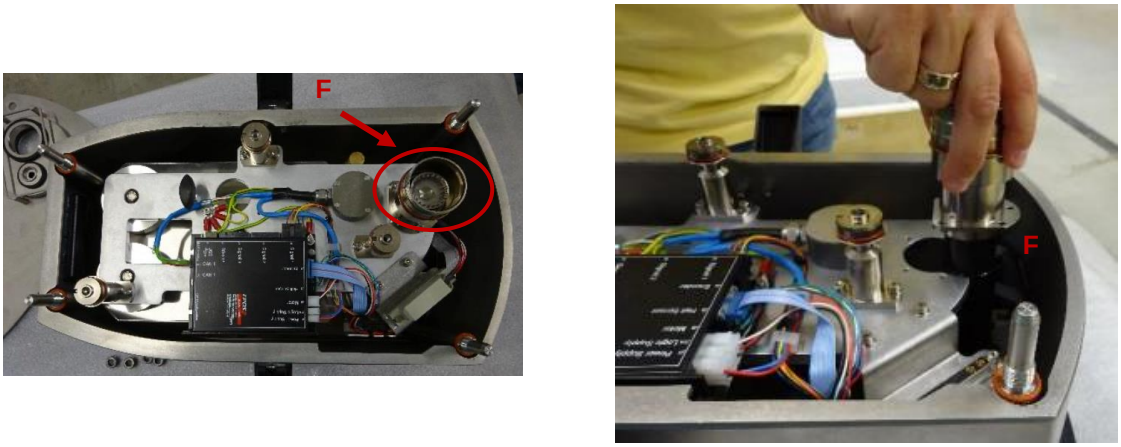

Figure 1.8 – Gearbox being assembled on the weighing scale box; F – Gearbox [33].

1.7.1 Detailed Analysis of Feeder's Components to be Selected for Each Run

The information indicated on this section about the feeder's components must be carefully analysed in order to make the most accurate decision about which of their tooling options should be chosen. The aim is to select the tool that would provide a lower variation on the feeding process and, for that, the relative standard deviation (RSD) must be the minimum possible.

RSD is the percentage of deviation of the massflow relatively to the defined setpoint measured per second. This deviation is valid either for an increase or for a decrease of the massflow regarding the setpoint. The higher is that difference, the higher is the RSD and the worst is the feeding process control.

1.7.1.1 Gearbox and Screw

On the GEA Compact Feeder it is possible to set three different types of gearboxes, each one with a defined gearbox ratio (Figure 1.9).

Gearbox 1 = 63:1
Gearbox 2 = 235:1
Gearbox 3 = 455:1

Figure 1.9 – Gearbox types and respective ratios.

Despite the feeder's motor speed range of operation being 0 – 9000 RPM, it was defined by GEA that it would be preferable to run between 1500 – 7500 RPM to have a safety of 1500 RPM for each side. This consideration makes it more probable to reach an optimal feeding process independently of the flowability of the materials.

On Table 1.3 the screw speed that each gearbox can reach considering the recommended range of motor speeds is presented. The gearbox 1 is the gearbox with the lowest ratio (63:1) and for that reason it is the one that can reach higher screw speeds. On the other hand, the gearbox with the highest ratio (gearbox 3) can run the feeder at the lowest screw speed, and for that reason it is the best gearbox to be used for low throughputs. Logically, the gearbox 2 must be set on the feeder for runs that are intend to operate at intermedium conditions that are not reachable by none of the other two gearboxes.

In a few words, a higher throughput requires a higher screw speed and, oppositely, a lower throughput demands a lower screw speed.

Table 1.3 – Range of stable screw speeds for each gearbox [30].

Gearbox Ratio	Screw Speed @ 1500 Motor RPM	Screw Speed @ 7500 Motor RPM
63:1	77	384
235:1	21	104
455:1	11	53

Furthermore, the feeder ordered came with two different types of concave screws, the coarse and fine. It is also important to refer that they are twin screws, which means that both, the 20C screw and the 10C screw, are in reality two screws each with 20 mm/rev and 10mm/rev, respectively (Figure 1.10).

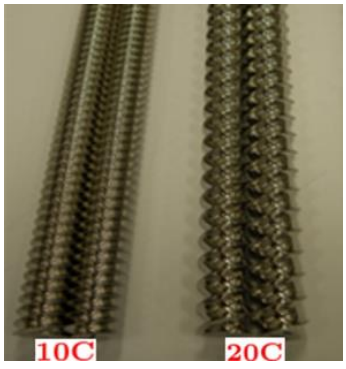

Figure 1.10 – Available screw types to set on GEA Compact Feeder; 10C – Fine concave screw; 20C – Coarse concave screw [30].

The step of choosing the appropriate gearbox and screw is decisive for the feeding process because it will have a direct impact on the RSD. Considering this, in cases where it is assembled on the feeder the 10C screw, a much lower amount of powder will be fed to the process in comparison to the 20C screw and for this reason the gearbox and screw selection must be done simultaneously to assure the defined setpoint [26] [33].

1.7.1.2 Agitator and Baffle

It is possible to set inside the feeder's hopper two different types of agitators, the symmetric and the asymmetric agitator (Figure 1.11).

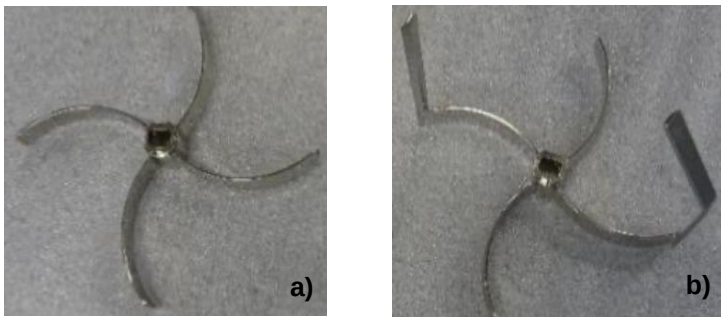

Figure 1.11 – Two different types of agitators. a) Symmetric agitator; b) Asymmetric agitator.

The agitators are composed of:

- Symmetric agitator – 4 C blades agitator wipes;
- Asymmetric agitator – 2 C blades and 2 combined C-anchor blades agitator wipes.

The asymmetric C-anchor blades prevent a number of pervasive diffusional problems within the hopper, such as ratholing and bridging (Figure 1.12).

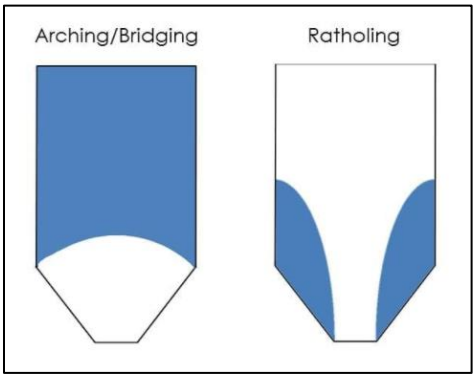

Figure 1.12 – Powders diffusional problems: bridging and ratholing [37].

It is also important to refer that when it is intended to feed materials to the continuous process with the tendency to form bridging it is recommended as well to add a static baffle to the hopper (Figure 1.7 – D).

1.7.1.3 Mesh

The GEA Compact Feeder has three possible meshes to be inserted at the output of the feeder's screw (Table 1.4). Their function is to reduce the RSD of the feeding process, although some materials might not be affected by any of the three meshes and for those cases it is preferable to run the feeder without a mesh.

Table 1.4 – Types of mesh and respective information.

Mesh	Grid	Hole Diameter (mm)
D8	Highest	8
D2	Intermediary	2
D1	Lowest	1

Regarding Table 1.4, the D8 mesh is the one with the biggest grid because its holes are 8 mm each and D1 is the smallest mesh measuring 1 mm per hole diameter. To better understand the impact that the diameter sizes have on the mesh sieving function, the previous table must be complemented with Figure 1.13.

D8 D2 D1

Figure 1.13 – The three meshes available to set on the feeder [26].

1.7.1.4 Topup

It is possible to set on the topup system one of the four topups that are available (1.6L/ 1.2L/ 0.8L/ 0.4L). However, the process of choosing the most appropriate one is dependent on the conditions at which the refill should occur. As so, the topup depends on the minimum volume of material that can be inside the feeder without provoking consequences to the feeding stability (minimum refill volume).

Considering this, the sum of the volumes of minimum refill volume and topup volume must make up 2L, as represented on Table 1.5.

Table 1.5 – Minimum refill volume and the correspondent topup that must be set on the feeder.

Min Refill Volume (L)	Topup volume (L)
< 0.4	1.6
< 0.8	1.2
< 1.2	0.8
< 1.6	0.4

1.8. Feeding Operational Principles

1.8.1 Initial Run

Firstly, an initial run is performed in order to calibrate the feeder and also define the initial FF array to prepare the feeder for the production run. For that purpose, the feeder's hopper must be totally filled (2L of working volume).

The FF is the ratio between the massflow and the feeding screw speed (Equation 1.1) and it depends on the amount of powder inside the hopper, on the materials' properties and on the screw type that is selected.

$$FF\ (g/rev) = \frac{Massflow\ (g/s)}{Screw\ Speed\ (rev/s)} \tag{1.1}$$

The FFs are stored on a FF array where each array's FF value is valid for a specific interval of powder's mass (Figure 1.14). At the same time that the FF array is updated, from the highest to the lowest number, the correspondent standard deviation (Stdev) is calculated by the feeder. A low value of Stdev means that the FF value was well actualised. On the other hand, a Stdev value of 1 g/rev means that the FF value is unknown, in other words, the value was not actualised.

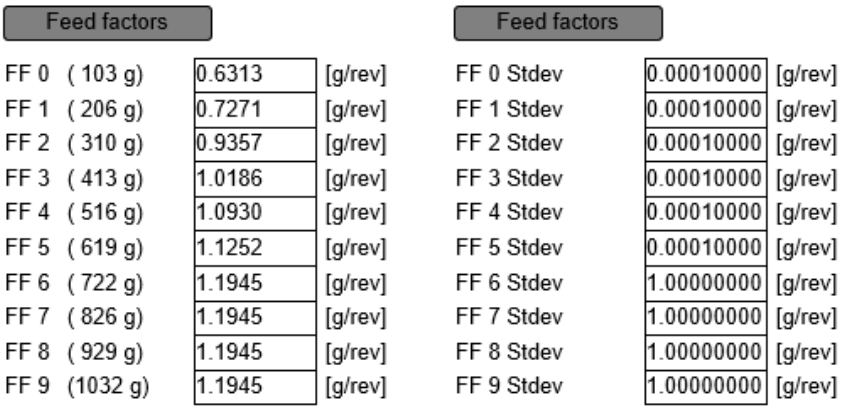

Figure 1.14 – An example of a FF array.

Regarding Figure 1.14, all FFs higher than FF 5 have Stdevs of 1 g/rev which means that the correspondent FFs were not calibrated. Considering this, the FF array was calibrated starting on FF 5 until the feeder got totally empty and the calibration was started with a mass of powder lower than 722g. This is the reason why both the calibration and the update of the correspondent Stdevs only are verified starting on FF 5 (619g).

1.8.2 Feeder's Run

To perform the feeding process for production purpose, the LIW feeding mode is activated. It is responsible for controlling the massflow to be as similar as possible to the defined setpoint.

The weighing cell is used to measure the amount of powder that is inside the hopper and to calculate the actual powder's massflow that is leaving the feeder according to the LIW principle.

The massflow control loop is a feedback loop that controls the velocity of the feeding screw by taking into account the massflow oscillations regarding the defined setpoint. The control loop is a cascaded design with a fast inner loop to control the motor velocity and the slow outer loop to control the mass flow. The inner loop is implemented by the servo driver. The outer loop is implemented as PID loop with gain scheduling which means that the optimal PID parameters for the outer loop are calculated by feeder control module based on the current powder behaviour and selected massflow filter (setpoint), but the user has the ability to define the aggressiveness of the control loop with the "TC multiplier" parameter [33].

The massflow control loop can operate in volumetric mode or gravimetric mode:

• In gravimetric mode the controller runs in closed loop mode, meaning that the massflow is used to correct the screw speed to maintain the setpoint;

• In volumetric mode the controller runs in open loop mode, meaning that the screw speed is calculated by dividing the setpoint over the stored FF from the array (Equation 1.2).

$$Screw\ Speed\ (rev/s) = \frac{Setpoint\ (g/s)}{FF\ (g/rev)} \tag{1.2}$$

It is important to refer that the gravimetric mode will only be activated when the massflow signal is stable, which is based on the RSD of the massflow regarding the defined setpoint.

To better understand what happens during the refill a more detailed explanation is followed.

1.8.2.1 Refill

When the mass inside the feeder gets to a minimum amount (Section 2.2.2.2), the refill is automatically performed by the feeder.

During the refill, the LIW Feeder that was operating in gravimetric mode is instantaneously changed into volumetric mode by the control system, because the weight loss cannot be accurately measured when material is entering and leaving the feeder at the same time [28].

Therefore, the feeder will simulate the weight signal based on the valve delay, the refill rate parameters and the topup weight parameters [33].

1.9 Feeder Software

First of all, it is important to refer that the feeder's weighing scale box is controlled by the feeder's control box (Figure 1.15) that is therefore connected to a laptop.

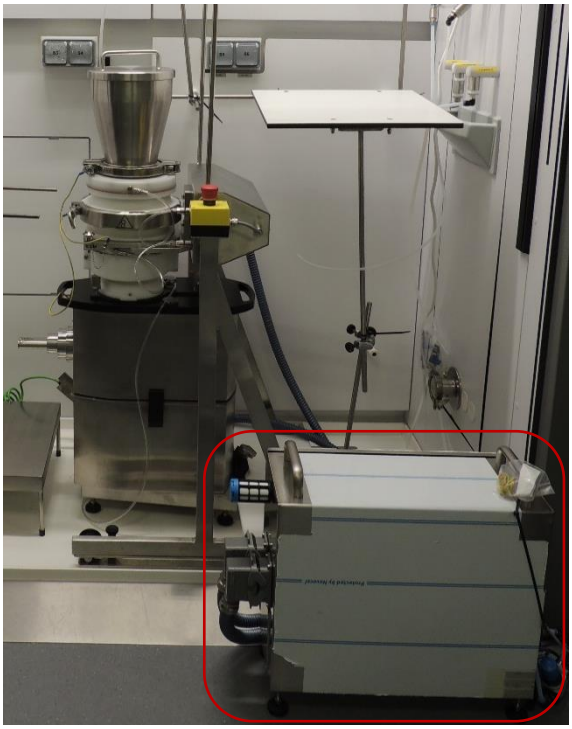

Figure 1.15 – GEA Compact Feeder as well as its control box (outlined in red).

Through the laptop the operator can command the feeder as well as visualise and record its performance parameters in real time. This last point is a great advantage of the equipment making it possible for the operator to take action during the feeding processes in case of deviations.

There are two main software used to perform this task: the Feeder Controlling Program and a remote datalogger, called TwinCAT ScopeView.

1.9.1 Feeder Controlling Program

The Feeder Controlling Program, developed by the GEA Group, is a local user interface of the GEA Compact Feeder, essential to control the equipment.

Before starting to operate the feeder, several trainings are needed to become familiar with this program, due to the huge variety of commands that are distributed through the following screens.

[Main]: This screen gives a summarised overview, with the feeder status and process readouts, of the controlled location(s) and the installed feeder(s), with a maximum of four (Figure 1.16). It is important to refer that during the experimental work only one feeder was tested and for this reason only “Location 1” was used, as it is possible to be verified on the bottom of the following screens’ figures.

Figure 1.16 – Feeder controlling program’s main screen.

[Location 1]: This screen gives a more detailed overview of the associated location/feeder, with the available control buttons, the process readouts and the alarm status and control. Through this screen the feeder calibration is managed and the feeder’s runs can also be controlled in cases where it is not intended to do the processing in an automated mode (Figure 1.17).

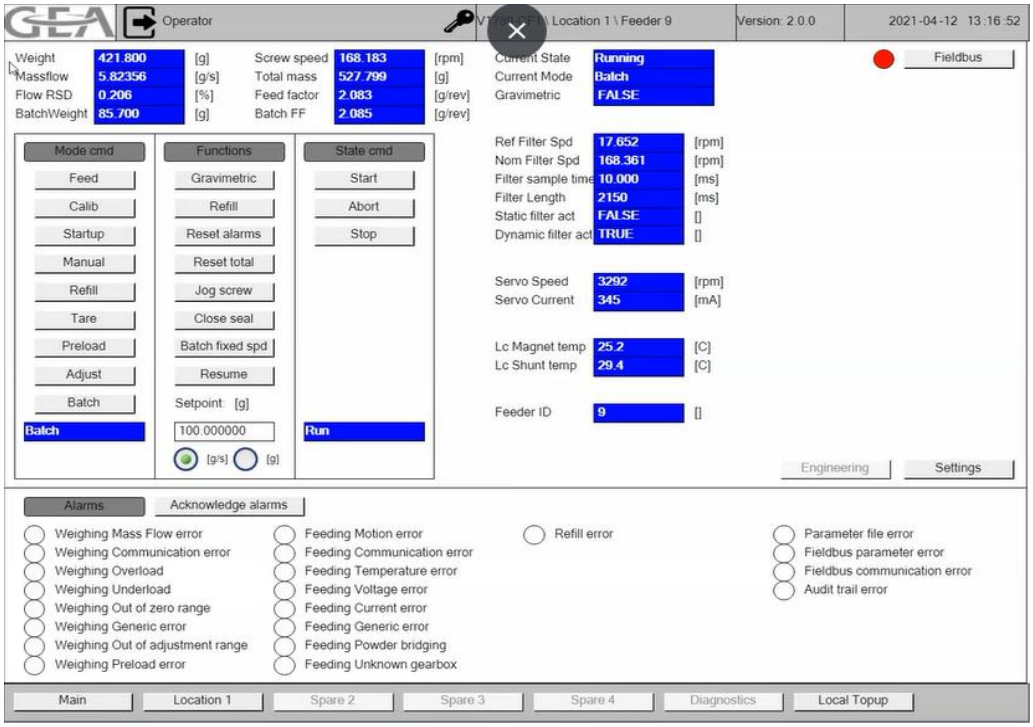

Figure 1.17 – Feeder controlling program's location 1 screen.

[Settings]: This screen gives access, for the associated location/feeder, to a subset of the available and editable parameters and process readouts for operation. Also, it is in this screen where the FF profile is presented (Figure 1.18).

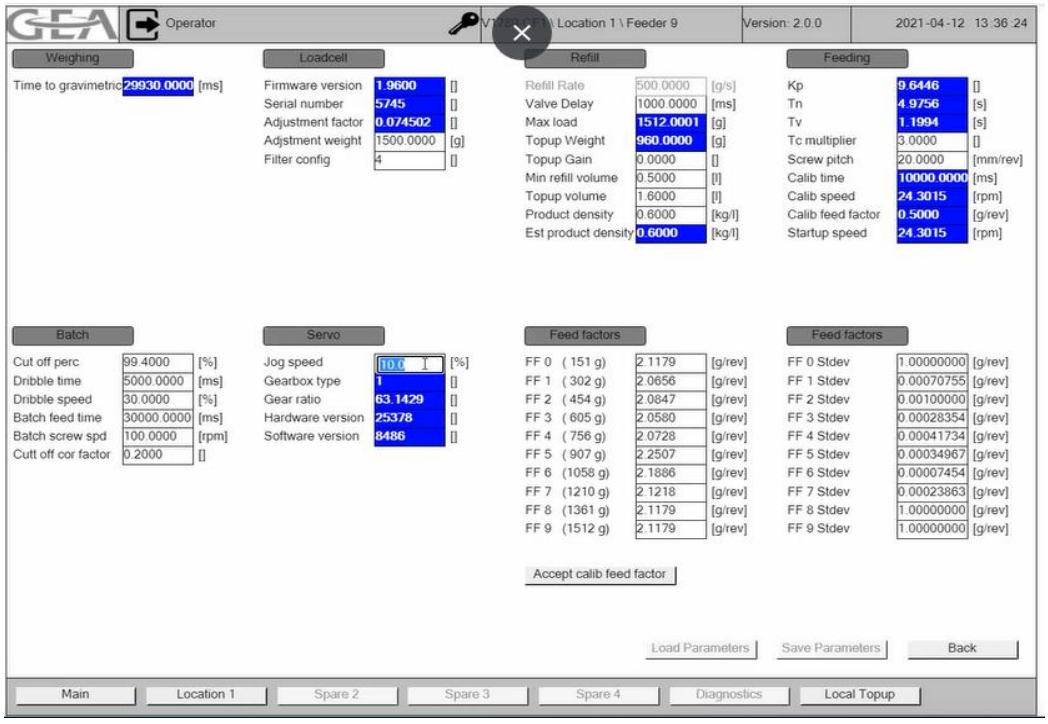

Figure 1.18 – Feeder controlling program's settings screen.

[Local Topup]: This screen gives a more detailed overview of the local topup, with the available control buttons, the process readouts, and the alarm status and control. It is through this screen that the feeder is controlled during the feeder's run, after the first run is performed. In other words, this is the screen that is used when the feeder is running automatically (Figure 1.19).

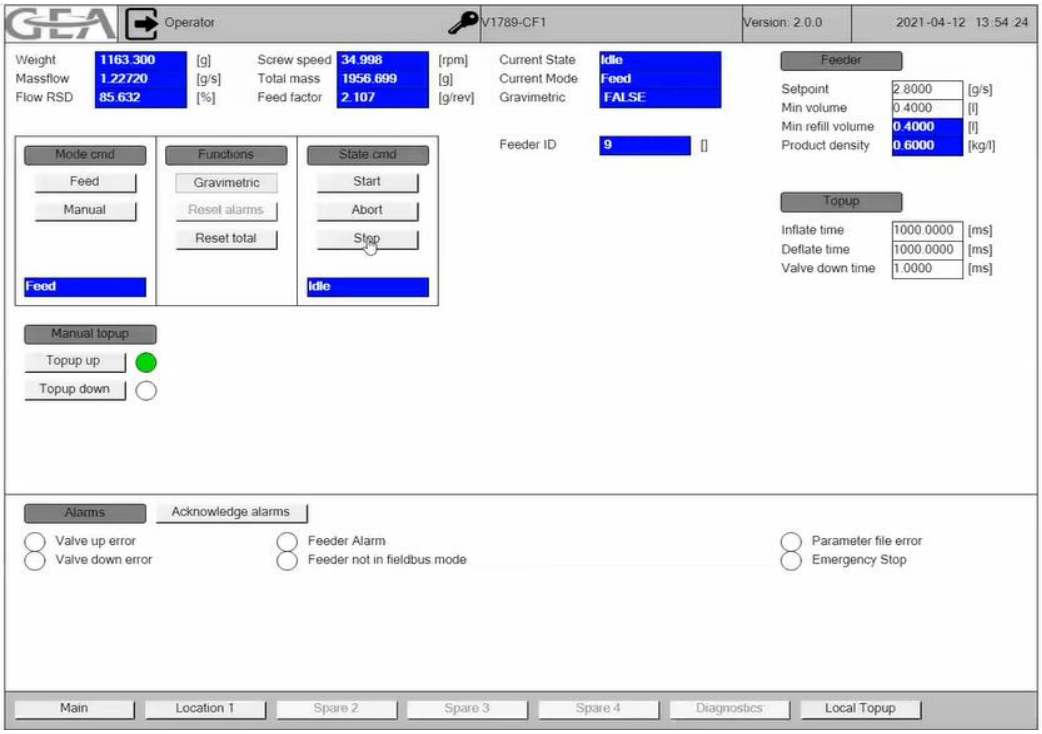

Figure 1.19 – Feeder controlling program's local topup screen.

Furthermore, in order to simplify the command of the Feeder Controlling Program, a software handling manual was developed by the author of this thesis with the goal of helping other operators by providing them a step-by-step guideline document.

1.9.2 TwinCAT ScopeView

A remote datalogger called TwinCAT ScopeView from Beckhoff is used for data logging. This program is useful to help the operator interpret and take action in real time regarding the equipment's behaviour.

In Figure 1.20, an example of a datalogger with all the considered variables in function of time is presented.

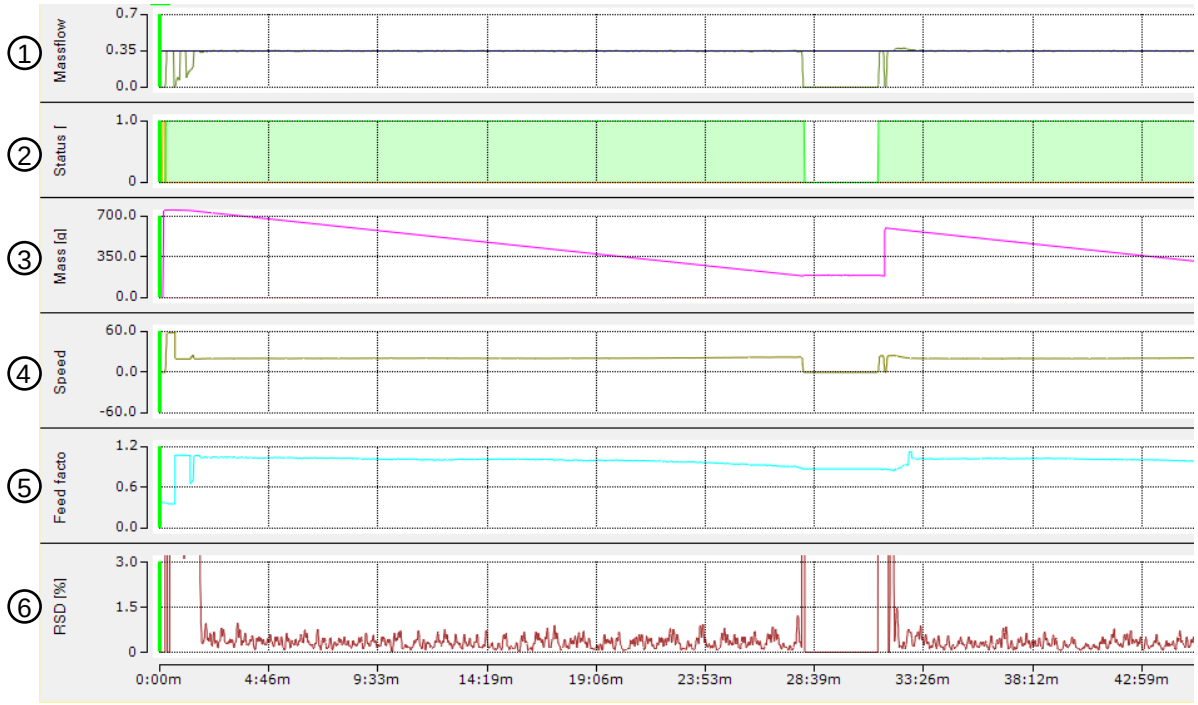

Figure 1.20 – Maximum setpoint feeder's run of Excipient F at a setpoint of 0.347 g/s. Graphic 1 – Massflow & Setpoint (g/s) vs time; Graphic 2 – Status [0-1] vs time; Graphic 3 – Mass (g) vs time; Graphic 4 – Speed (g/s) vs time; Graphic 5 – FF (g/rev) vs time; Graphic 6 – RSD [%] vs time.

On the graphic 1, the defined setpoint is presented by a black line. Massflow represents the output oscillations relatively to the setpoint (green line). The graphic 2 shows the mode of the system, i.e. if the feeder is in volumetric (status=0) or gravimetric mode (status=1). Notice that the thin orange area on the left side of the plot means that the feeder was also in volumetric mode.

The graphic 3 indicates the amount of mass that is still inside the feeder and the graphic 4 represents the screw speed over time.

The graphic 5 indicates the profile of mass per revolution over time.

Finally, the graphic 6 reflects the variability of the massflow regarding the pre-defined setpoint. This is one of the most important graphics for equipment handling because it indicates if the feeder is or not operating in controlled conditions regarding the guidelines.

Describing in a few words the Figure 1.20, the run is initiated with the feeder completely empty and as the "Start" button is pressed on local topup screen (Figure 1.19) the fill happens, consequently, all the feeder's parameters start to adapt to the run conditions. On the graphic 1 it is possible to observe that the massflow variable is trying to stabilize at the defined setpoint of 0.347 g/s and, as expected during that period, the RSD is truly high. After, approximately two minutes, the feeder starts to operate at stable conditions.

It is noticeable that, over time, the mass inside the feeder (graphic 3) is decreasing during the feeding process until reaching 28 minutes, approximately the time when the refill happens. During the refill time the feeder operates in volumetric mode being the graphic 2 on zero. It is also interesting to notice that every time that the topup valve rotates (in the beginning and in the end of the refill) an abrupt increase of the RSD is observed on graphic 6, due to the feeder's vibrations caused by the topup system action.

The described process is supposed to be repeated over time until the end of the production.

1.10 Powder Rheology

In order to analyse the materials' properties, the most important parameters to consider in this master thesis are measured by rheological tests, being the most widely used the Ring Shear Cell [13] [38]. Besides the flowability, it can also measure the bulk density (ρ_{bulk}) and the tap density (ρ_{tap}) through the Ring Shear Cell Tester which combined calculate the Hausner ratio (HR) and the Carr's index (CI) as indicated in Equation 1.3 and 1.4, respectively [39]-[41].

$$HR = \frac{\rho_{tap}\ (kg/L)}{\rho_{bulk}\ (kg/L)} \tag{1.3}$$

$$CI\ (\%) = \frac{\rho_{tap}\ - \rho_{bulk}\ (kg/L)}{\rho_{tap}\ (kg/L)} \times 100 \tag{1.4}$$

The ρ_{bulk} is the density before compaction and ρ_{tap} after compacting the powder in kg/L. After calculating for each material the value of these two indexes, flowability can be qualified, according to Table 1.6.

Table 1.6 – HR and CI compressibility indexes flow characterization [42].

CI (%)	Flow property	HR
≤ 10	Excellent	1.00-1.11
11-15	Good	1.12-1.18
16-20	Fair	1.19-1.25
21-25	Passable	1.26-1.34
26-31	Poor	1.35-1.45
32-37	Very poor	1.46-1.59
> 38	Very very poor	> 1.60

Ring Shear Cell: This test can provide useful information regarding powder flowability and also has the advantage of being precise and predictive.

For each preshear stress, the stress needed to shear the bed for three different consolidation stresses (as failure shear stress) are plotted against the normal stress, those points are represented on Figure 1.21 as Shear points and together they form a plot known as a yield locus.

The X axis represents the stress normal to the shearing power (consolidation stress), and the Y axis represents the shear stress. The most common method of treating shear data is the Mohr circle analysis, also shown in Figure 1.21. The Mohr circles are drawn in such a way that they are tangent to the yield locus. These circles represent the total stresses on the powder bed at the point of shear in any direction, in other words, it represents the pressures on all cutting planes. The 1st Mohr Circle is drawn tangent to the yield locus and crosses the X axis at the origin and at the unconfined yield strength (UYS). This parameter provides the maximum principal stress acting on a free surface required to cause failure. The 2nd Mohr Circle is drawn in a way that it is simultaneously tangent to the yield locus and it integrates a point of maximum shear and zero normal applied stresses (preshear point). Its intersection with the X axis provides the major principal stress (MPS) which is the maximum perpendicular stress at which the powder can be consolidated before it changes volume. Finally, the material's cohesion property (Tau,c) is given by the intersection of the yield locus with the Y axis [39] [43].

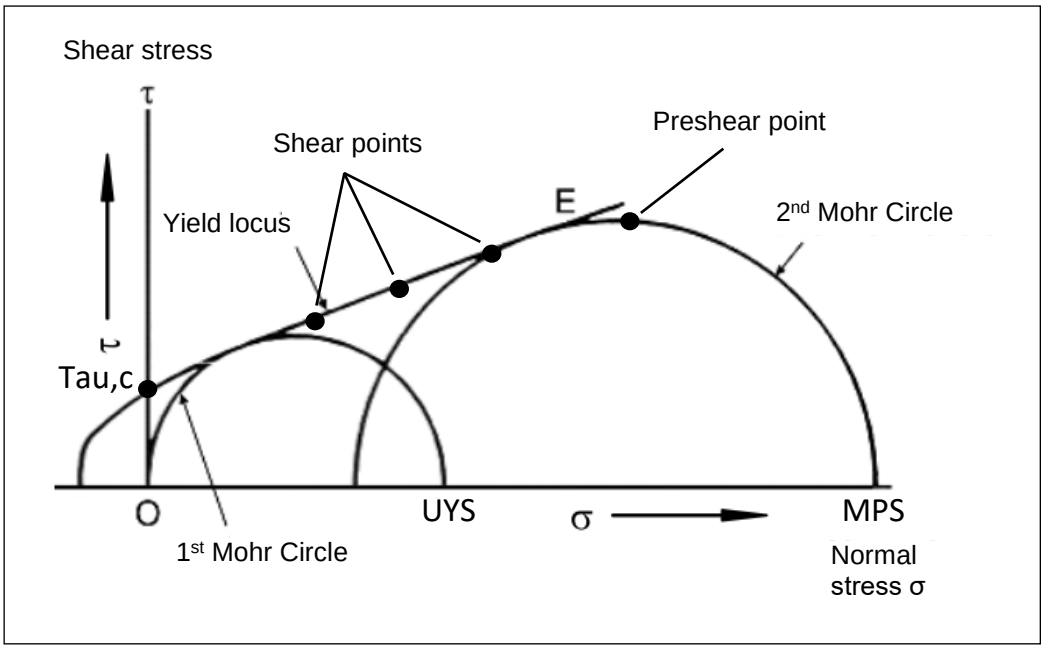

Figure 1.21 – Mohr circles analysis scheme and yield locus with shear points and preshear point.

Additionally, by plotting the UYS by the MPS, the flow function coefficient (ffc) is obtained (Equation 1.5).

$$ffc = \frac{MPS\ (Pa)}{UYS\ (Pa)} \tag{1.5}$$

The ffc at a given consolidating stress can be referenced against established flowability categories (Table 1.7) [25].

Table 1.7 – Flowability categories according to the materials' ffc classification [39].

ffc range	Flow type
ffc < 1	Not flowing
1 < ffc < 2	Very cohesive
2 < ffc < 4	Cohesive
4 < ffc < 10	Easy-flowing
10 < ffc	Free-flowing

It is also important to consider the materials' particle size in order to predict the flowability of a powder. Such considerations are displayed on Table 1.8.

Table 1.8 – Flow type categories according to the materials' particle size.

Particle size (μm)	Flow type
250 - 2000	Free-flowing
100 - 250	May flow freely
< 100	Flowing is a problem

Regarding the Table 1.8 flow type, the "May flow freely" classification must be clarified. It means that the materials with particle sizes within that range may flow freely if they have an aerodynamic shape and high flowability.

2. Materials & Methods

2.1 Materials

On the following sections the materials that were tested on the feeder will be described in detail as well as the equipment used for that materials' characterization.

2.1.1 Utilized Materials

As previously referred, one of the main goals of this project is to predict the behaviour of the studied materials inside the feeder.

Having this in consideration, some of the most commonly used materials in pharmaceutical formulations were tested on the feeder. On Table 2.1, all the studied materials are represented as well as their supplier and batch number.

Table 2.1 – Materials' supplier, batch number and role in a formulation. Material supplier's brochures are also referenced on the table, except for Copovidone SD which was produced in Hovione.

Material	Type of material	Supplier	Batch #	Quantity (kg)
Avicel PH102 [44]	Filler	DUPONT IE Wilmington, DA, USA	5510616.HQ00018	1.0
Avicel PH200 [44]	Filler	DUPONT IE Wilmington, DA, USA	5512500.HQ00002	1.0
Lactose Mono 316NF [45]	Filler	KERRY Tralee, Ireland	B590000392	0.5
Ligamed MF-2-V [46]	Lubricant	PETER GREVEN Bad Münstereifel, Germany	NA	0.5
Prosolv SMCC HD90 [47]	Filler	JRS PHARMA Rosenberg, Germany	D9SO308	2.0
Ac-Di-Sol [48]	Disintegrant	DUPONT IE Wilmington, DA, USA	110606.HQ00006	1.0
Copovidone SD	Binder	HOVIONE Lisbon, Portugal	NA	0.7

The majority of the materials tested on the feeder were fillers. This type of materials are used to increase the volume of the drug in a way that the patient, the end user, may consume [5]. Not only that, but they can also stabilize the product and, due to their good properties, help the manufacturing process [49]. It is also interesting to notice that this class of materials is commonly used at high percentages in the formulations. On the other hand, desintegrants (Excipient F) and lubricants (Excipient D) are used at lower percentages.

Excipient G is commonly used as a binder as referred on Table 2.1, however, for this study, it was considered as an API in order to simulate amorphous solid dispersion (ASD) from spray drying (SD). This was due to the fact that the laboratory security team does not allow the handling of APIs on the feeder, since the feeder's handling conditions, by the time that this experiment was done, could not match the company safety requirements. In fact, the Excipient G was produced guaranteeing a similar particle size and ρ_{bulk} comparing to the typical Hovione's ASD.

It is important to refer that the quantity indicated for each material on Table 2.1 does not correspond to the amount of mass that was truly used during the feeder's runs. Firstly, approximately 100g were initially collected for the materials' characterization and secondly, the feeder has a dead mass zone in which, during all the tests, an amount of the material's mass gets stuck inside the equipment (Appendix A).

Also, it should be considered that for each time that the feeder is disassembled, that dead mass is wasted during the cleaning process and the number of times that this procedure is performed depends on the difficulty found to achieve the feeder limits for each material.

Noticing that the maximum setpoint feeder's runs were always done before the minimum setpoint feeder's runs, the amount of mass available to achieve each of the materials minimum setpoint was always lower than to perform the maximum setpoint feeder's runs.

2.1.2 Equipment

2.1.2.1 Equipment Utilized for Materials' Characterization

The following equipment was used to characterise the materials' rheological properties, particle size and morphology. Also, it is important to describe the conditions in which each type of analysis was performed.

Two of the used equipment, the Ring Shear Tester and the Sympatec, allow a quantitative analysis of the measured parameters, being their respective values indicated on Appendix B. On the other hand, the scanning electron microscope (SEM) only allows a qualitative analysis.

2.1.2.1.1 Ring Shear Tester

The rheological properties of the materials and also the ρ_{bulk} and ρ_{tap} were characterized using a RST-XS.s Ring Shear Tester (Dietmar Schulze, Germany) (Figure 2.1). The applied normal load at pre-shear was 2000 Pa. Afterwards, the powders were sheared under three different consolidation stresses (shear points): 400, 1000 and 1600 Pa.

The Xs - Mr Shear Cell (30 mL volume) was used to measure both the densities under consolidation at pre-shear (ρconsolidation), the powders' cohesion (Tau,c) by using the yield locus to estimate the shear stress at zero normal load and the ffc to evaluate flowability. If it is intended to know with precision all the steps taken during this measurements, it is highly recommended to consult a book from D.Schulze named "Powders and Bulk Solids" [39].

Finally, it is important to refer that, unfortunately, all the parameters were measured only once, which, of course, has an error associated.

Figure 2.1 – RST-XS.s Ring Shear Tester [50].

2.1.2.1.2 Sympatec

The particle size distribution of the materials was measured by laser diffraction using the Sympatec HELOS-BR-RODOS-L-ASPIROS (Figure 2.2). This equipment combines a dry dispersion unit, RODOS/L, with the laser diffraction sensor, HELOS/BR. It offers a fast and repeatable particle size analysis for dry fine-grained materials (0.1 µm - 875 µm). Cohesive powders are also dispersed

and measured in a reliable way [51]. The dispersion pressure was 0.2 bar and the R5 lens was used. From this equipment the dv10, dv50, dv90, SMD and VMD of each material was recorded and each value was measured in triplicate and for this reason the data presented on Table B.1 (Appendix B) are average values.

Figure 2.2 – Sympatec HELOS-BR-RODOS-L-ASPIROS [51].

2.1.2.1.3 Scanning Electron Microscope

The Phenom ProX Desktop SEM (Figure 2.3) in high vacuum mode was used with a typical accelerating voltage of 15kV. With the usage of this equipment, it is possible to do a qualitative analysis about each material's powder particles shape, surface topography and morphology.

Figure 2.3 – Phenom ProX Desktop SEM.

2.1.2.2 Feeder

As previously referred, the GEA Compact Feeder is the centre of this thesis and for that reason, all the information about the equipment was already described on Section 1.7, 1.8 and 1.9.

However, it is important to refer that for the analysis on Section 3, all the data that was used from the TwinCAT ScopeView software was the one that was recorded on the feeder's stationary periods, which means that the data correspondent to the moments when the fill and the refill were register were not considered, since the feeder was running in volumetric mode.

2.2 Methods

The following methodology will be carried to define the maximum and minimum setpoint limits of the feeder for the different materials previously presented. This is of high importance because, when having these limits, it is known that between that ranges the operation conditions will be stable.

2.2.1 Define the Setpoint

The methodology defined to choose the initial setpoint to be tested on the feeder had in consideration the following logic.

As previously referred on Section 1.3, the CDC-10 process can run between a minimum of 1kg/h and a maximum of 25 kg/h. For each of these extremes, the materials' setpoints were calculated for both the minimum and maximum percentage in which each material is commonly used in the formulation (Table 2.2). Such percentages were based on literature in order to define the starting values for the experimental runs.

Table 2.2 – The most commonly percentages of materials used in formulations. Each material's percentage must be multiplied by the respective CDC-10 process limits indicated on top of the columns; on the last column the literature from where the respective percentages were defined is indicated, except for Excipient C and Excipient G whose information was provided by Hovione.

Material	1 kg/h	25 kg/h	References
Excipient A	20%	90%	[52]
Excipient B	20%	90%	[52]
Excipient C	10%	60%	Hovione
Excipient D	0.25%	1.5%	[53]
Excipient E	25%	50%	[47]
Excipient F	1%	5%	[52]
Excipient G	5%	60%	Hovione

Afterwards, in Equation 2.1 and Equation 2.2, calculations were made considering the percentages in formulation (% in formulation) to define the initial setpoint to be tested on the feeder (pre-defined setpoint) for the maximum ($MAX_{pre\text{-}defined}$ Setpoint) and the minimum ($MIN_{pre\text{-}defined}$ Setpoint) CDC-10 limits.

$$MAX_{pre-defined}\ Setpoint\ (kg/h) = \%\ in\ formulation\ \times 10^{-2} \times 25\ kg/h \quad (2.1)$$

$$MIN_{pre-defined}\ Setpoint\ (kg/h) = \%\ in\ formulation\ \times 10^{-2} \times 1\ kg/h \quad (2.2)$$

Afterwards, since the feeder controlling program requires the setpoint in g/s, both pre-defined setpoints must be converted from kg/h to the right units.

To test both limits on the feeder the procedure followed for each material was:

1st – Feeder's first run considering the maximum pre-defined setpoint;
2nd – Feeder's run with the maximum pre-defined setpoint;
3rd – Feeder's first run considering the minimum pre-defined setpoint;
4th – Feeder's run with the minimum pre-defined setpoint;
5th – Use the trial-and-error "methodology" to find the minimum stable setpoint.

It is important to refer that this procedure took into consideration the fact that all the pre-defined maximum setpoints were run at stable conditions. Eventually, for future cases where the feeding performance is unstable, that setpoint must be decreased until reaching a stable massflow, by the same methodology as indicated on the 5th step. This last step was frequently carried out for the pre-defined minimum setpoints, forcing to gradually increase the minimum setpoint until reaching the lowest stable setpoint possible. Noticed that it is considered that the feeder is operating at stable conditions when its RSD average value is below 4%.

In the literature, the most common used value is 5%RSD [25]. However, as this number is an average it might happen that in some cases, with average values below 5%RSD, there are huge massflow oscillations throughout the run. This situation was verified with the Excipient B minimum pre-defined setpoint (0.056 g/s). In fact, the average RSD was 5% but the oscillations were too big to consider that its massflow stability was reasonable, forcing the author of this thesis to proceed for the 5th step and to decrease the RSD limit to 4% for safety reasons.

2.2.2 Define Feeder's Components

A methodology was developed to define the appropriate equipment components to be set on the feeder for each condition shown on Table 2.2. All the reasoning and considerations taken during the process of choosing the most appropriated components are indicated below.

2.2.2.1 Gearbox and Screw

After calculating the setpoint through Equation 2.1 or Equation 2.2, in order to find out the best gearbox and screw to set on the feeder, the volume flow rate must be obtained for all the materials used (Equation 2.3).

$$Volume\ Flow\ Rate\ (L/h) = \frac{Setpoint\ (kg/h)}{\rho_{bulk}\ (kg/L)} \tag{2.3}$$

Afterwards, it is ascertain in which range between the maximum and the minimum volume flow rates, presented on Figure 2.4, the calculated value fits.

# used in HMI recipe	*Gearbox type*	*screw*	*Max [L/h]*	*Min [L/h]*
1	Gearbox 63	Screw P=D	113.6	7.1
		Screw P=D/2	56.7	3.5
2	Gearbox 235	Screw P=D	30.4	1.9
		Screw P=D/2	15.2	0.9
3	Gearbox 455	Screw P=D	15.7	1.0
		Screw P=D/2	7.8	0.5
	(@100rpm)	Screw P=D/2	-	0.10

Figure 2.4 – Table provided by GEA to help on gearbox and screw type selection.

In some cases, the volume flow rate is in between more than one interval, and, for such cases, the methodology adopted is to first choose the upper interval and select the correspondent gearbox and screw type to be assembled on the feeder.

In cases where, by the indicated methodology, it is not stable to use the selected components (gearbox and screw), the interval represented below on the table must be selected.

2.2.2.2 Topup Valve

In order to define the most adequate topup valve to be used, a first run is always performed with the 1.6L topup. This procedure was decided because the topup with highest volume allows fewer number of refills and reduces the time that the feeder is running in volumetric mode. This is the reason why the 1.6L topup is the preferable one.

After the referred first run, the data recorded on TwinCAT ScopeView is analysed and the moment when the disturbances start to happen (on the massflow, the speed and the FF) is identified. That point corresponds to the minimum mass (Min Mass) of material that should remain inside the feeder during the feeding process and, for that reason, on that moment the refill should happen. Afterwards, the minimum mass value, is divided by ρ_{bulk} (Equation 2.4).

$$Min\ Refill\ Volume\ (L) = \frac{Min\ Mass\ (kg)}{\rho_{bulk}\ (kg/L)} \tag{2.4}$$

In cases where the obtained volume is lower than the minimum refill volume (Min Refill Volume in Equation 2.4) of 0.4L, the topup of 1.6L can be used. On the other hand, if the volume is higher than the minimum refill volume of 0.4L, one of the other three topups should be chosen by the same logic (Table 1.5). Both examples will be analysed on Section 3.1.2.2.

Figure 2.5 is a summary slide, given by GEA during the virtual training, where an example with a set-by-set analysis of how the previously referred methodology should be applied is presented.

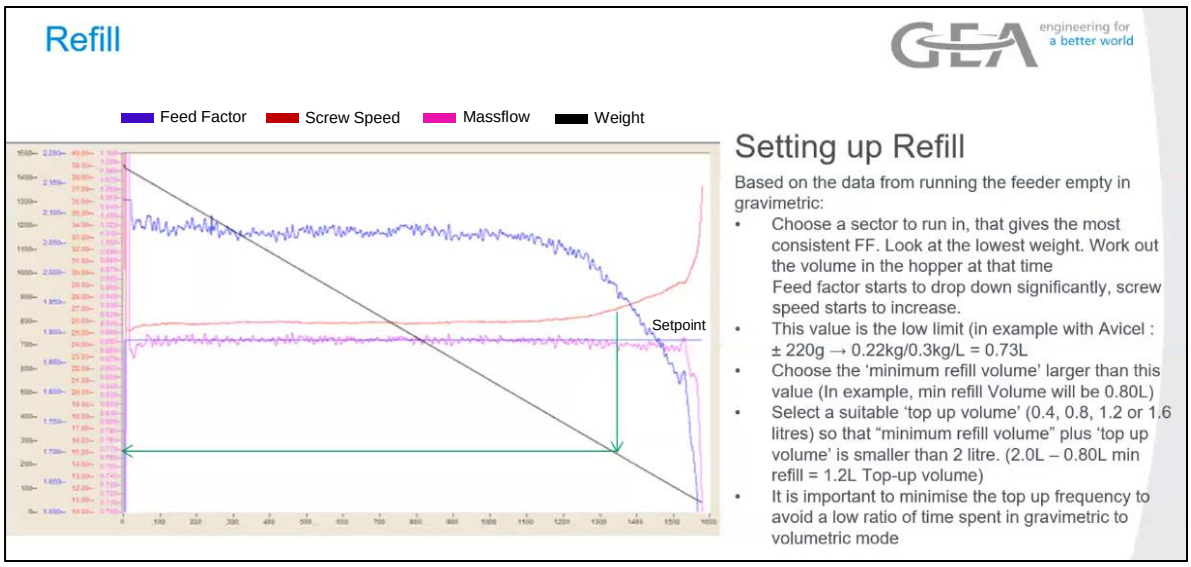

Figure 2.5 – GEA first run example. On the right side of the figure, it is also explained in detail the company reasoning based on the obtained results.

On Section 3.1.3 an example obtained from a first run experimental trial will be analysed in detail.

2.2.2.3 Agitator and Baffle

The selection of the agitator's type to be used is dependent on the material's flowability, as it will be explained on Section 3.1.1.

Figure 2.6 – Selection of the agitator type depending on the flowability.

Regarding Figure 2.6, for materials that have good flowability, the symmetric agitator is the indicated to be assembled on the feeder. Oppositely, for materials with bad flow properties, it is recommended to set on the feeder an asymmetric agitator. Moreover, when it is intended to perform the feeding of powders with undesired flowability it is also recommended the usage of a static baffle.

2.2.2.4 Mesh

The first run is always carried without the usage of a mesh. In cases where the RSD is below 3% there is no need to run the feeder with the mesh since it can be considered as already optimised.

When the RSD is over 3%, the running variability starts getting closer to the maximum stable RSD value of 4%, as indicated on Section 2.2.1. Considering this, it is of most interest to repeat the same run with the usage of meshes with the aim of obtaining a “safer” feeding process. The testing procedure is done as follows:

1st – Mesh with 8mm diameter hole (D8)
2nd – Mesh with 2 mm diameter hole (D2)
3rd – Mesh with 1 mm diameter hole (D1)

With this purpose, different meshes are tested beginning with the largest hole diameter (D8) and ending with the smallest one (D1). If the difference between the before and after RSD, with the usage of a mesh, is not significant the next mesh with a smaller hole diameter is tested (D2) and if the same is verified for D2, the remaining mesh must be tested (D1).

2.2.3 First Run

This run is necessary to calibrate the equipment, to calibrate the FF profile, as explained on Section 1.8.1, and to conclude about if the 1.6L topup is or not the most appropriate for the each material feeding process (Section 2.2.2.2).

It is recommended to perform this primary run with the feeder’s hopper completely full (to make up the 2L volume), although, as mentioned on Section 2.1.1, this condition was not possible to be achieved.

2.2.4 Feeder’s Run (for production purpose)

After defining all the feeder’s components and performing the first run, the feeder is ready to start the production. Usually, during this process, the feeder runs in automatic mode, this means that when the continuous production is started, by pressing the “Start” button (1) on the local topup screen (Figure 2.7), the only way that it would stop is either by pressing the “Stop” button (2) or by the activation of one or more feeder’s alarms (3).

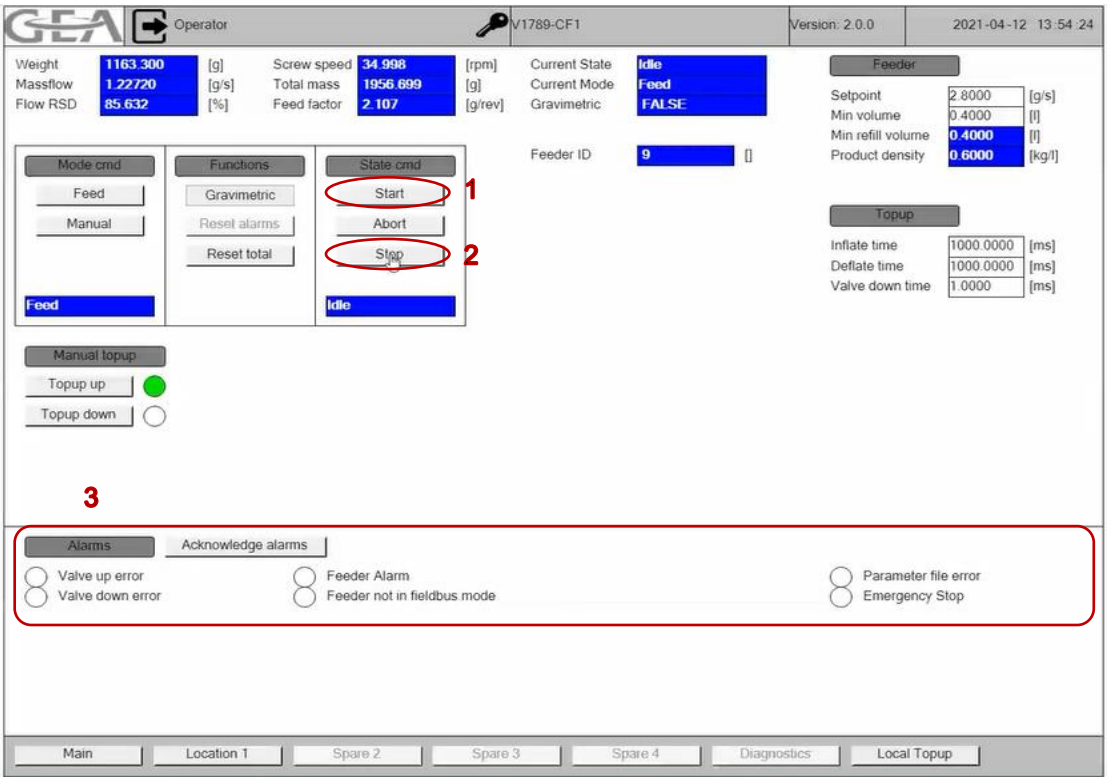

Figure 2.7 – Local topup screen with the indicated commands; (1) – Start button; (2) – Stop button; (3) – Feeder's alarms.

The autonomy of the feeder is a great advantage for continuous processes in a way that the feeder's system will automatically guarantee that the feeding process is always occurring in optimised conditions, because during the entire production time before the feeder gets out of control the refill is performed.

2.2.5 SIMCA®

SIMCA® 13.0.3 32-bit, by Sartorius, is used in this project for statistical analysis, using multivariate calibration and predictive modelling.

Firstly, the materials are characterized by the previously described equipment (Ring Shear Tester and Sympatec) to compile a multivariate dataset (Appendix B). Then, after the minimum and the maximum stable setpoints are found for each material, the correspondent feeder's components and feeder's parameters from each run are also organized as presented on Appendix C. Finally, to analyse all this dataset, PCA and PLS models are developed.

It is important to refer that all the methodology described in the following sections is a combination of the acquired knowledge provided by Hovione SIMCA's training and literature [54].

2.2.5.1 Significant Variables

In order to ensure that the PCA and PLS models are reliable, it is crucial to guarantee that there is not more than one X variable describing the same parameter. If so, the models will be overfitted, meaning that despite such models having a good fitting to the used set of data, they will not be able to fit additional data or predict future observations reliably [29].

Besides that, during the PLS model construction, the significant variables must be selected in order to make the model as simple as possible. This is achievable through the combined analysis of the coefficients and variable importance plot (VIP) graphics (explained on the following sections). By analysing both graphics at the same time, it is possible to eliminate progressively the X variables that are not impacting the most the response (Y).

2.2.5.1.1 Coefficients Graphic

The **coefficients graphic** shows which variables have a higher impact on the model. Also, through this graphic, it is possible to conclude about which of the significant variables are positively or negatively correlated to the Y of PLS models.

It is also important to refer that the values presented in coefficients graphics are the coefficients that are multiplied by the pre-processed data with mean centre and scaling (that pre-processing is automatically made by SIMCA). The program basically subtracts the average of each variable and then divides it by the respective standard deviation. For this reason, after the significant variables selection, each coefficient value must be unscaled in order to predict Y. In this way it becomes possible to multiply the “real” coefficient by the correspondent X variable and predict the Y value for new scenarios.

2.2.5.1.2 Variable Importance Plot

The **VIP** displays the overall importance of each variable (X) on the response (Y) cumulatively over all components. This graphic is a column plot sorted by descending order. The most relevant X variables for explaining Y are the ones with VIP values equal or higher than 1.

2.2.5.2 Components Graphic

2.2.5.2.1 Principal Component Analysis

During the PCA model development, while choosing the number of components to be used, the most important parameter to look up to is the goodness of fit (R2X). To ascertain about the goodness of the PCA model the following steps must be considered.

Firstly, the value of R2X should be analysed amongst each component. If the difference between these values is higher than 0.1, the next component should be chosen.

Secondly, having a high goodness of prediction from cross validation (Q2) is not as significant as having a high value of R2X. Considering this, if the difference between the two components' R2X values is not relevant, the previous component should be chosen even if the next component's Q2 is significantly higher (> 0.1). This is due to the fact that the model with less components will be simpler and, beyond that, the robustness between the two considered models will not be significant.

2.2.5.2.2 Partial Least Squares

The PLS development follows the same logic regarding the first step described for PCA models, but instead of R2X the goodness of prediction from calibration (R2Y) must be considered. In fact, R2X also exists on the PLS models, but it is not an important parameter to be taken into consideration.

Regarding the second step of Section 2.2.5.2.1, the fact that the next component has a higher Q2 value than the previous one plays a more important role. Therefore, in these cases, the next component should be chosen, instead of the previous one.

In fact, for the PLS models, the Q2 is the most important parameter to be considered because it gives the perception of how well Y is predicted. In addition to guaranteeing that the Q2 value is the biggest possible, it is also important to verify if the difference between the R2Y and the Q2 is not too big. If so, it means that the model is being influenced by variables overfitting.

It is important to refer that there is a minimum value of acceptance of 0.7 for the R2X and R2Y, for the PCA and PLS models, respectively. Obviously, the higher their values are the better the models will be.

2.2.5.3 Observed vs Predicted Graphic

Besides the components graphic, the **observed vs predicted graphic** is also really important to conclude about the PLS models viability.

This graphic displays the actual value versus the value predicted by the model for the selected response Y. Moreover, the Root Mean Square Error of the Estimation (the fit) for observations in the workset (RMSEE) and Root Mean Square Error, computed from the selected cross validation round (RMSEcv) is also displayed and, in order to have a good PLS model it is important that their values are as approximate as possible (same order of magnitude).

On **observed vs predicted graphic** it is possible to apply a regression line to all the obtained scores and to conclude, through the coefficient of determination (R2) value, about the linearity of the predictive system. The higher the R2 value is the better is the PLS model developed.

2.2.5.4 Scores Graphic

The **scores graphic** gives the information about how similar or different each material is, in terms of powder's characteristics, regarding other materials that are being compared.

The closer the materials are positioned on the plot, the more similar will those materials be, oppositely, the farther the materials are from each other's the more different will those materials be.

The **scores and loadings graphics** complement each other, because the positioning of the materials in a given direction on the scores plot is influenced by the variables that are lying in the same direction on the loadings plot.

2.2.5.5 Loadings Graphic

The **loadings graphic** displays the correlation structure of the variables (X).

In cases where the variables are closely positioned, they are directly proportional. If two variables describe between them approximately 90° regarding the graphic's origin, it means that they are not dependent. If two variables describe an angle of approximately 180° relatively to the graphic's origin, it means they are related in an inverse proportion.

2.2.5.6 Hotelling's T2Range Graphic

The **Hotelling's T2Range graphic** represents the information considered by the PCA model. The bigger the material's T2Range value the higher is the distance from the origin in the model plane (scores space) for each selected observation.

2.2.5.7 DModX Graphic

Oppositely to the **Hotelling's T2Range graphic**, the **DModx graphic** shows the model missed information, also known as residues. The higher the material's residue the less information is captured by the model about that material.

It is also important to verify if the residues values of all the materials plotted are lower than the DCrit(0.05) to guarantee that the model is reliable.

3. Results & Discussion

1) On Section 1 it is indicated the design space of GEA Compact Feeder for all the materials tested. Moreover, it is important to analyse in detail how the three major results groups (the materials' properties, the feeder's components, the feeder's parameters) impacted the experimental data that is presented on Table 3.1, in order to show the importance of continuing to develop a database to accelerate and simplify all the pre-production decisions about the appropriate process conditions, as well as the best materials to be combined in the formulation.

2) Afterwards, alternatives to avoid the first run are analysed such as to predict the FF profile and the topup volume.

3) Over Section 3, the impact that running the powders through the feeder has on the materials' properties is studied.

4) On Section 4 the applicability of the final ranges of stable setpoints and how that information should be used by those responsible for the production process will be described.

5) At the end, two case studies will be analysed (Section 5). The first one exemplifies how a new production should be scrutinized by considering Section 4 discussion. The second explains the utility that the Digital Twin program has by simulating the feeder's behaviour before starting the drug production.

3.1 Section 1: Resume Section of the Optimized Feeder's Runs

The Table 3.1 gives a general idea of the minimum and maximum setpoints that are possible to run on the feeder at stable conditions (< 4%RSD as defined on Section 2.2.1) as well as the feeder's components used on each process. It is important to refer that in order to avoid diffusional problems, the baffle was always assembled on the feeder for all the runs performed.

Considering the discussion made on Section 2.2.2.3 for the materials that have good flowing properties (Excipient A, Excipient B, Excipient C and Excipient E), the symmetric agitator was set on the hopper and for the rest of the materials (Excipient D, Excipient F and Excipient G) the asymmetric agitator was the chosen one. The reasons that fundament these decisions are analysed in detail on the following Section 3.1.1.

Table 3.1 – Table of all the experimental results obtained from the seven materials processed through the feeder.

Material	Range	Gearbox	Screw (mm/rev)	Topup (L)	Agitator Type	Mesh	Setpoint (g/s)	RSD (%)
Excipient A	MAX	63:1	20	1.6	Symmetric	NA	6.250	1.41
	MIN	455:1	10			NA	0.056	0.95
Excipient B	MAX	63:1	20	1.6	Symmetric	NA	6.250	1.18
	MIN	455:1	10			NA	0.080	1.36
Excipient C	MAX	63:1	20	1.6	Symmetric	NA	4.167	0.20
	MIN	455:1	10			NA	0.120	3.69
Excipient D	MAX	455:1	10	0.8	Asymmetric	NA	0.104	1.28
	MIN	455:1	10			NA	0.017	3.18
Excipient E	MAX	63:1	20	1.6	Symmetric	NA	3.472	0.23
	MIN	455:1	10			D2	0.140	3.76
Excipient F	MAX	455:1	10	1.6	Asymmetric	NA	0.347	0.37
	MIN	455:1	10			D8	0.050	3.10
Excipient G	MAX	63:1	20	1.6	Asymmetric	NA	4.167	0.89
	MIN	455:1	10			NA	0.020	2.69

In order to obtain the final results presented on Table 3.1, four months of trial-and-error experiences were necessary. It is considered by the author of this thesis that feeding stability can be guaranteed by running between the presented materials' maximum and minimum limits, although the following sections must be carefully analysed in order to be aware of all the information that must be considered during future works that intend to feed the studied materials on the CDC-10.

3.1.1 Materials' Properties Analysis

The feeding performance depends not only on the design of the equipment, control systems and setpoint, but also on the material flow properties. Thus, to better understand the selection of the feeder's components presented on Table 3.1, the powder flow properties of the tested materials must be characterized, to prevent the powder from sticking to the equipment walls, and to guarantee a low feed rate variability [55].

3.1.1.1 Materials' Characterization

The materials feeding performance is affected by their powders flow. It is influenced by a diversity of parameters, being some of the most relevant ones the particle morphology, particle size and flowability (density and ffc) [32] [56] [57].

3.1.1.1.1 Particle Morphology

The particles' morphology is possible to be defined based on their shape and angularity. More elongated particles lead to a lower flowability, whereas the spherical ones provide better flow properties [39].

In order to identify the morphology of all the studied materials, the SEM was used and the images from Figure 3.1 were obtained.

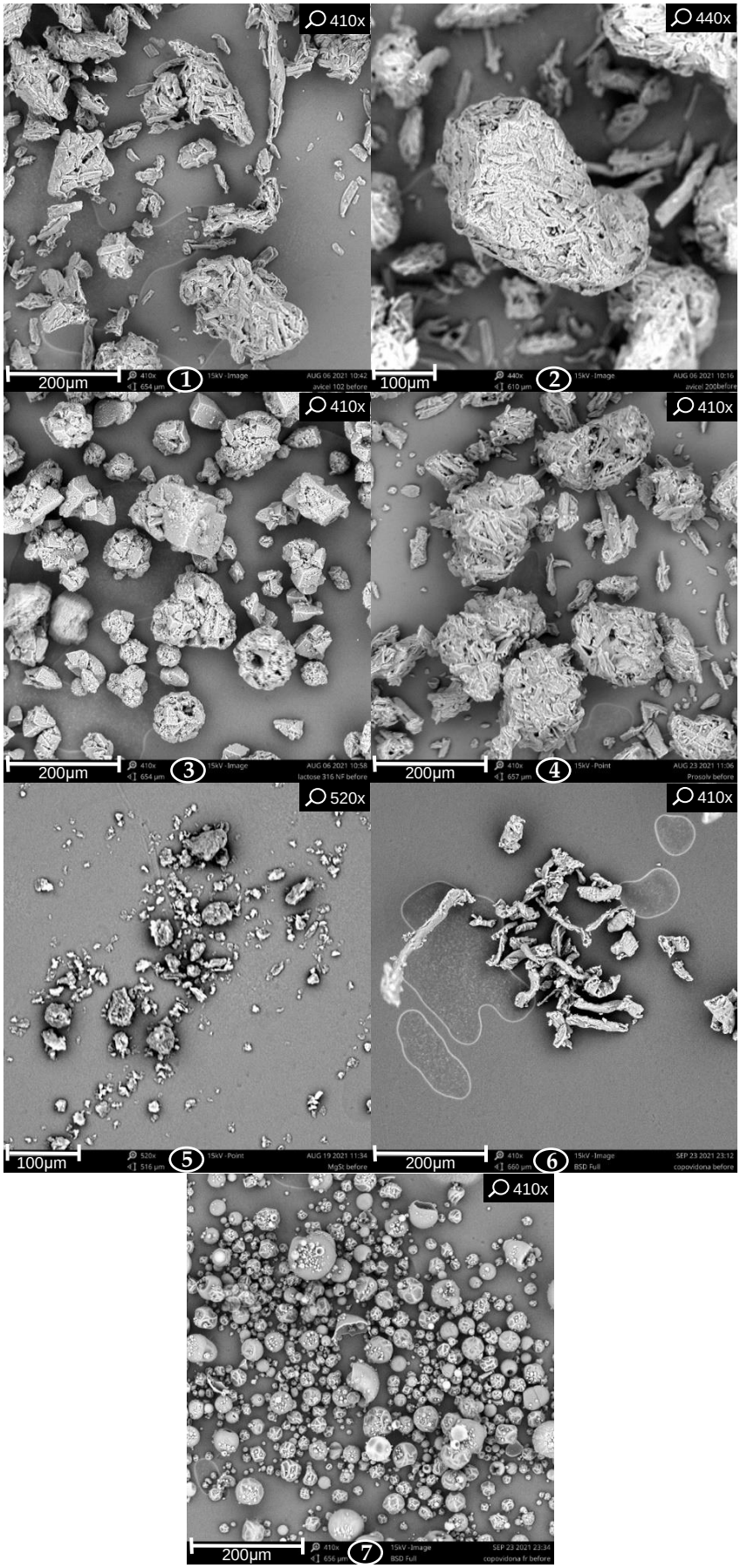

Figure 3.1 – SEM materials´ images. (1) – Excipient A; (2) – Excipient B; (3) – Excipient C; (4) –Excipient D; (5) – Excipient E; (6) – Excipient F; (7) – Excipient G.

Regarding Figure 3.1 the following descriptions were made:

- Excipient A (1) and Excipient B (2) are characterized by their irregular shape, although Excipient B has a higher circularity than Excipient A and this difference can be noticed between both SEM images [58] [59];

- Excipient D (4) is also an irregular powder in terms of morphology and it has a crystal structure of high quality Magnesium Stearate [46];

- Excipient E (5) has a homogenous distribution of colloidal anhydrous silica (CSD) on the microcrystalline cellulose (MCC) which is the reason why it has a very similar shape to Excipients A and B (regard their SEM images) [47];

- Excipient F (6) is a material characterized by a fibrous morphology and on Figure 3.1 – (6) it is possible to observe its elongated particles [48];

- Excipient G (7) and Excipient C (3) are both produced via SD and, as a consequence, their particles are easily recognisable by their spherical shape.

Based on the description of the images extracted from the SEM, Table 3.2 was created in order to resume the type of morphology that each material has.

Table 3.2 – Morphology of all the characterized materials.

Material	Morphology
Excipient A	Irregular [60]
Excipient B	Irregular [61]
Excipient C	Spherical [62]
Excipient D	Irregular [53]
Excipient E	Irregular [63]
Excipient F	Fibrous [64]
Excipient G	Spherical [65]

Regarding Table 3.2, most of the materials are irregularly shaped. Excipients C and G have a spherical morphology due to their materials' drying process and Excipient F is the material that stands out by possessing a fibrous morphology.

Despite the majority of the materials having an irregular morphology, there are differences between their flowability. For this reason, further materials' properties analysis are followed.

3.1.1.1.2 Flowability

There are two different ways to evaluate how a material flows through the feeder: the ffc, measured in the Ring Shear Tester, and the HR and the CI (Section 1.10).

Firstly, by considering the ffc, a material can be classified from a not flowing to a free-flowing powder, in which for a higher ffc value the flowability of the material is better [39].

Considering the intervals presented on Table 1.7 the materials were classified on Table 3.3.

Table 3.3 – Materials' ffc classification.

Material	ffc	Flow Type
Excipient A	7.03	Easy-flowing
Excipient B	10.51	Free-flowing
Excipient C	9.75	Easy-flowing
Excipient D	2.90	Cohesive
Excipient E	8.89	Easy-flowing
Excipient F	5.61	Easy-flowing
Excipient G	4.19	Easy-flowing

The materials that have the best flowing performance are Excipients B, C, E and A, from the highest to the lowest ffc. The remaining materials are the ones with the worst flowability, by the same logic.

Excipient B is considered a free-flowing material. The problem associated with this class of materials is the tendency that they have to "flush" through the feeder, which could cause a high variability on the flowrate [31]. In fact, the referred situation seems to be noticed by comparing both minimum setpoint values of Excipients A and B in the experimental results (Table 3.1).

Despite the fact that Excipient B presents higher flowability than Excipient A, the first mentioned could not stabilize at the initial defined setpoint of 0.056 g/s as Excipient A, amongst the RSD limits pre-defined on Section 2.2.1. Considering this, an increment of the minimum setpoint from 0.056 g/s to 0.08 g/s was required, in order to avoid more material than the intended from getting out of the feeder.

Besides Excipient G being characterized as an easy-flowing material, during the experimental feeder's runs it has a cohesive performance. Something really common that is used to be verified on feeder's runs with cohesive materials is its adherence to the equipment, namely to the screws (Figure

3.2 – 1) [56]. It is also possible to observe on Figure 3.2 – 2 that the same situation was noticed for Excipient D, which was classified as a cohesive material.

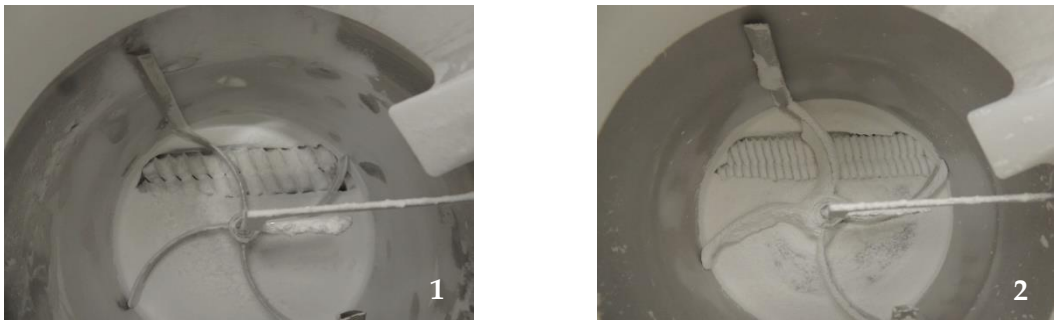

Figure 3.2 – Real images of the equipment hopper after feeder's runs. 1 – Image from Excipient G feeder's run; 2 – Image from Excipient D feeder's run.

There are also two other classifications to quantify the materials' flow properties, the HR and the CI (Table 1.6). Although, as both of them rank materials by the same classification, it was opted to use only one, the HR, to classify the materials regarding ρ_{bulk} and ρ_{tap}.

In opposition to the ffc classification, the lower is the HR value the higher is the material flowability. Hence, considering Table 3.4, it is possible to rank by the HR value the materials by increasing order: Excipients E, B, A, C, F, G and D.

Table 3.4 – Materials' HR classification.

Material	HR	Flow property
Excipient A	1.10	Excellent
Excipient B	1.05	Excellent
Excipient C	1.11	Excellent
Excipient D	1.65	Very very poor
Excipient E	1.04	Excellent
Excipient F	1.13	Good
Excipient G	1.53	Very poor

It is really interesting to compare both flowability studies and conclude about both the analysis differences and similarities (Table 3.5).

Something interesting to notice is that the material with the best flowability based on the HR classification is not the same as by the ffc classification. However, the best four materials classified with excellent flow properties coincide with the four materials with the highest ffc values. This reveals that materials can be grouped into two different groups, the ones with best flowing performance: Excipients A, E, C and B; and the ones with the worst flowing performance: Excipients F, G and D.

Table 3.5 – Comparative table of both materials' flowability indexes.

Material	HR	Flow property	ffc	Flow Type
Excipient A	1.10	Excellent	7.03	Easy-flowing
Excipient B	1.05	Excellent	10.51	Free-flowing
Excipient C	1.11	Excellent	9.75	Easy-flowing
Excipient D	1.65	Very very poor	2.90	Very cohesive
Excipient E	1.04	Excellent	8.89	Easy-flowing
Excipient F	1.13	Good	5.61	Easy-flowing
Excipient G	1.53	Very poor	4.19	Easy-flowing

Another aspect to be taken into consideration is that the difference between the HR number of Excipients B and E is not considerable and the same happens between Excipients A and C. In other words, it seems that the gravity force does not distinguish with accuracy materials with high flowability.

For further studies, if all the analysed materials have really different rheological properties, such as happens between Excipients F, G and D, the HR index would perform a reliable comparison. As so, it would be possible to avoid the usage of the Ring Shear Tester, measuring only the ρ_{bulk} and ρ_{tap} in order to calculate the HR which constitutes a much simpler process.

For the materials used in the present study, it is noticeable that the ffc confers a more sensible comparison of the differences between the powders flowability and for that reason ffc will be the comparison parameter for the following analysis.

3.1.1.1.3 Particle Size

As it was previously referred, another property that has a direct impact on the flowability is the particle size and for the comparative analysis, the particle size median (dv50) value is a fair parameter to be taken into consideration, as it represents the size of 50% of the material's particles.

The higher the particle size the better is the powder flowability and considering the intervals presented on Table 1.8 the materials were classified on Table 3.6. Generally, an increase on the particle size improves the powder flow due to an increment on the body forces that overcome the cohesion and friction forces [66].

Regarding Table 3.6, four of the materials are differentiated from the others by having big particle sizes, Excipients B, C, E and A, by decreasing order. The remaining materials have totally different ranges of particle sizes being all of them lower than 50 μm.

Table 3.6 – Particle size value of 50% of each material's particles (dv50).

Material	dv50 (µm)	Flow type
Excipient A	113.5	May flow freely
Excipient B	196.0	May flow freely
Excipient C	124.0	May flow freely
Excipient D	6.2	Flowing is a problem
Excipient E	121.9	May flow freely
Excipient F	43.1	Flowing is a problem
Excipient G	37.7	Flowing is a problem

As previously referred on Section 1.10, it is important to consider more rheological properties to define if the particle size offers more advantages or disadvantages for the respective material flow. Hence, the following section was created.

3.1.1.1.3.1 Flow Analysis based on Materials' Properties

In order to reach a conclusion about the materials' influence on the stability of the feeding process it is important to compare the different materials' properties previously analysed.

Regarding Table 3.7, it is curious to notice that the material with the best flowability has an irregular shape, however more need to be taken into consideration. In fact, Excipients A and B are both good choices among the others Avicels in terms of flowability for continuous processes and for direct compression, namely for tablet production [44]. Despite the fact that these two materials have similar moisture content, Excipient B was designed with improved flow and this was possible due to a larger average particle size (approximately 200 µm) comparing with Excipient A [59].

Table 3.7 – Comparison between the most relevant parameters to characterize the materials flowing performance.

Material	ffc	dv50 (µm)	Morphology
Excipient A	7.03	113.5	Irregular
Excipient B	10.51	196.0	Irregular
Excipient C	9.75	124.0	Spherical
Excipient D	2.90	6.2	Irregular
Excipient E	8.89	121.9	Irregular
Excipient F	5.61	43.1	Fibrous
Excipient G	4.19	37.7	Spherical

Another comparison to be made is between Excipients C and E. Now, their differences on flowability are more dependent on their morphological characteristics. As Excipient C is produced via SD its particles are spherical while Excipient E has irregular shaped particles. However, as Excipient E is produced in order to have an optimal flow [47], it occupies the third place on ffc ranking.

Excipient F is differentiated from the other materials by its particle morphology. Its elongated shape forces the particles to align, which increases their frictional behaviour [67]. Furthermore, Excipient F has a small particle size which also contributes for its diffusional issues (ffc = 5.6).

Other interesting material is Excipient G. Despite its spherical shape it is one of the worst materials in terms of flowability, due to the fact that its particle size is the second lowest. Furthermore, it is possible to observe on the SEM image of Excipient G (Figure 3.1 – (7)) that it has a rugose surface. This characteristic increases the number of contacts between different particles, which also increases adhesive forces [68].

Finally, as expected, the worst material is the lubricant, however Excipient D differentiates from the traditional Magnesium Stearates for having improvements on flowability, being recurrently used on continuous productions [46].

3.1.1.1.4 Cohesion

In many instances, the materials' cohesive nature is strictly related with flowability causing difficulties on the feeding process [57]. Through the Ring Shear Tester it is also possible to conclude about the cohesive forces between the particles, this parameter is named cohesion and is represented by Tau,c [69].

On Table 3.8 it is possible to observe that the materials with the highest cohesion are the ones with the worst flowability. All cases are in accordance with the previous ffc analysis, except for Excipient B. However, there is almost no difference between the Tau,c value of Excipients B and C, and, for this reason, not much relevance should be given to this specific situation.

Table 3.8 – Comparison between materials cohesion and flowability.

Material	Tau,c (Pa)	ffc
Excipient A	134.0	7.03
Excipient B	92.2	10.51
Excipient C	92.0	9.75
Excipient D	340.7	2.90
Excipient E	109.7	8.89
Excipient F	185.2	5.61
Excipient G	228.3	4.19

Another parameter that seems to affect the materials' flow is compressibility, because highly cohesive materials also showed high compressibility [32]. This property is also important to be analysed because it will be of high importance on further analysis (Section 3.2).

3.1.1.1.5 Compressibility

It is possible to create a comparative analysis between all the studied materials about the compressibility property resorting to the FF values obtained during each material's first run.

Each FF profile depends on the initial mass used to calibrate the feeder, due to the fact that the higher the weight above the screws, the higher is the amount of material that can fit in each screw revolution. However, this phenomenon only happens for materials with high compressibility and to better understand this concept the following graphic is presented (Figure 3.3).

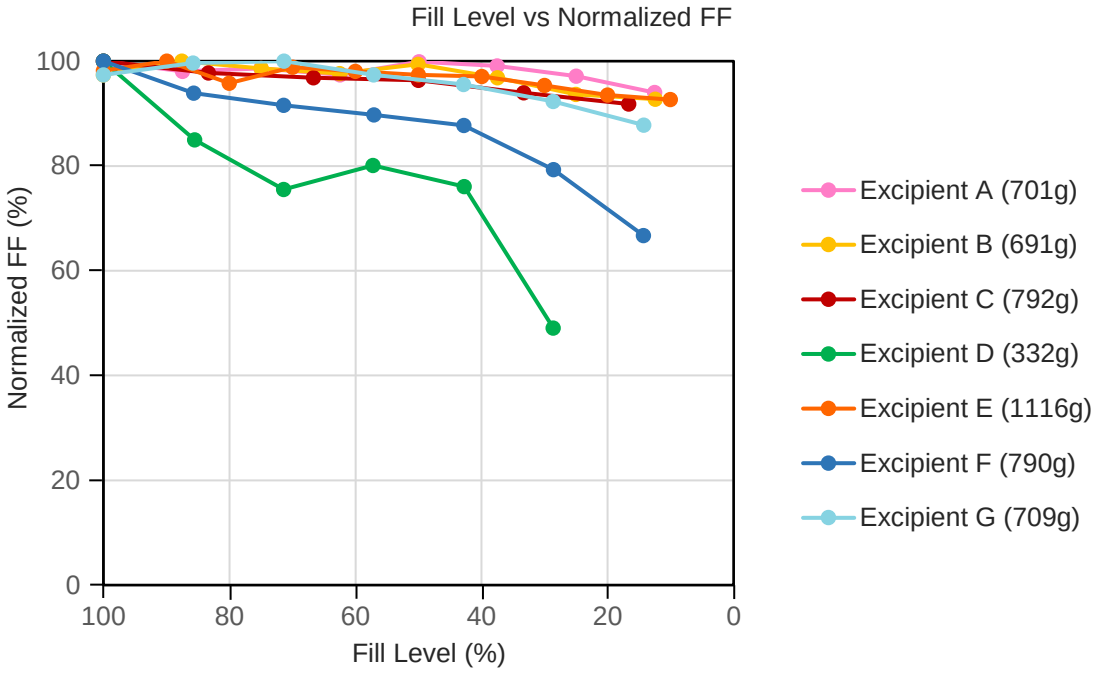

Figure 3.3 – Graphic of the normalized FF in function of the fill level.

By analysing Figure 3.3 it is possible to understand how dependent the FF value is from the fill level in a way that its decrease generates a decrease on the FF profile as well. However, there are some cases where the referred situation is more notorious than others. In fact, the materials that present on Figure 3.3 a more negative slope are the ones that have higher compressibility, because at the beginning of the run, when the feeder was totally filled, a higher amount of powder was capable to fit in each screw revolution.

In this way, as the feeder is emptied, the FF value logically decreases more abruptly because the weight of the material above the screw is no longer that significant.

It is noticeable that Excipient D is by far the most compressible material, then Excipient F is the material with the second highest compressibility, followed by Excipient G. The rest of the materials do not seem to be much affected by the upper material´s mass.

In order to give credibility to the previous conclusions, it is important to compare the initial mass used during the feeder's first run (when the FF profiles were recorded) of the compressible materials with the others.

From all the materials, Excipient D is the one with the lowest initial mass, this means that in a different scenario, with a higher amount of mass inside the feeder, it is expectable that its negative slope will be even more accentuated.

Despite the fact that Excipient F has approximately the same initial mass as the other materials, its slope is accentuated which gives no doubts about the compressibility of Excipient F. Finally, the same conclusion is applied for Excipient G regarding the fact that it also possesses almost the same amount of initial mass.

As a final remark, by comparing the compressibility results with the Section 3.1.1.1.4 conclusions, the three most compressible materials are the ones with the highest cohesion.

3.1.1.2 PCA

In order to validate the previous conclusions from Section 3.1.1.1, a PCA was done considering the raw material properties database (Appendix B) with the aim of identifying the similarities and differences between the tested materials.

3.1.1.2.1 PCA considering all Rheological Properties and Particle Size (PCA.M1)

Initially, by considering Table B.1, B.2 and B.3, a PCA with all the measured rheological properties and particle size parameters were done (Figure 3.4).

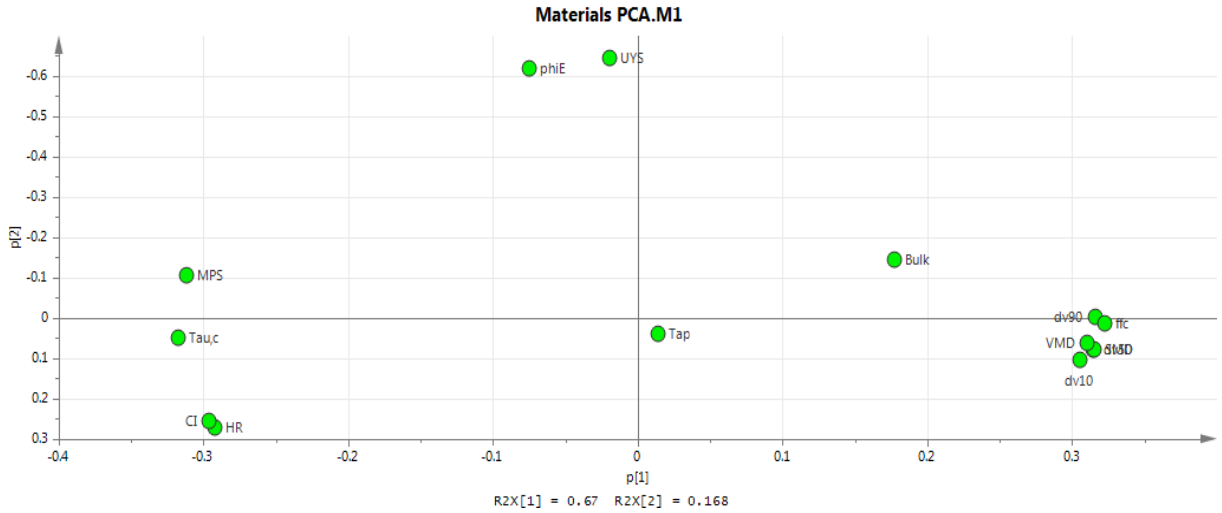

Figure 3.4 – Materials PCA.M1's loadings graphic considering the rheological properties, measured at 2000 Pa, and the particle size parameters.

It is important to refer that the PCA.M1 has a model fitting of R2X = 0.837 and a predictability of Q2 = 0.46 (Table 3.9) which, for the reasons described on Section 2.2.5.2.1, represents a good model.

Table 3.9 – Materials PCA.M1 model's information.

Model 1	R2X	R2X[1]	R2X[2]	Q2	Rank
Materials PCA	0.837	0.670	0.168	0.460	2

3.1.1.2.2 PCA considering only One Representative Materials' Property to characterize each Parameter (PCA.M2)

Secondly, it was observed that some of the materials' properties (X variables) present on PCA.M1 represent the same parameter. This means that some variables are dependent from others and for this reason, as indicated on Section 2.2.5.1, the model is misrepresented [29].

An example is the HR and the CI. Both variables are representative of the ρ_{bulk} and ρ_{tap}, as so, only one of these four should be used on the model. Taking this into consideration, the HR was the chosen one. The same situation is verified for the ffc that is calculated through MPS and UYS (Equation 1.5) and for that reason only ffc was considered on the model (Table B.3).

Regarding the variables that classify the materials' particle size, it was also necessary to select one representative parameter. After a lot of considerations, the dv50 was selected mostly due to the similarity of its values to the ones from literature and by its closeness to the SMD values (Table B.1).

Considering the new loadings graphic for PCA.M2 (Figure 3.5), it is possible to verify that the flowability and particle size are positively correlated, this means that the materials with high dv50 will have high flowability. Oppositely, Tau,c and HR are negatively correlated to flowability and of course positively correlated with each other. As so, materials with high cohesion and high HR will have bad flowability. Relatively to the bulk friction angle (phiE), it is situated 90 degrees from the others rheological properties, which means that it does not impact them directly.

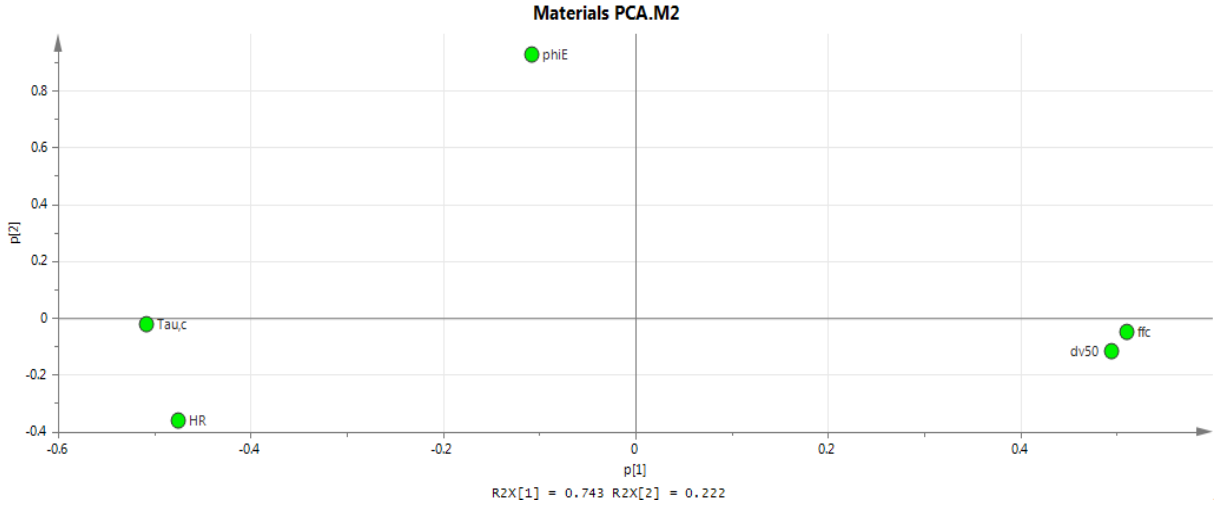

Figure 3.5 – Materials PCA.M2's loadings graphic considering only one representative materials' property to characterize each parameter.

On PCA.M2, it is detected an increase of the R2X and the Q2 values (Table 3.10) in comparison with the PCA.M1, that means that this second PCA model confers even more credibility and also validates the model that was previously done.

Table 3.10 – Materials PCA.M2 model's information.

Model 2	R2X	R2X[1]	R2X[2]	Q2	Rank
Materials PCA	0.965	0.743	0.222	0.748	2

As previously referred on Section 2.2.5, the scores and loadings graphics are complementary, because the positioning of the materials in scores graphic (Figure 3.6) is influenced by their materials' properties distribution on the loadings graphic (Figure 3.5).

Regarding Table 3.10, it is important to notice that this PCA model is constituted by two components (Rank) and that the first component (R2X[1]) has a higher impact on the model than the second one (R2X[2]). This means that on Figure 3.6 the materials that are more separated regarding the X axis (component [1]) are more differentiated in terms of rheological properties than the materials that are more distanced from the Y axis (component [2]).

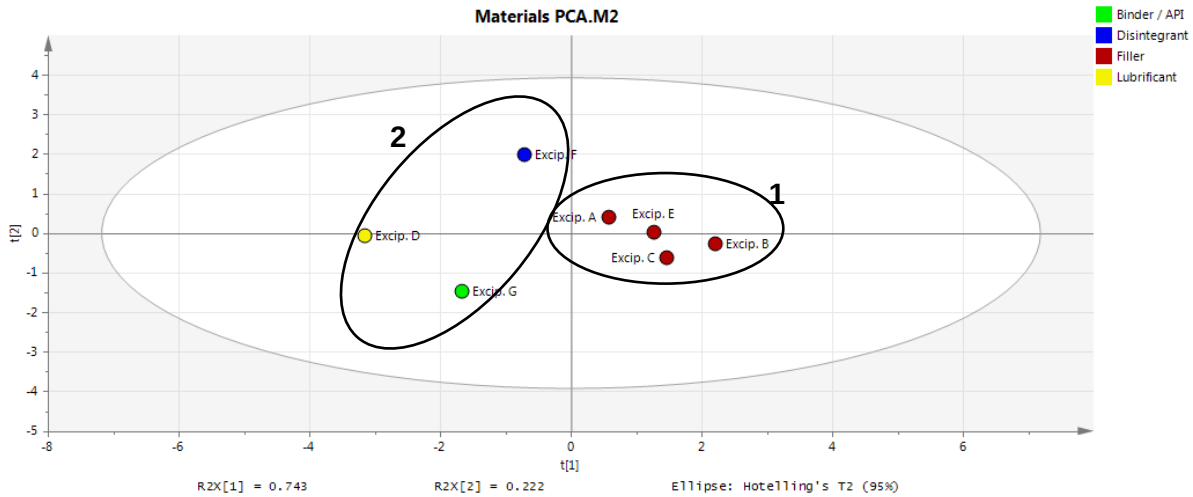

Figure 3.6 – Materials PCA.M2's scores graphic considering independent materials' properties. (1) – Group 1; (2) – Group 2.

Analysing the scores graphic, it is possible to notice that the materials used in a formulation for filling purpose (red-coloured) are positioned closer to each other than the rest of the materials. This is related with the fact that they have similar properties (Group 1) and since they are positioned on the right side of the graphic it means that they possess good flow properties. On the other hand, materials situated on the left side of the Y axis (Group 2) are more cohesive and are consequently the ones with worse flowability.

The reason why Excipients F and G are the materials that are placed on the extremities regarding the Y axis is due to their phiE values. Excipient F is the material with the highest phiE value and Excipient G is the material with the lowest, as it can be observed on Table 3.11.

The phiE is the rheology property that quantifies the angle (interaction) formed between the material's powder particles. The lower is the phiE, the better is the influence of the powder shape on flowability [70].

Table 3.11 – Resume table of all the materials phiEs.

Material	phiE (º)
Excipient A	40.8
Excipient B	38.2
Excipient C	36.3
Excipient D	41.4
Excipient E	38.8
Excipient F	48.0
Excipient G	34.1

The Hotelling's graphic (Figure 3.7) represents the information that is considered by the PCA model and, as the R2X is 0.965, the model covers approximately 97% of the data.

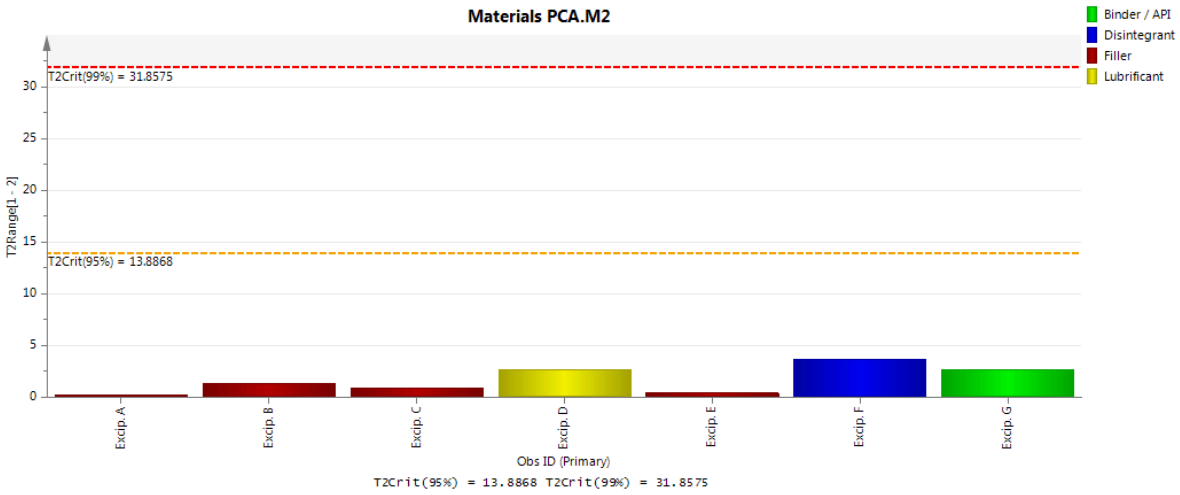

Figure 3.7 – Materials PCA.M2's Hotelling´s T2Range graphic considering independent materials' properties.

Regarding Figure 3.7, the bigger the T2Range value is the more different is a material from the others, in terms of materials' properties. As so, to complement the Hotelling's T2Range graphic, the T2Ranges values were specified on Table 3.12.

Considering all the materials, Excipient F is the one that stands out the most, followed by Excipient D and then by Excipient G.

Table 3.12 – T2Range values from Materials PCA.M2 model.

Material	T2Range
Excipient A	0.24
Excipient B	1.38
Excipient C	0.92
Excipient D	2.69
Excipient E	0.44
Excipient F	3.67
Excipient G	2.66

Oppositely, the DModx graphic (Figure 3.8) informs about the missed information, also known as residues, and for this model it represents approximately 3% (100% - 97%) of the data.

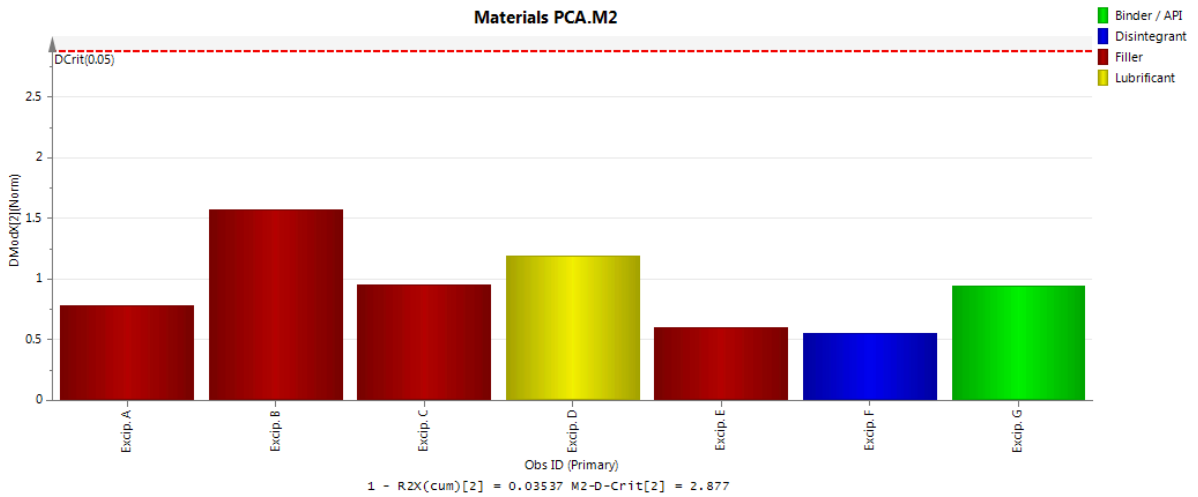

Figure 3.8 – Materials PCA.M2's DModx graphic considering independent materials' properties.

Considering Table 3.13, it is possible to notice that Excipient B is the material with less information captured by the PCA model. Fortunately, as displayed on Figure 3.8, its value is lower than the DCrit (0.05) which means that the model is reliable.

Table 3.13 – Materials PCA.M2's DModx values considering independent materials' properties.

Material	DModX
Excipient A	0.79
Excipient B	1.58
Excipient C	0.96
Excipient D	1.19
Excipient E	0.60
Excipient F	0.56
Excipient G	0.94

The analysis of the DModX graphic makes it possible to conclude that there are no outliers on the PCA.M2 model.

3.1.2 Feeder's Components

To better understand how all the feeder's components represented on Table 3.1 were selected, a more detailed analysis was performed.

3.1.2.1 Gearbox and Screw

In Table 3.14 the calculated setpoints (mass flow rates) and volume flow rates for the minimum and the maximum percentages that each material is normally added to the formulation are presented.

Table 3.14 – Theoretical values obtained from the initial calculations.

	Feeder's Limits						
	MIN (1 kg/h)			ρ_{bulk} (kg/L)	**MAX (25 kg/h)**		
Parameters / **Materials**	**% formula-tion**	**Setpoint (g/s)**	**Volume Flow Rate (L/h)**		**% formula-tion**	**Setpoint (g/s)**	**Volume Flow Rate (L/h)**
Excipient A	20%	5.6×10^{-2}	0.59	0.34	90%	6.250	66.18
Excipient B	20%	5.6×10^{-2}	0.57	0.35	90%	6.250	64.29
Excipient C	10%	2.8×10^{-2}	0.17	0.58	60%	4.167	25.86
Excipient D	0.25%	6.9×10^{-4}	0.01	0.24	1.5%	0.104	1.56
Excipient E	25%	6.9×10^{-2}	0.56	0.45	50%	3.472	27.78
Excipient F	1%	3.0×10^{-3}	0.02	0.47	5%	0.347	2.66
Excipient G	5%	1.4×10^{-2}	0.14	0.36	60%	4.167	41.67

It is interesting to notice that all the maximum setpoints defined by the calculations were able to be run on the feeder at stable conditions. On the other hand, the same was not possible to achieve for the minimum setpoints, in fact, in some cases, the final obtained setpoint was much higher than the value defined during calculations. That is the case of Excipients D and F (compare Table 3.1 and Table 3.14 setpoints). These results clearly show that the major adversity against the feeder's stability will be on productions that require low throughputs.

After the volume flow rate calculation (Equation 2.3) it is possible to define the gearbox and the screw for each feeder's run by resorting to a table provided by the supplier (Figure 3.9).

# used in HMI recipe	Gearbox type	screw	Max [L/h]	Min [L/h]
1	Gearbox 63	Screw P=D	113.6	7.1
		Screw P=D/2	56.7	3.5
2	Gearbox 235	Screw P=D	30.4	1.9
		Screw P=D/2	15.2	0.9
3	Gearbox 455	Screw P=D	15.7	1.0
		Screw P=D/2	7.8	0.5
	(@100rpm)	Screw P=D/2	-	0.10

Figure 3.9 – Table provided by GEA to help on gearbox and screw type selection [33]. P=D=20 mm/rev=20C; P=D/2=10 mm/rev=10C.

The following tables (Table 3.15 and 3.16) contain the feeder's components selected by following the methodology explained on Section 2.2.2.1.

Table 3.15 – Feeder's components selected based on the methodology applied considering the minimum limit.

Material	MIN Volume Flow Rate (L/h)	Gearbox	Screw (mm/rev)
Excipient A	0.59	455:1	10
Excipient B	0.57	455:1	10
Excipient C	0.17	455:1	10
Excipient D	0.01	455:1	10
Excipient E	0.56	455:1	10
Excipient F	0.02	455:1	10
Excipient G	0.14	455:1	10

Table 3.16 – Feeder's components selected based on the methodology applied considering the maximum limit.

Material	MAX Volume Flow Rate (L/h)	Gearbox	Screw (mm/rev)
Excipient A	66.18	63:1	20
Excipient B	64.29	63:1	20
Excipient C	25.86	63:1	20
Excipient D	1.56	235:1	10
Excipient E	27.78	63:1	20
Excipient F	2.66	235:1	20
Excipient G	41.67	63:1	20

In cases where the minimum volume flow rate was lower than 0.5 L/h the gearbox 455:1 and 10C screw were set (Table 3.15). In fact, it is indicated on Figure 3.9 table lower level "@100rpm" and

this means that the feeder will be working on conditions that are not possible to be guaranteed stability by the supplier for volume flow rates lower than 0.5 L/h.

It is important to refer that there were some exceptions where, by considering the materials' rheological properties, the final gearbox and screw selected were different.

One of them is the run to define the maximum setpoint of Excipient D. Considering its volume flow rate value, the gearbox 235:1 and 10C screw (Table 3.16) could have been used. However, the maximum setpoint calculated (Table 3.14) were truly low and to guarantee a precise control of the feeding process it was selected, by prevention, the gearbox 455:1 and the 10C screw.

To the second exception, Excipient F, the gearbox 235:1 and the 20C screw could have been set on the feeder (Table 3.16), however a similar situation occurs relatively to its maximum setpoint and, for that reason, it was selected to set on the feeder the gearbox 455:1 and the 10C screw as well.

It would be interesting for further studies to try these two materials maximum setpoints with the set up indicated on Table 3.16, because no adversities were found in order to achieve a stable setpoint (RSD < 4%) with the gearbox 455:1 and the 10C screw, which makes it possible that these same conditions can be also achieved with the components suggested by the calculations.

3.1.2.2 Topup

The topups were selected for all the materials by following the procedure described on the Section 2.2.2.2. To demonstrate its applicability, two opposite scenarios will be analysed in detail.

In order to select the most appropriate topup, the first thing to be identified is the amount of mass that still remains inside the feeder when the FF graphic starts to drop significantly and the speed graphic (screw speed) starts increasing. The amount of mass that is present at the turning point (minimum mass) is the key for the reasoning applied on the following examples.

The first example is a case in which the calculated volume is inferior to 0.4L, making the 1.6L topup the selected one to be assembled on the feeder (Example 1). For the Example 2, two cases in which the calculated volume is superior to 0.4L are presented, leading to the decision of choosing a different topup.

Example 1:

As it is possible to identify on Figure 3.10, the turning point of Excipient C is approximately 99g.

Afterwards, that minimum mass value must be converted into the corresponding units (kg) and divided by the ρ_{bulk} (Equation 2.4). Now, it is possible to compare the volumes and decide, based on the minimum refill volume, what the appropriate topup for Excipient C is.

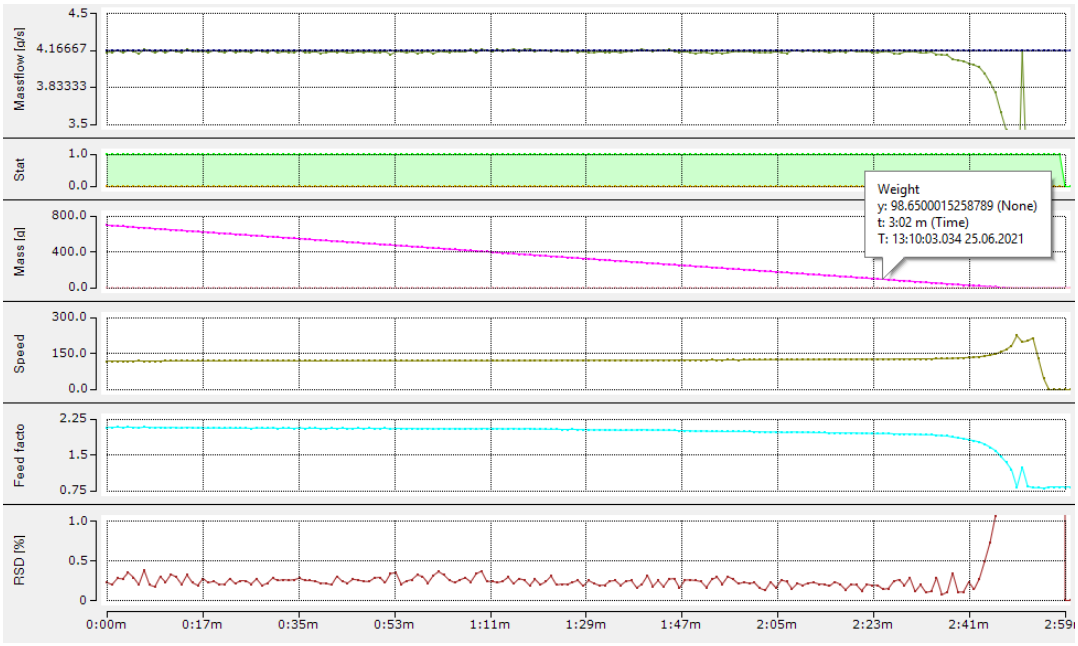

Figure 3.10 – First run of Excipient C recorded on TwinCAT ScopeView.

As observed on Equation 3.1 the minimum refill volume is 0.17L and as it is lower than 0.4L the topup with the highest volume can be utilized (1.6L).

Notice that for the majority of the materials, the minimum refill volume was lower than 0.4L and for that reason the topup of 1.6L was the one that was used the most.

$$99\ g \longrightarrow 0.099\ kg$$

$$Min\ Refill\ Volume = \frac{0.099\ kg}{0.58\ kg/L} = 0.17\ L < 0.4\ L \tag{3.1}$$

Example 2:

On this example two materials will be analysed. As the process to identify the minimum mass was already demonstrated on Example 1, that explanation was not repeated on the second example.

Regarding Equation 3.2 and 3.3 it is possible to verify that both materials have minimum refill volumes higher than 0.4L.

Excipient F

$$Min\ Refill\ Volume = \frac{0.204\ kg}{0.47\ kg/L} = 0.43\ L\ >\ 0.4\ L \tag{3.2}$$

Excipient D

$$Min\ Refill\ Volume = \frac{0.175\ kg}{0.24\ kg/L} = 0.73\ L >\ 0.4\ L \tag{3.3}$$

Considering the calculations of Excipient F, the 1.2L topup should have been used. However, by the time that this decision was made, the information about the rheological properties of Excipient F were not available. In fact, as the minimum refill volume was not that different from 0.4L it was considered that setting on the feeder the 1.6L topup would not constitute a problem.

As was previously explained on Section 3.1.1.1.5, Excipient F is a material with high compressibility and that characteristic might have interfered during the process of defining the minimum stable setpoint. It is important to refer that an improvement on both Excipient F feeder's runs stability might have been obtained if the topup of 1.2L was used. As so, it is advised for future works to repeat the process with the 1.2L topup and verify if it is possible to find a lower minimum setpoint at stable conditions.

About Excipient D, it is possible to verify on Equation 3.3 that the minimum refill volume of Excipient D is also higher than 0.4L. However, instead of choosing the 1.2L topup, as it is indicated by the calculations since the minimum refill volume is lower than 0.8L (1.2L + 0.8L = 2L), it was opted to follow the supplier instructions. During the virtual training, the supplier had informed that for any magnesium stearate it is highly recommended to use the 0.8L Topup.

3.1.2.3 Mesh

It was previously explained on Section 2.2.2.4 the complete process of decision for the usage or not of the mesh during the feeder's runs.

In fact, only two materials (Excipients F and E), both at the minimum setpoint, required the usage of a mesh. The reasons why this feeder's component was essential for both feeder's runs improvement are followed.

During the process of finding the Excipient F minimum setpoint, it was verified that the RSD average value of the run, without the usage of a mesh, was 3.59%. In fact, running the feeder without a mesh would not constitute a problem because that value is lower than 4%, although by setting the mesh on the feeder resulted on a considerable decrease of the RSD value, approximately 0.5% decrease, which without any doubt is a good improvement of the stability of the process.

That improvement on the process stability was even more notorious for the minimum setpoint of Excipient E where the usage of a mesh made it possible to lower the RSD from 4.34%, without a mesh, to 3.76%, with a D2 mesh. In other words, by using the D2 mesh, the feeding of Excipient E at a setpoint of 0.14 g/s passed from an instable process to a stable one.

Other aspect that was observed during the laboratorial experiments was that for all the materials that the D1 mesh was tested, its usage was not useful to improve the feeding performance. Moreover, there were only a few cases where it was possible to feed with the D1 mesh. In most cases, this mesh blocked the feeding process and, in response to that, the alarms: "Feeder Alarm" and "Feeding Current error" were activated which caused the feeder stoppage.

It is considered that the feeder's blockage might be related with two main reasons: the properties of the materials and high massflows. In what concerns the first cause, materials with high cohesion have a higher tendency to form aggregates, which induces the mesh's holes saturation. On the other hand, high massflows force the material to be fed at high velocity and that speed generates an increase of the pressure that is applied on the mesh, which can also "block" the mesh's holes.

3.1.3 Feeder's Parameters

It is truly important to understand how the feeder's parameters variate during the feeder's runs. The best way to understand its behaviour is by analysing the data registered by the feeder recording program (Figure 3.11).

Regarding Figure 3.11, it is noticeable that, over time, the mass inside the feeder (graphic 3) starts decreasing because, as expected, the equipment is feeding the material. At the same time, the FF (graphic 5) is decreasing as well, since the amount of material inside the feeder is getting low. In opposition, the speed (graphic 4) is getting higher in an effort to keep the massflow as close as possible to the setpoint (the black line on graphic 1).

It is notorious that a turning point exists (yellow line) where both plots, speed and FF, intensify their increasing and decreasing, respectively. That line marks the point where it is important to do the refill, in order to avoid the continuous production getting out of control, as occurs at the end of Figure 3.11.

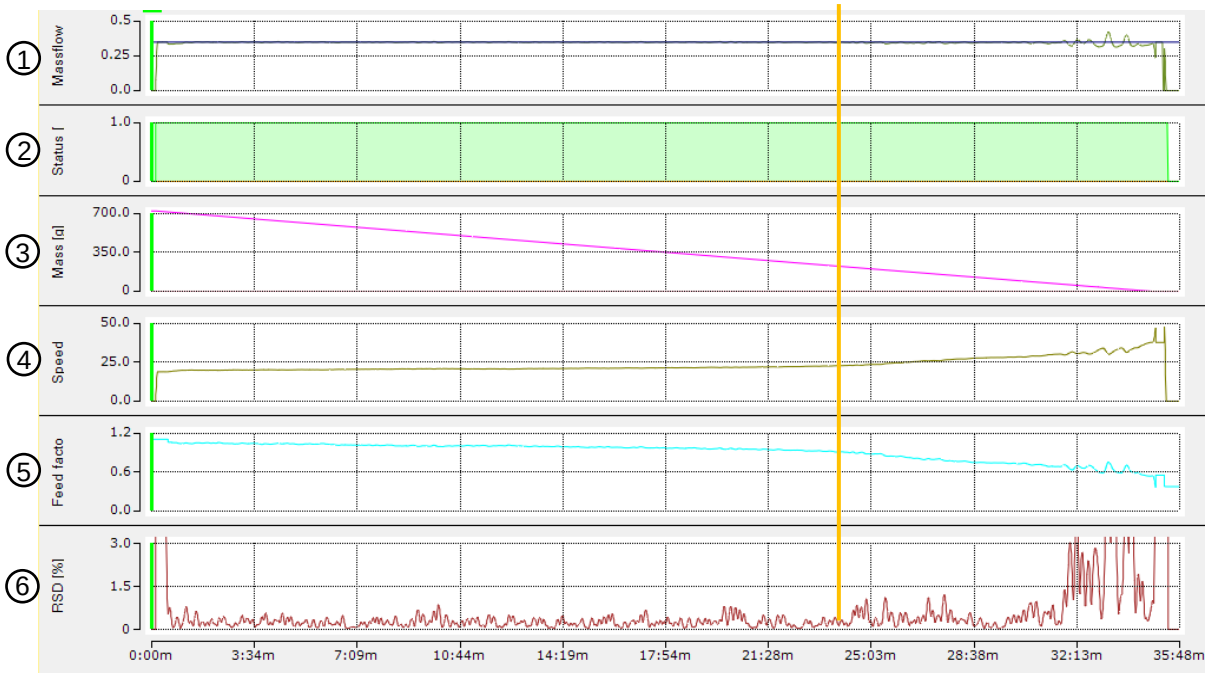

Figure 3.11 – First Run of Excipient F at a Setpoint of 0.347g/s. Graphic 1 – Massflow & Setpoint (g/s) vs time; Graphic 2 – Status [0-1] vs time; Graphic 3 – Mass (g) vs time; Graphic 4 – Speed (g/s) vs time; Graphic 5 – FF(g/rev) vs time; Graphic 6 – RSD [%] vs time.

To verify the previous occurrences, a PCA model (Figure 3.12) was created in order to better understand how the feeder's parameters are related.

Regarding Figure 3.12, the FF (Feed Facto) and Weight variables are directly proportional to each other as they are closely positioned. On the other hand, the screw velocity (ScrewVeloc) is symmetrically placed to them, which means that a decrease on the parameters situated on the left side of the graphic will generate an increase of the screw velocity. The same conclusion was previously described, since the screw velocity in the PCA model corresponds to the speed (graphic 4) on Figure 3.11.

Both the MassFlow and the RSD variables do not have a big impact on the model due to the fact that they are positioned approximately 90º relatively to the remaining feeder's parameters. It is also interesting to highlight that the reason why they do not interfere is because they represent oscillations of the feeding process. RSD as the relative standard deviation of the massflow is obviously dependent from it, although their correlation is not that strong due to the fact that an increase on the RSD can be generated by an increase or a decrease of the massflow relatively to the setpoint. In other words, it is not just an increase of the massflow that increases the RSD.

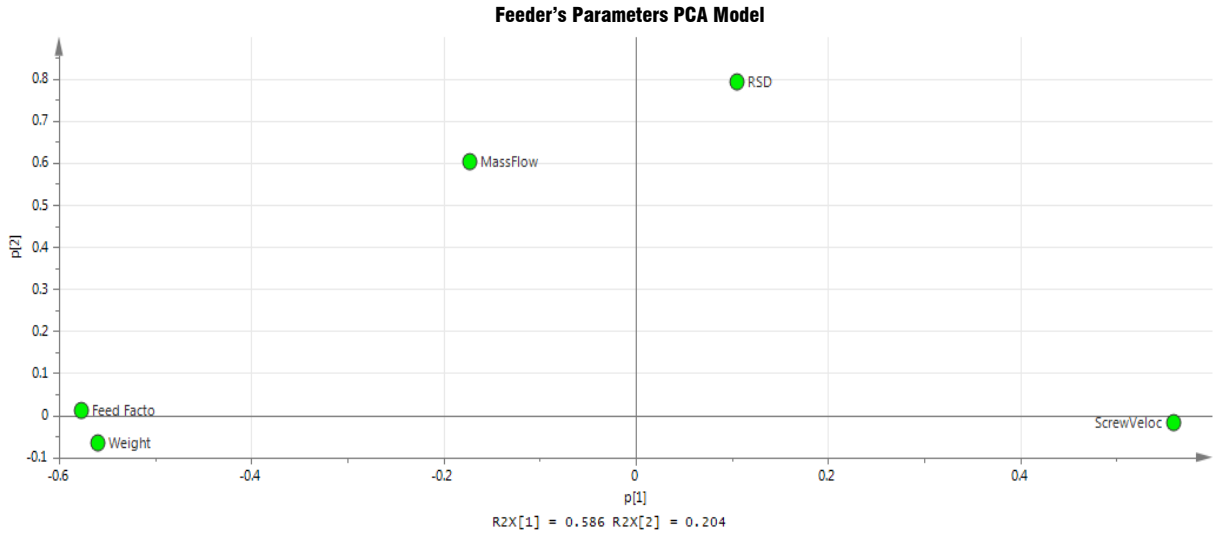

Figure 3.12 – Loadings graphic of the feeder's parameters PCA model.

3.2 Section 2: Feed Factor

FF is a parameter that has a great importance on the feeding process, as previously mentioned on Section 1.8.1. For this reason, it is interesting to know which variables impact the most the FF value.

It is important to refer that, from now on, the FF value considered for each material is actually an average of all the FF values recorded from each feeder's run and not from the first run. In other words, the considered FF values used to do the average are the ones that were used during the feeder's runs, guided by the FF profile obtained from the first runs.

3.2.1 Most Important Variables that affect Feed Factor

In order to understand which variables have an influence on the FF profile, a PLS model was developed with all the materials' properties, the feeder's components and the feeder's parameters. After a screening, the most significant parameters are presented on the final FF PLS model. It is important to refer once more that, as indicated on Section 2.2.5.1, for the final model only one variable was used to represent each parameter.

The final FF PLS model is represented by the variables that have a higher impact on the FF value (Figure 3.13).

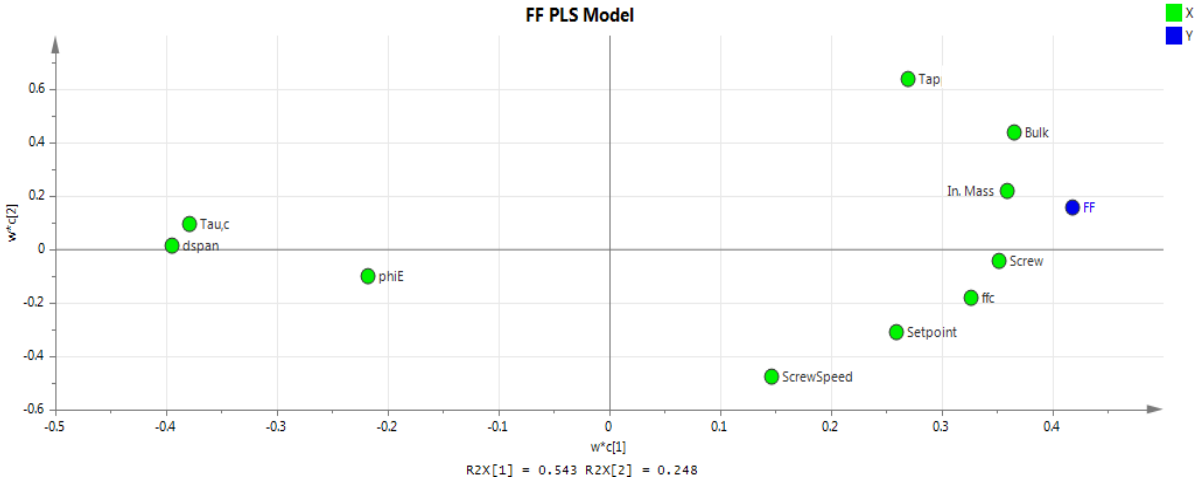

Figure 3.13 – Loadings graphic of the FF PLS model.

After analysing the FF PLS model, it is possible to notice that the FF depends directly on the initial mass (In. Mass), density (Bulk and Tap), Screw, ffc and Setpoint because they are the parameters that are more closely positioned to the FF. The ScrewSpeed does not have an impact on the model due to the fact that it does approximately 90º with the FF, considering the origin. The parameters located on the left side of the plot are inversely proportional to the FF.

It is important to refer that the FF PLS model (Table 3.17) is a really good model due to having really high values of R2Y and Q2. Also, the RMSEE and RMSEcv are similar values and lastly the R2 presented on Figure 3.14 is extremely high, this means that the model has a good fitting to all the materials considered for this analysis. In conclusion, it is more than fair to consider that the FF PLS model is a robust model and that it is not affected by overfitting.

Table 3.17 – FF PLS model's information.

Model	R2Y	Q2	RMSEE	RMSEcv	Rank
FF PLS	0.983	0.945	0.092	0.138	2

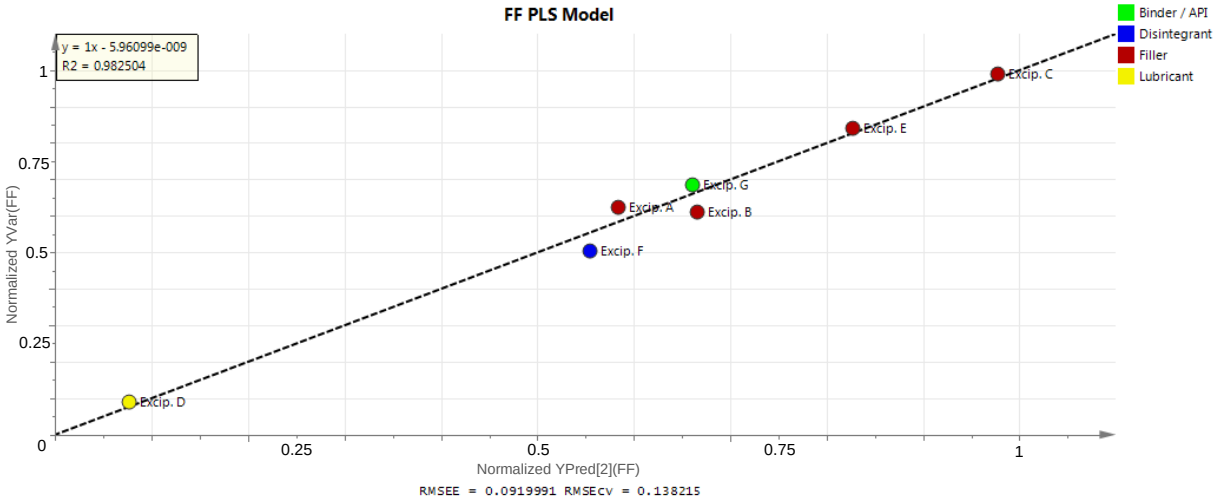

Figure 3.14 – Observed vs predicted normalized graphic of FF PLS model.

For a more detailed study, the coefficients graphic was considered, Figure 3.15. There are two main groups of variables. The ones with a positive impact (Group 1) and the ones with a negative impact (Group 2).

It is important to refer that the variables that cause a negative impact are actually inversely proportional to the FF, this means that their increase generates a decrease of the FF. Moreover, it is noticeable that there are two parameters that do not seem to have a strong impact on the FF, being these the screw speed and the setpoint. Nevertheless, a more detailed analysis will be performed on Section 3.2.2 about how the setpoint affect the FF values obtained from the experimental runs.

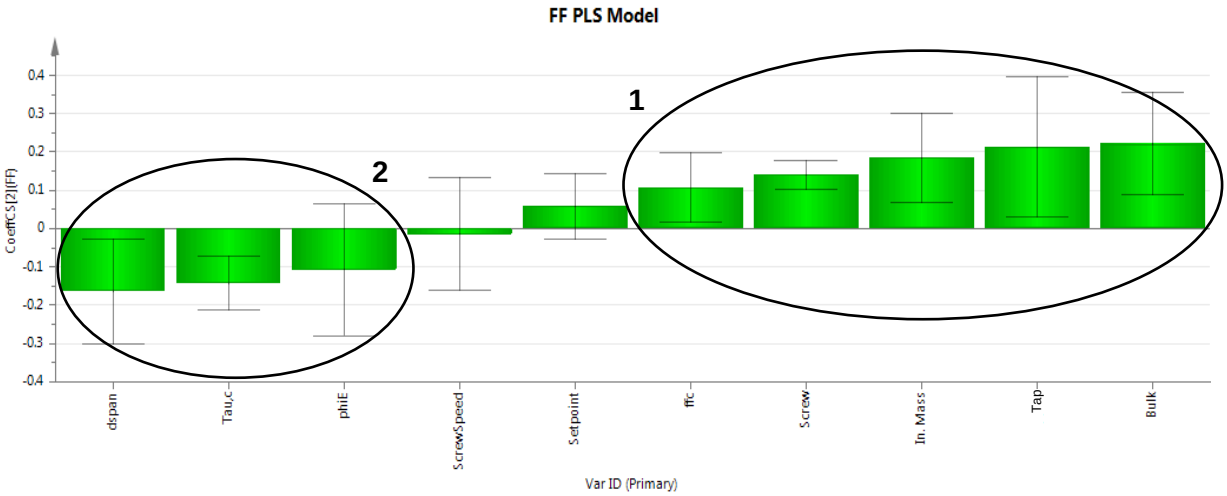

Figure 3.15 – Coefficients graphic of FF PLS model. Group 1 – Variables with a positive impact on FF; Group 2 – Variables with a negative impact on FF.

Regarding Figure 3.15, in Group 1, it is evident that the materials' density has a big impact on the FF due to the fact that a higher density enables that a higher amount of mass can be fitted per screw revolution. The initial mass of the material presented on the feeder´s hopper before the run starts also plays an important role on the FF value, mostly for compressible materials.

The influence of the screw can be explained by the fact that screws with a higher volume will be able to transport a higher volume of material per revolution, thus resulting on a higher FF value.

It is interesting to notice that the referred impact that the materials' density, screw and initial mass have on the FF was also verified on literature [32].

Finally, as expected, the materials' ffc is also a parameter to be taken into consideration since it depends on the phiE and the particle size, being the last one represented on the model as dspan. For this reason, only the ffc parameter will be considered for further analysis. The relation between those three variants is: the higher the particle size (the lower the dspan) and the lower the phiE is, the higher is the ffc.

The only parameter that was not analysed yet on Group 2 is cohesion (Tau,c) and, as predicted, it has a negative impact on the FF. That is mostly due to the fact that materials with a high cohesiveness also showed a high compressibility (Section 3.1.1.1.5) and compressibility has a strong negative impact on the FF average values because these are truly dependent on the amount of material that is inside the hopper on top of the screw.

3.2.2 Validation of Feed Factor PLS Model

Now it is important to verify if the previous conclusions made during the model analysis are in accordance with the FF values obtained from the feeder's runs. For that effect a table with all the main parameters was created, Table 3.18.

Table 3.18 – Resume table with all the parameters that mostly impact the FF.

Material	FF_MAX (g/rev)	ρ_{bulk} (kg/L)	Initial Mass (g)	ffc	Screw (mm/rev)
Excipient A	1.25	0.34	701	7.03	20
Excipient B	1.22	0.35	691	10.51	20
Excipient C	1.98	0.58	792	9.75	20
Excipient D	0.18	0.24	332	2.90	10
Excipient E	1.68	0.45	1116	8.89	20
Excipient F	1.01	0.47	790	5.61	10
Excipient G	1.37	0.36	709	4.19	20

Regarding Table 3.18, there are two materials that can be set apart from the others for having the highest values of FF: Excipients C and E. Despite the fact that Excipient E has the highest initial mass, the ρ_{bulk} of Excipient C is much higher. Furthermore, as indicated on Section 3.1.1.1.5 these

two materials are not affected by compressibility and this is the reason why the ρ_{bulk} impacts more the FF value than the initial mass. It is also important to refer that despite both materials having a really good flowability, the ffc of Excipient C is proven again to be superior.

It is curious to notice that despite Excipient B having the highest ffc, its FF is not that high and that is because, comparatively to the previous two referred materials, it possesses a lower ρ_{bulk}.

In fact, Excipients A, B and G have approximate values of ρ_{bulk}, initial mass and the run was also performed with the same screw type, so there must be a reason for the superiority of the FF of Excipient G. That reason might be related with its particle morphology. However this parameter is not possible to be quantified and introduced on the model (as complement of the following information Section 3.1.1.1.1 should be consulted). Actually, Excipient C, the material with the highest FF, and Excipient G are produced via spray drying, making the particles spherically shaped. It is possible that the spherical morphology helps during the screws filling and comparing with Excipients A and B irregular shapes it might be an obstacle for the particles' arrangement inside each screw revolution.

Until this point, for all the described materials, the screw type of 20C was the selected for the feeder's runs and for that reason it was not a decisive parameter. From now on, the materials that required the 10C screw will be analysed. The difference between the FF values of the two materials that used the 10C screw from the other materials' FF is stunning.

Excipient D is by far the material with the lowest FF because it possesses the lowest ρ_{bulk} and ffc, as well as the lowest initial mass. The last parameter referred is even more emphasized by the fact that, even though it was the case that had the less initial mass, it still was the material that suffered the most with compressibility (Section 3.1.1.1.5).

Excipient F is the material with the second highest ρ_{bulk}, as so, it was expected that its FF value would be higher, although, as previously referred, the screw with the lowest volume was used and that is the reason why a less amount of mass is transported per each revolution in comparison with the other materials. This relation can also be visualized by comparing the values of FF MAX with the FF MIN, presented on Table 3.19, where the feeder's runs that utilized the 10C screw have a lower value of FF, since smaller screws transports lower material's mass per revolution.

Table 3.19 – FF MIN is the FF value that corresponds to each material's minimum setpoint at stable conditions. FF MAX is the FF value that corresponds to each material's maximum setpoint at stable conditions.

Material	FF MIN (g/rev)	Screw (mm/rev)	Setpoint MIN (g/s)	FF MAX (g/rev)	Screw (mm/rev)	Setpoint MAX (g/s)
Excipient A	0.36	10	0.056	1.25	20	6.250
Excipient B	0.28	10	0.080	1.22	20	6.250
Excipient C	0.49	10	0.120	1.98	20	4.167
Excipient D	0.14	10	0.017	0.18	10	0.104
Excipient E	1.47	10	0.140	1.68	20	3.472
Excipient F	0.90	10	0.050	1.01	10	0.347
Excipient G	0.14	10	0.020	1.37	20	4.167

Even though the difference between both screws' volumes is roughly half (20C=4.6128 cm^3/rev; 10C= 2.3022 cm^3/rev), their FF values do not follow that behaviour. In fact, considering the materials that changed from the 20C to the 10C screw to run the feeder at the minimum setpoint, their FF MIN is much lower than half the of the FF MAX. However, the referred occurrence is not verified for Excipient E and for that reason it is recommended for further studies to repeat its run with the same conditions in order to notice if the obtained FF MIN is still similar.

Something that is also interesting to refer is that Excipients D and F use the 10C screw for both minimum and maximum setpoints and yet their FF MAX is also higher than their FF MIN. As so, there must be something more affecting the FF values and that might be related with the setpoint, due to the fact that for both runs of the same material the same feeder's components were set, as so the only variant was the setpoint. Even though the setpoint's variant has a low impact on FF PLS coefficients graphic (Figure 3.15), it still as some interference on it.

It is interesting to report that based on the results a relation like: the higher the setpoint the higher the FF value, is verified. Moreover, it was informed by the feeder's supplier that in fact the FF is not totally independent from the throughput, because it was previously identified by the company that the FF values changes with different setpoint values. Additionally, the supplier had also referred that "the faster the run the better the screws have to be filled", it seems to exist a compaction of the powders inside the screws that rotate with higher velocity. However, it is important to point out that it is necessary to carry out more tests and include a greater diversity of materials to have a clearer conclusion about this topic.

In conclusion, regarding the previous analysis, in terms of the materials' properties, a material with good flowability, which includes high particle size and low phiE, low cohesion and high density will ensure an optimal screw filling. In terms of the feeder's components, the most relevant parameters for a higher FF are the screw type and also the amount of mass (initial mass) that is introduced on the feeder per refill.

3.2.3 Feed Factor Prediction

FF is a parameter that is essential to guarantee the process stability as explained on Section 1.8.

As previously referred, by analysing the FF PLS Model (Section 3.2.1), the two factors that affect the most the FF are the screw type and the materials' properties. The initial mass also has an impact, but the amount of mass that can be dropped inside the hopper without impacting the FF, owing to materials compressibility, was also considered on the data utilized to create the models. Due to the fact that for all the materials a first run was performed before the feeder's run, and owed to that initial run, the appropriate topup was able to be chosen. This means that for every single new scenario that aims to avoid the first run, the appropriate topup must be predicted after predicting the $FF_{predicted}$ (this process will be explained on Section 3.2.4.2).

Taking all of this into consideration, for a new material or a new process condition, such as new percentages for the materials in the formulation or an alteration of the total production massflow, a $FF_{predicted}$ can be achieved.

Resorting to SIMCA Program two PLS models were created. It was decided that to better predict the FF it is important to develop a model for both types of screws. One considering all the FF values from the runs performed with a screw of 20 mm/rev (FF 20C Model) and the other taking into account the FF values obtained on runs that the 10 mm/rev screw was set (FF 10C Model).

Table 3.20 – FF 20C and FF 10C models' information.

PLS Model	R2Y	Q2	RMSEE	RMSEcv	Rank
FF 20C	0.966	0.941	0.069	0.070	1
FF 10C	0.944	0.914	0.140	0.112	2

First and foremost, it is critical to note that the FF 20C PLS model and FF 10C PLS model are excellent models due to their high values of R2Y and Q2 (Table 3.20). Furthermore, for both models, the RMSEE and RMSEcv values are really similar and, beyond that, both have high R2 values, as represented on Figure 3.16 and 3.17. In conclusion, it is safe to consider that both models are not affected by overfitting and that their predictions can be trusted.

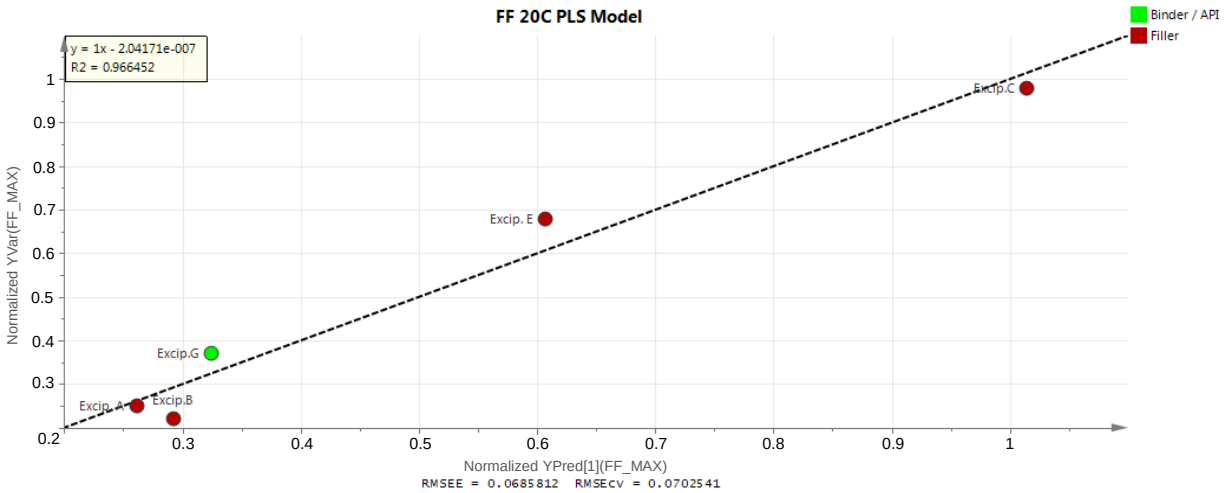

Figure 3.16 – Observed vs predicted normalized graphic for FF 20C PLS model.

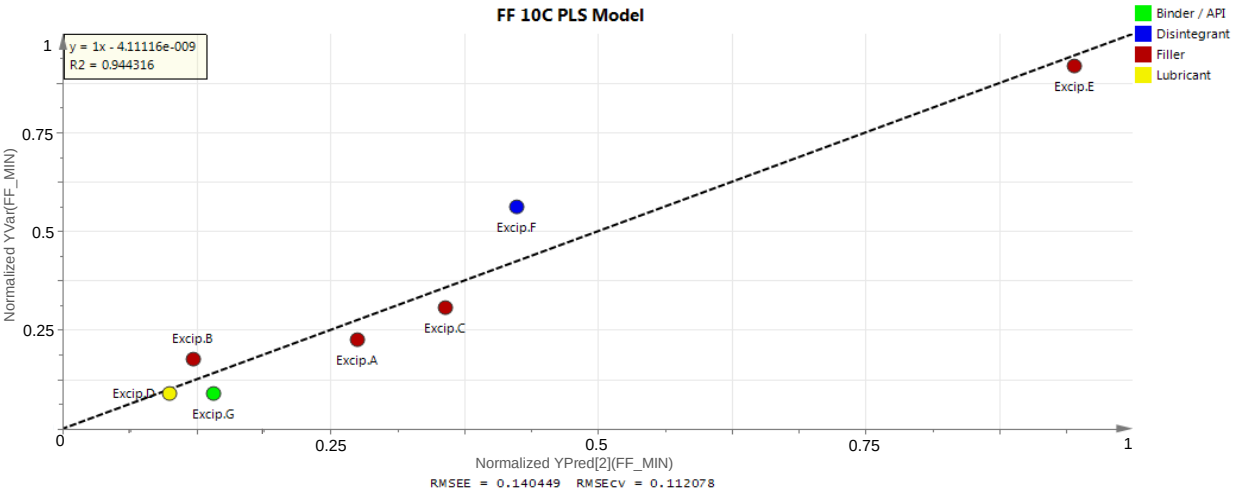

Figure 3.17 – Observed vs predicted normalized graphic for FF 10C PLS model.

On Table 3.21 it is possible to identify both the final models' significant variables. For the model that predicts the FF for the feeder's runs that use the 20C screw there is only one main variable, the ρ_{bulk}. For cases where the 10C screw might be set on the feeder there are two significant variables, dv10 and ffc, which must be considered.

Table 3.21 – FF 20C PLS model and FF 10C PLS model significant variables.

PLS Model	Significant Variables	
FF 20C	Bulk	
FF 10C	dv10	ffc

Both coefficient's plots (Figure 3.18) are also interesting to analyse because they show which of the previously referred significant variables have a higher impact on the model, in other words, which variables are highly correlated with the FF (the Y of both the PLS models). Also, through the

coefficient's plot it is possible to conclude about which of the significant variables are positive or negative correlated with the FF. Thus, it can be concluded that the bulk and ffc are positive correlated and that dv10 is negatively correlated to the FF on their respective models.

Something also interesting to refer is that for both predictive models, all the significant variables considered are also present as significant on FF PLS model on Section 3.2.1.

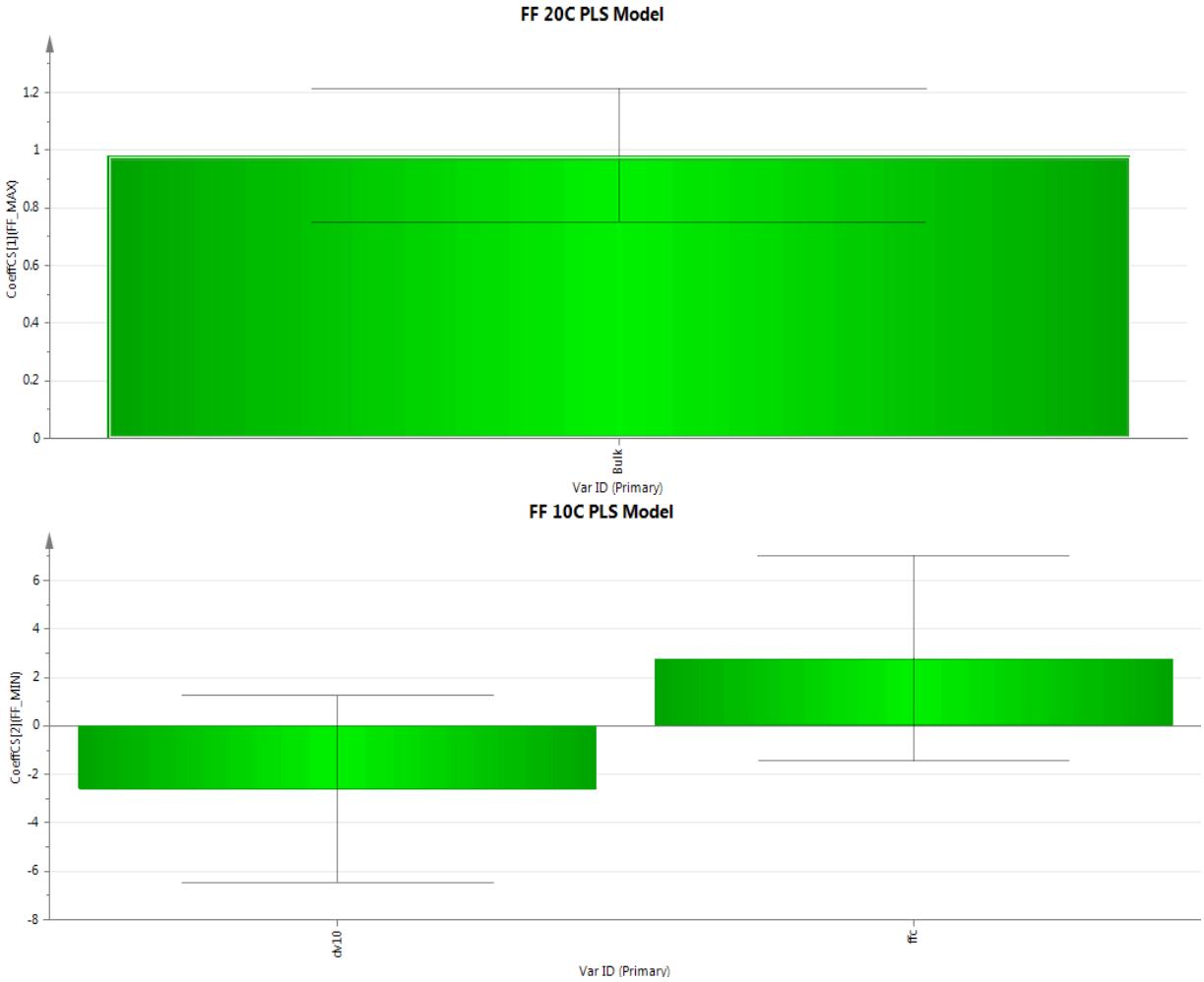

Figure 3.18 – Coefficients graphic of both FF PLS models.

To select which of the models should be utilized for a new scenario, it is mandatory to first do the screw selection and for that the methodology explained on Section 2.2.2.1 must be followed.

If it is decided that the 20C is the right screw to be set on the feeder, the equation present on Table E.1 must be utilized.

To demonstrate the viability of the created model, it is presented on Table 3.22 the comparison between both FF and it is possible to notice that the $FF_{predicted}$ values are similar to the FF 20C obtained from the experimental runs. Afterwards, it was decided to calculate the average of these differences

to attribute a range of variation (0.05 g/rev). The utility of this interval will be analysed during Table 3.23 discussion.

Table 3.22 – Experimental FF and $FF_{predicted}$ values of the PLS FF 20C model. The difference between the two values is also presented as well as the average of that differences.

Material	FF 20C (g/rev)	$FF_{predicted}$ 20C (g/rev)	Difference between FF and $FF_{predicted}$ (g/rev)	Average of the difference (g/rev)
Excipient A	1.25	1.27	0.02	0.05
Excipient B	1.22	1.30	0.08	
Excipient C	1.98	2.00	0.02	
Excipient D	----------			
Excipient E	1.68	1.61	0.07	
Excipient F	----------			
Excipient G	1.37	1.32	0.05	

In cases where the 10C is the fittest screw, the equation that must be used is the one presented on Table E.2.

Table 3.23 – Experimental FF and $FF_{predicted}$ values of the PLS FF 10C model. The difference between those two values is also presented as well as the average of that differences; the materials identified with MAX means that their FF values are from the maximum setpoint runs.

Material	FF 10C (g/rev)	$FF_{predicted}$ 10C (g/rev)	Difference between FF and $FF_{predicted}$ (g/rev)	Average of the difference (g/rev)
Excipient A	0.36	0.44	0.08	0.09
Excipient B	0.28	0.19	0.08	
Excipient C	0.49	0.57	0.08	
Excipient D	0.14	0.16	0.02	
Excipient E	1.47	1.51	0.05	
Excipient F	0.90	0.68	0.23	
Excipient G	0.14	0.22	0.08	
Excipient D MAX	0.18	0.25	0.07	
Excipient F MAX	1.01	0.77	0.24	

Firstly, the $FF_{predicted}$ 10C of each material (Table 3.23), calculated through the developed model considering all the materials' data collected from the minimum setpoint's runs, was compared to the original values as it was previously done for the $FF_{predicted}$ 20C model (Table 3.22).

It is of most importance to refer that during Excipients D and F feeder's runs, for both maximum and minimum setpoint, the 10C screw was utilized. For that reason, it was found to be interesting to apply the FF 10C model on both cases in order to understand its veracity.

As the materials' properties of these two materials were already considered for the model, the $FF_{predicted}$ 10C of Excipients D MAX and F MAX would be the same as for Excipients D and F, respectively. So, to the values obtained by $FF_{predicted}$ 10C model to Excipients D and F, it was added the average of the difference (0.09 g/rev) due to the fact that the experimental FF 10C of the Excipient D MAX (0.18 g/rev) and Excipient F MAX (1.01 g/rev) were higher than the values of Excipient C (0.14 g/rev) and Excipient F (0.90 g/rev). In a different scenario where it is intended to calculate the $FF_{predicted}$ at the minimum setpoint, the value of 0.09 g/rev should be subtracted.

After analysing the difference between FF and $FF_{predicted}$ of Excipients F MAX and D MAX it is possible to conclude that the value of Excipient D MAX is in between the interval, because 0.07 g/rev is lower than 0.09 g/rev, this means that the model was well succeeded. On the other hand, the same was not observed for Excipient F MAX because its difference is much higher than 0.09 g/rev, although it is interesting to compare the difference between FF and $FF_{predicted}$ of the Excipient F and F MAX (written in red on Table 3.23). In fact, both values are really similar, which means that the robustness of this model should not be totally discarded. For this reason, it is of most interest to investigate more about the viability of this model with more materials on future works.

3.2.4 After Feed Factor Prediction

By predicting the $FF_{predicted}$ it is no longer necessary to perform the first run. The $FF_{predicted}$ makes it possible to define the FF profile as well as to predict the optimal topup to be set for new feeder's runs.

3.2.4.1 Feed Factor Profile Prediction

The first run used to be important to define a FF profile before starting the feeder's runs. During the first run the FF values are automatically set on feeder controlling program settings' screen as shown in Figure 3.19, and that profile is used during the second run, the feeder's run (for production).

Considering Figure 3.19 it is possible to understand that inside the hopper there was only around 1200 g at the beginning of the first run, because the FF8 and the FF9 have a Stdev of 1 g/rev, which means that their bins FF values were not updated. The same was noticed for FF0, which means that at the moment when the picture was taken the first run was still on process.

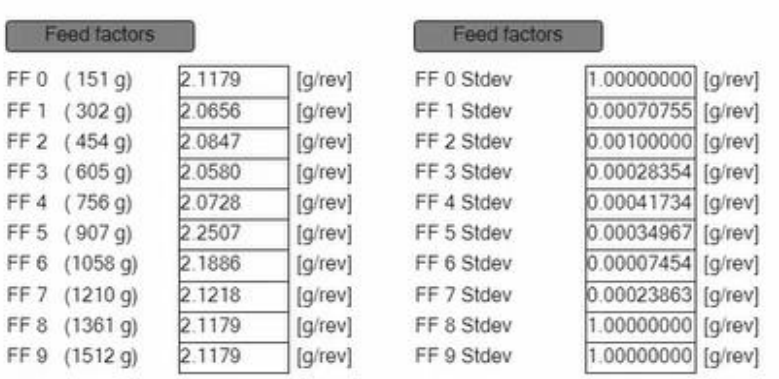

Feed factors			Feed factors		
FF 0 (151 g)	2.1179	[g/rev]	FF 0 Stdev	1.00000000	[g/rev]
FF 1 (302 g)	2.0656	[g/rev]	FF 1 Stdev	0.00070755	[g/rev]
FF 2 (454 g)	2.0847	[g/rev]	FF 2 Stdev	0.00100000	[g/rev]
FF 3 (605 g)	2.0580	[g/rev]	FF 3 Stdev	0.00028354	[g/rev]
FF 4 (756 g)	2.0728	[g/rev]	FF 4 Stdev	0.00041734	[g/rev]
FF 5 (907 g)	2.2507	[g/rev]	FF 5 Stdev	0.00034967	[g/rev]
FF 6 (1058 g)	2.1886	[g/rev]	FF 6 Stdev	0.00007454	[g/rev]
FF 7 (1210 g)	2.1218	[g/rev]	FF 7 Stdev	0.00023863	[g/rev]
FF 8 (1361 g)	2.1179	[g/rev]	FF 8 Stdev	1.00000000	[g/rev]
FF 9 (1512 g)	2.1179	[g/rev]	FF 9 Stdev	1.00000000	[g/rev]

Figure 3.19 – A FF profile given by feeder's supplier during the virtual training.

Basically, the feeder's hopper maximum fill weight ($m_{maxfill}$ in Equation 3.4) is divided into 10 equal mass-sized virtual bins, where bin 10 corresponds to the top 10% of the hopper section mass and bin 1 represents the bottom 10% [30].

To obtain the mass of material that is present per bin, Equation 3.4 must be used.

$$m_{maxfill}(kg) = 1.2 \times V_{refill}\ (L) \times \rho_{bulk}(kg/L) \tag{3.4}$$

To better understand the applicability of Equation 3.4, an example is followed (Equation 3.5). For the practical example, Excipient A was the chosen material and, as it was previously indicated, its ρ_{bulk} is 0.34 kg/L and by default the feeder considers always a refill volume (V_{refill}) of 2L, which is the amount of material that is expected to be inside the feeder after every refill.

$$m_{maxfill} = 1.2\ \times 2\ L\ \times 0.34\, kg/L = 0.816\ kg = 816\ g \tag{3.5}$$

As the $m_{maxfill}$ is 816g, the mass correspondent to each virtual bin will be that amount divided by 10, which is the number of sections that are present on the FF profile (Table 3.24).

Table 3.24 – An example of the mass-sized virtual bins.

Virtual bins	Mass-sized virtual bins (g)
FF0	82
FF1	163
FF2	245
FF3	326
FF4	408
FF5	490
FF6	571
FF7	653
FF8	734
FF9	816

At the end, regarding the previously calculated $FF_{predicted}$, it is possible to calculate the correspondent FF values across all bins, although this process requires further studies and there is a need to resort to more programs [27].

3.2.4.2 Topup Prediction

Avoiding the first run has consequences on the topup selection process, since it is dependent of the minimum refill volume, as explained on Section 3.1.2.2.

In fact, the ideal topup to be set on a feeder for a specific material depends a lot on the material's compressibility because, as previously highlighted on Section 3.1.1.1.5, it is harder to keep the feeding process at stable conditions if the amount of material that is fed per revolution is not always the same. To avoid this situation, it is mandatory to predict what the proper refill volume should be.

For a more compressible material, the usage of the 1.6L topup is not advised due to the fact that when a big amount of material drops on the feeder's hopper, the material's compressibility plays a negative role in the feeding process. For this reason, there should always exist a compromise between the number of refills and the non-usage of a topup that enhances the negative effect of the material's compressibility, so as to obtain a stable and optimised feeding process.

Two possible paths were found:

I. One hypothesis is by inserting the FF profile (after achieving all the FF values that correspond to each bin as referred on Section 3.2.4.1) on Figure 3.3 and conclude about

the compressibility of the material. If the slope is highly negative, it means that defining a topup with a lower volume than 1.6L would be a good decision;

II. An alternative way is by measuring all the studied materials' compressibility on the Ring Shear Tester. In fact, this is another functionality of the equipment [56]. After that, the data might be introduced on a PLS model similar as the previously done on Section 3.2.1 and it is expectable that the compressibility variable will be inversely proportional to the FF [32]. This means that, for future works, the higher the material compressibility is the lower will the average FF be.

In fact, having values to quantify compressibility constitute a great help for more reliable conclusions, such as:

- If the compressibility value of the new material is close to any of the compressibility values of the compressible materials that were studied in this thesis. The topups with lower volumes must be set on the feeder;

- If the compressibility value is similar to the values obtained for materials that are not compressible, the topup with the biggest volume (1.6L) should be chosen.

The two previous indicated paths to better define the topup are interesting to explore during future works. However, in order to have more reliable conclusions, a higher variety of tests for compressible materials should be performed, to identify in which cases each of the smaller topups (0.4L, 0.8L, and 1.2L) should be selected.

It is also important to refer that the topup as a feeder's component was not able to be included in any of the models due to the fact that only in one case the 1.6L topup was not used. Considering this, it is granted that that model would not confer any robustness to its predictions. However, by considering more materials and by applying the topup variable on future models, it is expected that it will be mostly related with the materials' properties and not with the feeder's parameters or the feeder's components. This relation was also emphasized by the supplier that confirms that the topup type is mostly dependent on the material that will be used on the production. This means that for a new material the same topup can be used for both maximum and minimum setpoints.

3.3 Section 3: Impact of Feeding Performance on Materials' Properties

Another goal of this thesis is to study if after running the materials through the feeder there are noticed any changes on the materials' properties.

As referred on Section 2.1.1, before each new material was run on the feeder, approximately 100g were collected for analysis on the Ring Shear Tester, Sympatec and SEM. The exact same procedure was followed after the material passed through the feeder and the same properties were analysed.

After the analysis of all the materials' properties for the before and after the feeder's runs samples, they were compared. The most outstanding result was the flowability property, because for all the materials the same type of deviation was noticed. The best way to illustrate these deviations is by plotting each material' before and after feeder's runs flow functions (plots the relation between the UYS and the MPS).

It is important to refer that in fact on Section 2.1.2.1.1 it is indicated that for this thesis only a pre-shear stress of 2000 Pa was considered. However, it is necessary to have more than one point to plot a flow function and compare the materials' properties. As each pair of UYS and MPS (each point) is obtained through the yield locus curve that is formed at each pre-shear consolidation stress, it is mandatory to do more testing about the pre-shear stresses on the materials. Considering this, it was applied to all the materials, before and after running through the feeder, a pre-shear consolidation stress of 1000 Pa followed by consolidation stresses of 300, 500 and 800 Pa, and a pre-shear consolidation stress of 3000 Pa followed by consolidation stresses of 600, 1500 and 2400 Pa.

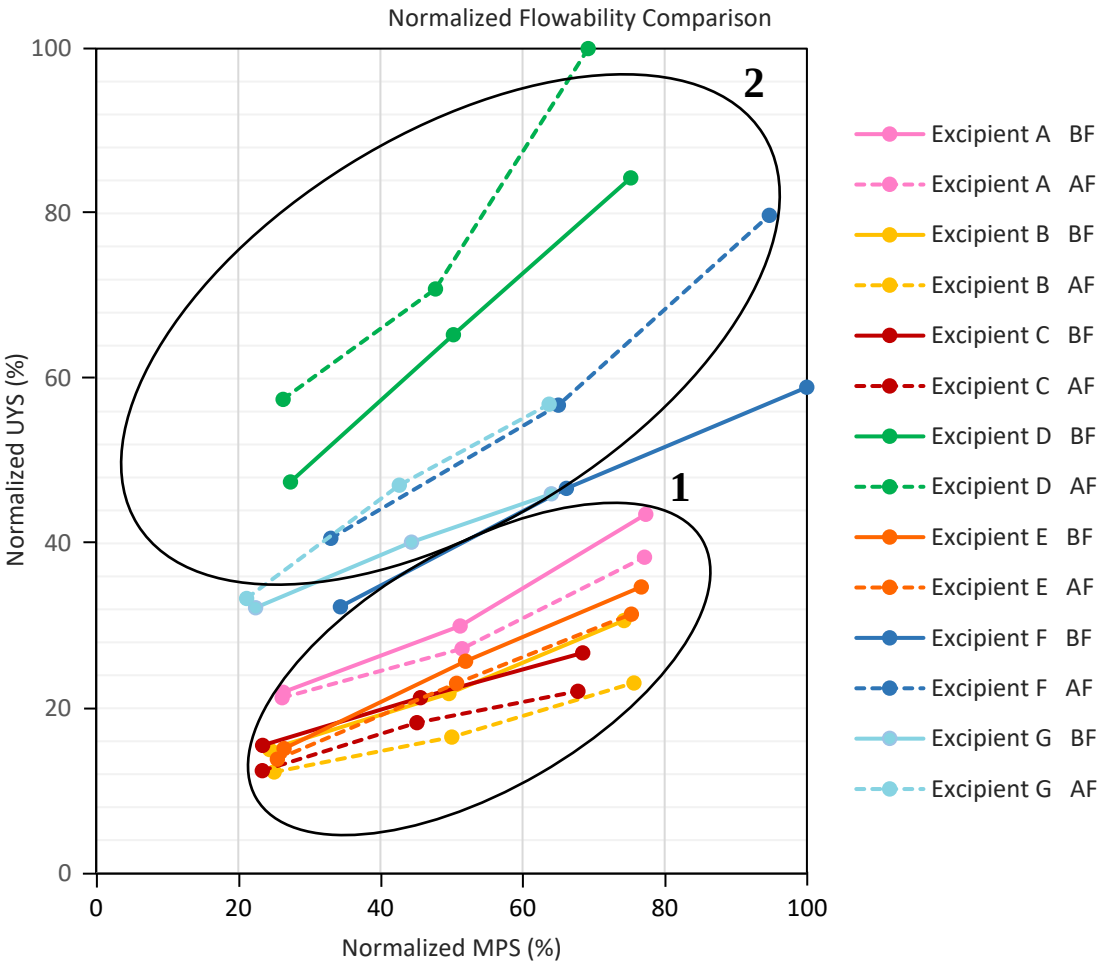

Figure 3.20 – Comparison between the materials' flowability. Flow functions of all the materials before and after running through the feeder; the dashed lines represent the materials' flowability after running through the feeder (AF); the continuous lines represent the materials' flowability before running through the feeder (BF); Group 1 is constituted by Excipients A, B, C and E; Group 2 is constituted by Excipients D, F and G.

Figure 3.20 represents the flowability of each material. As the UYS values are lower for Group 1 materials their ffc is higher, which, as previously analysed on Section 3.1.1.1.2, means that these materials have better flowability than the Group 2 materials.

The materials represented in Group 1 have easy-flowing properties, while the ones represented in Group 2 don't flow that well. Additionally, for the same material in Group 1, it seems that the flowability improves after the powder runs through the feeder, as the dashed lines are below the continuous lines. On the other hand, the opposite seems to happen with Group 2 materials, in which their flowability properties get worse after the feeder's run, as the dashed lines are above the continuous lines.

In the same Ring Shear Tester where the flowability is measured, the cohesion is also measured. In fact, it seems like there is an inverse proportion between the cohesion and the flowability.

Group 1 materials' cohesion decreases AF (Table 3.25), thus improving the flowability, while in Group 2 the cohesion increases AF (Table 3.26), thus decreasing the flowability.

Table 3.25 – Comparative table of the before (BF) and after (AF) feeder's runs cohesion measured at 2000 Pa for the Group 1 materials.

Tau,c (Pa) Group 1							
Excipient A		**Excipient B**		**Excipient C**		**Excipient E**	
BF	AF	BF	AF	BF	AF	BF	AF
134.0	127.7	92.2	79.7	92.0	83.0	109.7	105.0

Table 3.26 – Comparative table of the before (BF) and after (AF) feeder's runs cohesion measured at 2000 Pa for the Group 2 materials.

Tau,c (Pa) Group 2					
Excipient D		**Excipient F**		**Excipient G**	
BF	AF	BF	AF	BF	AF
340.7	375.3	185.2	230.0	228.3	247.7

In conclusion, cohesion is probably one of the parameters that directly affects the flowability of each material before and after the feeders' runs. Although, the previous analysis can only be applied amongst the tested materials, due to the lack of information available in the literature regarding this topic. Therefore, further studies to verify if this is also applied to other materials would be of much interest.

In addition, more powder properties should be taken into consideration, such as electrostatic charging since a material that has electrostaticity will be more cohesive. For this reason, the usage of a static eliminator on the materials before the feeders' runs should be tested [71]. Later, it should be analysed if the previously referred occurrences on the materials flowing performance continue to be verified after the feeders' runs.

3.4 Section 4: Stable Setpoints Final Ranges Applicability

The CDC-10 continuous process has a nominal output of 10 kg/h and can work between a range of 1 - 25 kg/h, as previously referred on Section 1.3. Considering this information, the minimum and maximum limitations of the stable setpoints were decided to be analysed in separate.

3.4.1 Upper Limitation – 25 kg/h

First, it is important to refer that, during the feeder's runs, no superior limitations, for the studied materials in the considered maximum percentages usually used in a formulation, were noticed. This means that it was possible to achieve all the defined setpoints without getting the feeder throughput out of control. Moreover, it is important to refer that the feeder's maximum setpoint presented on Table 3.27, does not reflect the maximum feeder's limitations itself but the setpoint that must be set on each material feeder in order to operate at the correspondent maximum percentage in formulation.

Table 3.27 – Resume table of all Max % in formulation and the correspondent Feeder´s Max Setpoint for a CDC-10 Max Total Setpoint production.

Target function	**API**	**Filler 1**	**Filler 2**	**Filler 3**	**Disinte-grant**	**Lubri-cant**	**Filler 4**
Material	Excipient G	Excipient A	Excipient B	Excipient C	Excipient F	Excipient D	Excipient E
Max % in formulation	60.0	90.0	90.0	60.0	5.0	1.5	50.0
Feeder´s Max Setpoint (g/s)	4.167	6.250	6.250	4.167	0.347	0.104	3.472
Feeder´s Max Setpoint (kg/h)	15.0	22.5	22.5	15.0	1.3	0.4	12.5
CDC-10 Max Total Setpoint (kg/h)	25	25	25	25	25	25	25

It is important to refer that to produce the final product (100% of the formulation) (Equation 3.6), the CDC-10 maximum total setpoint (CDC – 10 Max Total Setpoint) must be calculated considering that for each material the feeder's maximum setpoint (Feeder's Max Setpoint) corresponds to a respective maximum percentage in formulation (Max % in formulation).

$$CDC - 10\ Max\ Total\ Setpoint\ \ (kg/h)\ = \frac{Feeder's\ Max\ Setpoint\ \ (kg/h)}{Max\ \%\ in\ formulation} \times 100 \qquad (3.6)$$

Regarding Table 3.27 it is possible to conclude that all the CDC-10 maximum total setpoint are 25 kg/h. This means that the defined conditions for each scenario are possible to be used on a CDC-10 production line.

In cases that intend to use a different percentage in the formulation and/ or a different setpoint it is important to verify if the CDC-10 maximum total setpoint does not overcome 25 kg/h. If so, one of that two parameters (percentage in formulation or setpoint) must change to guarantee a maximum of 25 kg/h production.

3.4.2 Lower Limitation – 1 kg/h

Considering the CDC-10 lower limitation, the same type of analysis was made (Table 3.28).

Table 3.28 – Resume table of all Min % in formulation and the correspondent Feeder´s Min Setpoint for a CDC-10 Min Total Setpoint production.

Target function	**API**	**Filler 1**	**Filler 2**	**Filler 3**	**Disinte-grant**	**Lubri-cant**	**Filler 4**
Material	Excipient G	Excipient A	Excipient B	Excipient C	Excipient F	Excipient D	Excipient E
Min % in formulation	5.00	20.00	20.00	10.00	1.00	0.25	25.00
Feeder´s Min Setpoint (g/s)	0.020	0.056	0.080	0.120	0.050	0.017	0.140
Feeder´s Min Setpoint (kg/h)	0.072	0.200	0.288	0.432	0.180	0.063	0.504
CDC-10 Min Total Setpoint (kg/h)	1.44	1.00	1.44	4.32	18.00	25.06	2.02

In Equation 3.7, the CDC-10 minimum total setpoint (CDC – 10 Min Total Setpoint) is calculated considering that for each material the feeder's minimum setpoint (Feeder's Min Setpoint) corresponds to a respective minimum percentage in formulation (Min % in formulation).

$$CDC - 10\ Min\ Total\ Setpoint\ \ (kg/h)\ = \frac{Feeder's\ Min\ Setpoint\ \ (kg/h)}{Min\ \%\ in\ formulation} \times 100 \qquad (3.7)$$

Regarding Table 3.28 it is possible to notice that Excipients F and D have the highest CDC-10 minimum total setpoint values (written in red). This is related with their low formulation percentages considered, making them two critical materials to be aware of.

As lubricant is always used at low percentages it is commonly the formulation limiting material [72]. Although, in a formulation where Excipient D would not be present the Excipient F would be the limiting material.

Considering a perfect scenario where all the materials feeder´s runs would be able to run stably with the setpoint defined by the calculations, previously presented on Section 3.1.2.1, this would not constitute a problem, because all the materials' CDC-10 minimum total setpoint would have been 1 kg/h (Table 3.29) as it was 25 kg/h for all the CDC-10 maximum total setpoint (Table 3.27).

Table 3.29 – Resume table of all Min % in formulation and the correspondent Feeder´s Min Setpoint for a CDC-10 Min Total Setpoint ideal production.

Target function	**API**	**Filler 1**	**Filler 2**	**Filler 3**	**Disinte-grant**	**Lubri-cant**	**Filler 4**
Material	Excipient G	Excipient A	Excipient B	Excipient C	Excipient F	Excipient D	Excipient E
Min % in formulation	5.00	20.00	20.00	10.00	1.00	0.25	25.00
Feeder´s Min Setpoint (g/s)	1.4×10^{-2}	5.6×10^{-2}	5.6×10^{-2}	2.8×10^{-2}	3.0×10^{-3}	6.9×10^{-4}	6.9×10^{-2}
CDC-10 Min Total Setpoint (kg/h)	1	1	1	1	1	1	1

This means that the materials with the highest CDC-10 minimum total setpoint (Excipients F and D) on Table 3.28 were the ones with higher difficulty to be run on the feeder at such small setpoints and minimum percentages in formulation. Moreover, it is not even possible to run Excipient D on the GEA Compact Feeder with such a low minimum percentage in the formulation, because a CDC-10 minimum total setpoint of 25.06 kg/h surpasses the CDC-10 maximum total setpoint (25 kg/h). Considering this, for future productions, a slightly increase on the minimum percentage in the formulation or a slightly decrease on the feeder's minimum setpoint should exist.

Considering the CDC-10 minimum total setpoint of Excipient F, it is not recommended to increase its value, because 18 kg/h is higher than the CDC-10 nominal value of 10 kg/h. Besides that, it does not allow a big range of operation for the other feeders responsible for feeding the rest of the materials, which represents a reduction of flexibility for the CDC-10 process. Furthermore, its high throughput would require a high velocity in all the equipment used on this process, leading to major process oscillations that would certainly affect the product quality.

Since it will not be possible to decrease the Excipient F feeder´s minimum setpoint, because the referred minimum setpoint on Section 3.1 is the lowest possible for all the studied materials at stable RSD, there are two different options remaining:

I. Raise the minimum percentage in the formulation;

If Excipient F was projected at 2% in formulation, its CDC-10 minimum total setpoint would be 9 kg/h, which is a much reasonable condition to run the process. In cases where this increase is not possible, by considering the feeder's stable conditions or by forcing the product to get out of specifications, there is another possibility.

II. Change the material for another with better flow properties at higher percentage in formulation.

At some point, certain materials could not be fed stably at higher percentages than the maximum limit. As a consequence, the material cannot be used on that production.

E.g. Sodium Stearyl Fumarate can run at stable conditions at higher concentrations, 2% in formulation, than Excipient D (Table 3.29) and for this reason it constitutes a good alternative as a lubricant [52].

In conclusion, the lower the material CDC-10 minimum total setpoint is, the more flexible is its percentage in a formulation, because if the feeder is stable at a minimum condition, it will be possible to operate in control in any higher value as well. In other words, the lower is the CDC-10 minimum total setpoint the larger is the range of stable working conditions for that material to run on the feeder.

A good example is Excipient A, which is the material with the lowest CDC-10 minimum total setpoint (1 kg/h), as it coincides with the CDC-10 process lower limitations it will be stable to operate at any value within the continuous process range.

3.5 Section 5: Case Studies

3.5.1 Case Study 1

On the first case study, an example of a formulation will be analysed to simulate the appliance of the results and reasoning from the previous section (Section 3.4). For this case, only some of the tested materials were integrated on the production process and at different percentages in the formulation. As a consequence, their feeders will be running at different feeder´s minimum setpoint (Table 3.30).

Table 3.30 – Resume table of all Min % in formulation and the correspondent Feeder´s Min Setpoint and CDC-10 Min Total Setpoint for the materials considered on the case study 1.

Target function	**API**	**Filler 1**	**Filler 2**	**Disinte-grant**	**Lubricant**
Material	Excipient G	Excipient C	Excipient E	Excipient F	Excipient D
% in formulation	40	10	44	5	1
Feeder´s Min Setpoint (kg/h)	0.072	0.432	0.504	0.180	0.063
CDC-10 Min Total Setpoint (kg/h)	0.180	4.320	1.145	3.600	6.264
Each Feeder´s Setpoint at 6.264 kg/h (kg/h)	2.506	0.626	2.756	0.313	0.063
Feeder´s Max Setpoint (kg/h)	15.0	15.0	12.5	1.3	0.4

Regarding Table 3.30, the limiting material is Excipient D because it has the highest CDC-10 minimum total setpoint, which means that, for this example of production, the CDC-10 must work at a CDC-10 minimum total setpoint of 6.264 kg/h (written in red).

To better explain the effect that this information has on a formulation, the setpoint that each feeder must run in response to the defined conditions was added to the table (each feeder´s setpoint at 6.264 kg/h), calculated by Equation 3.7. Afterwards, it is important to verify if all the materials have their setpoint values between the minimum and maximum stable setpoints by comparing them with each material feeder´s minimum setpoint and feeder´s maximum setpoint (written in blue on Table 3.30). Fortunately, as all the values are between both setpoints, it means that it is possible to start the CDC-10 production on that conditions.

In conclusion, as it was done for this case study, the same reasoning can be applied for all the productions that are intended to be started on the CDC-10.

3.5.2 Case Study 2

On the second case study it was resorted to Digital Twin, which is a web app created by Hovione, to help on the behaviour prediction of the feeders that are intended to be run on the CDC-10.

The Digital Twin CDC line can simulate the running of a maximum number of six feeders, which means that the formulations can only be constituted by a maximum of six materials. In cases where the process must contain a lubricant, the usage of a second blender is mandatory. The first blender is responsible for blending all the excipients with the API and the second is necessary to homogenize the lubricant with the previously blended materials and, for that reason, the feeder responsible for feeding the lubricant is only introduced after the first blender (Section 1.3). Notice that all these requirements are considered by the web app.

To calibrate the virtual feeders, it is necessary to upload an Excel document with the required dynamic parameters (massflow, screw speed and weight) in function of the time. Considering the document, the program defines the **parameters of the feeder**: ff_min, ff_max, beta and the process noise, placed on the left top of Figure 3.21.

The **conditions of the feeder** must be manually introduced in accordance to the intended conditions for each formulation. However, the "P", "I" and "D" should be tested by trial-and-error in order to find out the most adequate profile.

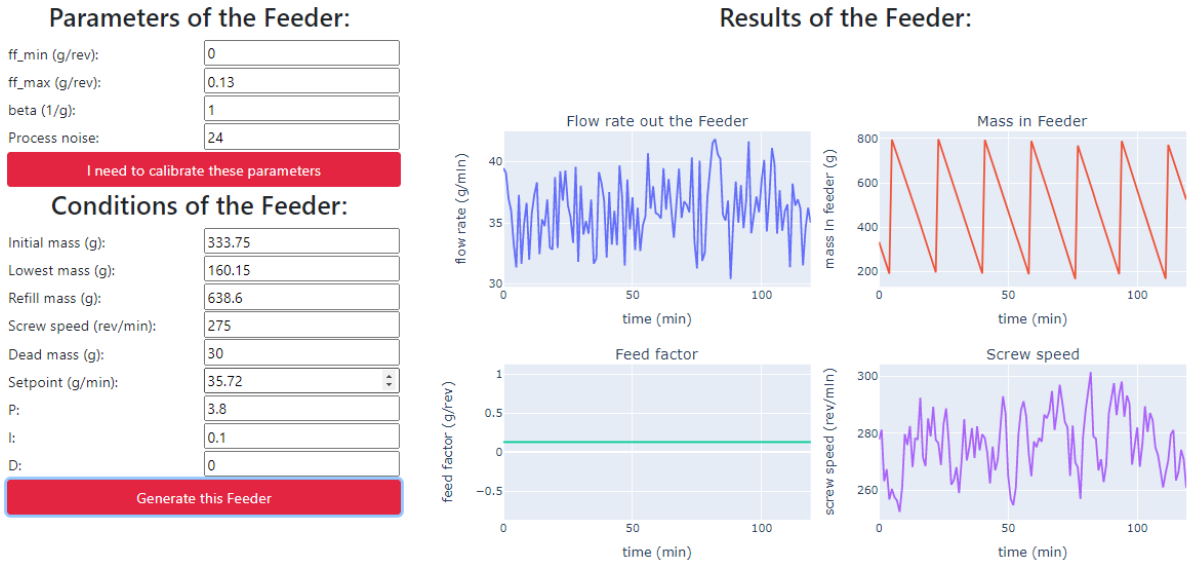

Figure 3.21 – Digital twin feeder's panel.

It is important to refer that this predictive analysis is useful merely to confer an initial idea of what is expected to happen on the feeder equipment for a new scenario. The information about the expected feeder's behaviour is displayed on the graphics placed on the right side of Figure 3.21 (**results of the feeder**). An initial idea of how the flow rate profile will be is plotted, as well as the screw speed and the FF profile. Furthermore, on the mass in feeder plot, it is possible to observe the frequency at which the refills are expected to happen.

It is interesting to notice that the FF plot on Figure 3.21 is a constant line and to better understand the reasons that lead to that occurrence, Equation 3.8 must be analysed.

$$ff_{apparent}(W) = ff_{max} - (ff_{max} - ff_{min}) \times e^{-\beta \times W} \quad (3.8)$$

$ff_{apparent}$ – apparent FF value (g/rev)
ff_{max} – maximum FF value (g/rev)
ff_{min} – minimum FF value (g/rev)
W – amount of mass inside the feeder (g)
β (beta) – represent the changes in FF as a function of mass remaining in the feeder (g^{-1})

Regarding Equation 3.8 [73], it is possible to identify two main possibilities for the FF profile not presenting a decreasing tendency:

I. In cases where the ff_max is equal to the ff_min, the FF profile will be a constant line with the ff_max value;

II. On the other hand, if beta is really close to zero the FF profile will be a constant line with the ff_min value.

In conclusion the FF plot consistency reflects either that the powder is not compressible and for that reason it does not show a notorious decrease on the FF values during time (I), or that the amount of material that is processed through the feeder during the experience is too little to generate an impact on the FF profile (II).

It is important to refer that to obtain the **parameters of the feeder** it is necessary to first test the materials on the feeder so as to collect the massflow, screw speed and weight from their feeder's runs. In order to make this web app useful and predict the feeder's behaviour for a new process condition or for a never before tested material, PLS models, considering the data collected from the already tested feeder's runs (Appendix D), were developed with the aim of predicting the ff_min, ff_max and beta for both types of screws (Table 3.31).

The process noise is not that important to predict, due to the fact that it is just a variable that Digital Twin adds to confer a more realistic character to the virtual feeder. In other words, the noise variable was introduced on the web app programming with the aim of simulating the oscillations that happen inside the “real” feeder.

Table 3.31 – Resume table of all the PLS models’ information created to predict the parameters of the feeder.

Model / Model properties	ff_min 20C	ff_max 20C	beta 20C	ff_min 10C	ff_max 10C	beta 10C
R2Y	0.950	0.975	0.858	0.934	0.948	0.575
Q2	0.879	0.943	0.759	0.825	0.881	0.363
RMSEE	0.233	0.080	0.289	0.104	0.155	0.007
RMSEcv	0.219	0.078	0.215	0.159	0.269	0.007
Rank	3	2	2	3	3	2

The majority of the models are robust because their RMSEE and RMSEcv values are similar and not only do they have Q2 values higher than 0.7 but also high values of R2Y (Section 2.2.5). The only model that does not constitute a good prediction is the beta 10C, although not achieving a good predictive model for this parameter does not constitute a problem, because all the feeder’s runs where the 10C screw was used always had a beta value equal or close to 1, as it can be seen on Table 3.32. Taking this into consideration, it is a good decision to define beta 10C = 1, for a first trial, on future scenarios.

Table 3.32 – Resume table of all the beta 10C values calculated by the Digital Twin program.

Material	beta 10C
Excipient A	1.02
Excipient B	1.00
Excipient C	1.00
Excipient D	0.99
Excipient E	1.00
Excipient F	1.00
Excipient G	1.00

To create a good methodology, it is important to simplify the model by identifying its significant variables. The Table 3.33 shows the most significant materials’ properties that should be measured in order to predict the **parameters of the feeder**.

Table 3.33 – Significant variables for all the PLS models created to predict the parameters of the feeder.

Models	Significant Variables		
ff_min 20C	dv50	ffc	Tau,c
ff_max 20C	dv50	Tau,c	----
beta 20C	dv50	ffc	----
ff_min 10C	dv50	Tau,c	phiE
ff_max 10C	dv10	ffc	phiE

Finally, the coefficients that must be multiplied by the significant materials' properties as well as the respective equations that must be used to predict all **parameters of the feeder** are represented on Table E.3, Table E.4, Table E.5, Table E.6 and Table E.7.

In conclusion, by using these models, it is possible to virtually predict, on the Digital Twin, the feeders' behaviour for any new productions that intend to use a maximum of six feeders. Furthermore, after their virtual calibration, it is also possible to simulate the CDC-10 production and conclude about the characteristics of the mixed materials.

4. Conclusions & Future Work

First of all, it is important to refer that the experimental plan was successfully executed as it was proposed to test the maximum number of materials as possible. More materials were not tested due to safety restrictions and material's supplying constraints. Considering all the seven studied materials, the main goals of the thesis were achieved. However, it is necessary to test a higher range of different materials on future work to achieve more accurate conclusions.

A methodology that enables an efficient equipment calibration as well as an accurate selection of the feeder's components, in order to provide optimised feeding conditions, was successfully developed. Moreover, it was also possible to define a range of the feeder's operation that guarantees a stable massflow for all the studied materials.

Meanwhile, a database that considers the materials' properties was also developed, with which it was possible to conclude about the materials similarities and differences to better predict their performance during the feeder's runs.

Flowability is one of the most important rheological parameters to be taken into consideration for the feeding processes due to the fact that it "includes" more materials' properties in it. In other words, materials that possess bad flowability also have a lower particle size, higher cohesion and lower Hausner ratio (HR). Considering this analysis, through all the materials tested, Excipients D, F and G are expected to be the materials that cause more adversities during the feeding optimization, which was confirmed throughout the experimental trials.

For future works, it is important to continue developing this database in order to eventually make it so embracing that it would be possible to avoid the first run. In other words, for every new material that is intended to be used on the CDC-10 production, its properties would be similar to one of the materials that were already characterized on the database. As it is identified a similar material in terms of properties, it is a fair procedure to set the same feeder's components that were used to run the material already characterized on the database as well as know the approximate range of stable massflows that the new material might be run in.

After a deeper research, another alternative was found to avoid the first run, at least until having a more complete database, which consists in the prediction of the feed factor (FF) profile and the topup volume, since both are the main reasons why the first run is performed.

Considering that the FF depends on the process conditions, the materials' properties and the feeder's components two partial least squares (PLS) models were created in order to predict its average value ($FF_{predicted}$). As the FF profile is defined by the FF values, further studies must be carried out as described on Section 3.2.4.1.

To predict the topup volume, the two paths suggested on Section 3.2.4.2 must be tested either to conclude which one is the most appropriate or even check if a combination between both would work better in a way that one may validate the other.

It is important to emphasize that by the time that these alternatives were elaborated, the practical part of this project had already been ceased and thence finalising it has become impossible due to time limitations.

Finally, it was also found interesting to find out if the process of feeding causes any modifications on the materials' properties. In fact, the materials' flowability seems to be affected by the feeder. It was observed that for the materials that already have good flowing properties the flowability improves after the feeder's running. On the other hand, for the materials with bad flowing properties, its flowability had decreased after passing through the feeder. Unfortunately, no information was found on literature regarding this topic which means that for a more robust conclusion more materials must be analysed in order to validate or not the reported situation.

5. References

[1] M. A. P. McAuliffe *et al.*, “The Use of PAT and Off -line Methods for Monitoring of Roller Compacted Ribbon and Granule Properties with a View to Continuous Processing,” *Org. Process Res. Dev.*, vol. 19, no. 14, pp. 158–166, 2015, doi: 10.1021/op5000013.

[2] K. Plumb, “Continuous processing in the pharmaceutical industry: Changing the mind set,” *Chem. Eng. Res. Des.*, vol. 83, no. A6, pp. 730–738, 2005, doi: 10.1205/cherd.04359.

[3] C. Blackshields and A. Crean, “Continuous Powder Feeding for Pharmaceutical Solid Dosage Form Manufacture: A Short Review,” *Pharm. Dev. Technol.*, vol. 23, no. 6, pp. 554–560, 2018, doi: 10.1080/10837450.2017.1339197.

[4] S. L. Lee *et al.*, “Modernizing Pharmaceutical Manufacturing : from Batch to Continuous Production,” *J. Pharm. Innov.*, vol. 10, no. 3, pp. 191–199, 2015, doi: 10.1007/s12247-015-9215-8.

[5] L. Pernenkil, “Continuous Blending of Dry Pharmaceutical Powders,” 2008.

[6] K. Marikh, H. Berthiaux, V. Mizonov, and E. Barantseva, “Experimental study of the stirring conditions taking place in a pilot plant continuous mixer of particulate solids,” *Powder Technol.*, vol. 157, no. 1–3, pp. 138–143, Sep. 2005, doi: 10.1016/j.powtec.2005.05.020.

[7] W. E. Engisch and F. J. Muzzio, “Method for characterization of loss-in-weight feeder equipment,” *Powder Technol.*, vol. 228, pp. 395–403, 2012, doi: 10.1016/j.powtec.2012.05.058.

[8] S. Simonaho, J. Ketolainen, T. Ervasti, M. Toiviainen, and O. Korhonen, “Continuous manufacturing of tablets with PROMIS-line — Introduction and case studies from continuous feeding , blending and tableting,” *Eur. J. Pharm. Sci.*, vol. 90, pp. 38–46, 2016, doi: 10.1016/j.ejps.2016.02.006.

[9] T. Page *et al.*, “Equipment and Analytical Companies Meeting Continuous Challenges,” *J. Pharm. Sci.*, vol. 104, no. 3, pp. 821–831, 2015, doi: 10.1002/jps.24282.

[10] M. Fonteyne *et al.*, “Process analytical technology for continuous manufacturing of solid-dosage forms,” *TrAC - Trends Anal. Chem.*, vol. 67, pp. 159–166, 2015, doi: 10.1016/j.trac.2015.01.011.

[11] S. Chattoraj and C. C. Sun, “Crystal and Particle Engineering Strategies for Improving Powder Compression and Flow Properties to Enable Continuous Tablet Manufacturing by Direct Compression,” *J. Pharm. Sci.*, vol. 107, no. 4, pp. 968–974, 2018, doi: 10.1016/j.xphs.2017.11.023.

[12] Y. Suzuki *et al.*, “Control strategy and methods for continuous direct compression processes,” *Asian J. Pharm. Sci.*, vol. 16, no. 2, pp. 253–262, 2021, doi: 10.1016/j.ajps.2020.11.005.

[13] B. Van Snick *et al.*, “Continuous direct compression as manufacturing platform for sustained release tablets,” *Int. J. Pharm.*, vol. 519, no. 1–2, pp. 390–407, 2017, doi: 10.1016/j.ijpharm.2017.01.010.

[14] M. Hopkins, “LOSS in weight feeder systems,” *Meas. Control*, vol. 39, no. 8, pp. 237–240, 2006, doi: 10.1177/002029400603900801.

[15] G. GEA, “Continuous processing - Solutions for Oral Solid Dosage Forms,” p. 42, 2020, Accessed: Sep. 05, 2021. [Online]. Available: https://www.gea.com/en/binaries/Pharmaceutical-Continuous-Processing-for-oral-solid-dosage-forms_tcm11-31710.pdf

[16] A. Basu, A. De, and S. Dey, “Techniques of Tablet Coating: Concepts and Advancements: A Comprehensive Review,” *J. Pharm. Pharm. Sci.*, vol. 2, no. 4, pp. 1–6, 2013, [Online]. Available: https://www.rroij.com/open-access/techniques-of-tablet-coating-concepts-and-advancements-a-comprehensive-review.php?aid=34923

[17] A. D. Karande, P. W. S. Heng, and C. V. Liew, “In-line quantification of micronized drug and excipients in tablets by near infrared (NIR) spectroscopy: Real time monitoring of tabletting process,” *Int. J. Pharm.*, vol. 396, no. 1–2, pp. 63–74, 2010, doi: 10.1016/j.ijpharm.2010.06.011.

[18] R. Weinekötter and L. Reh, “Continuous Mixing of Fine Particles,” *Part. Part. Syst. Charact.*, vol. 12, no. 1, pp. 46–53, 1995, doi: 10.1002/ppsc.19950120108.

[19] J. Scicolone, D. Hausner, J. Palmer, A. Birkmire, J. Holman, and F. Muzzio, “Optimizing Loss-in-Weight Feeding of Poorly Flowing Materials,” *Pharm. Technol. - APIs, EXCIPIENTS, Manuf. 2020*, no. 4, pp. 24–28, 2020, Accessed: Oct. 09, 2021. [Online]. Available: https://cdn.sanity.io/files/0vv8moc6/pharmtech/04d37a1f59614cc941d329d741dc28dd7a9b04f5.pdf/PTSupp0920_ezine (Watermark)_LINKED.pdf

[20] J. J. Cartwright, J. Robertson, D. D’Haene, M. D. Burke, and J. R. Hennenkamp, “Twin screw wet granulation : Loss in weight feeding of a poorly flowing active pharmaceutical ingredient,” *Powder Technol.*, vol. 238, pp. 116–121, 2013, doi: 10.1016/j.powtec.2012.04.034.

[21] B. Van Snick *et al.*, “Impact of material properties and process variables on the residence time distribution in twin screw feeding equipment,” *Int. J. Pharm.*, vol. 556, pp. 200–216, 2018, doi: 10.1016/j.ijpharm.2018.11.076.

[22] M. S. Escotet-Espinoza *et al.*, “Using a material property library to find surrogate materials for pharmaceutical process development,” *Powder Technol.*, vol. 339, pp. 659–676, 2018, doi: 10.1016/j.powtec.2018.08.042.

[23] J. Palmer *et al.*, “Mapping key process parameters to the performance of a continuous dry powder blender in a continuous direct compression system,” *Powder Technol.*, vol. 362, pp. 659–670, 2020, doi: 10.1016/j.powtec.2019.12.028.

[24] C. Allenspach, P. Timmins, G. Lumay, J. Holman, and T. Minko, “Loss-in-weight feeding , powder flow and electrostatic evaluation for direct compression hydroxypropyl methylcellulose (HPMC) to support continuous manufacturing,” *Int. J. Pharm.*, vol. 596, p. 120259, 2021, doi: 10.1016/j.ijpharm.2021.120259.

[25] T. Li, J. V. Scicolone, E. Sanchez, and F. J. Muzzio, “Identifying a Loss-in-Weight Feeder Design Space Based on Performance and Material Properties,” *J. Pharm. Innov.*, vol. 15, pp. 482–495, 2020, doi: 10.1007/s12247-019-09394-4.

[26] W. E. Engisch and F. J. Muzzio, “Loss-in-Weight Feeding Trials Case Study : Pharmaceutical Formulation,” *J. Pharm. Innov.*, vol. 10, pp. 56–75, 2015, doi: 10.1007/s12247-014-9206-1.

[27] I. K. Yadav *et al.*, “Influence of material properties and equipment configuration on loss-in-weight feeder performance for drug product continuous manufacture,” *Powder Technol.*, vol. 348, pp. 126–137, 2019, doi: 10.1016/j.powtec.2019.01.071.

[28] W. E. Engisch and F. J. Muzzio, “Feedrate deviations caused by hopper refill of loss-in-weight feeders,” *Powder Technol.*, vol. 283, pp. 389–400, 2015, doi: 10.1016/j.powtec.2015.06.001.

[29] B. Van Snick *et al.*, “A multivariate raw material property database to facilitate drug product development and enable in-silico design of pharmaceutical dry powder processes,” *Int. J. Pharm.*, vol. 549, no. 1–2, pp. 415–435, 2018, doi: 10.1016/j.ijpharm.2018.08.014.

[30] F. Tahir *et al.*, “Development of feed factor prediction models for loss-in-weight powder feeders,” *Powder Technol.*, vol. 364, pp. 1025–1038, 2020, doi: 10.1016/j.powtec.2019.09.071.

[31] Y. Wang, T. Li, F. J. Muzzio, and B. J. Glasser, “Predicting feeder performance based on material flow properties,” *Powder Technol.*, vol. 308, pp. 135–148, 2017, doi: 10.1016/j.powtec.2016.12.010.

[32] B. Bekaert *et al.*, “Determination of a quantitative relationship between material properties, process settings and screw feeding behavior via multivariate data-analysis,” *Int. J. Pharm.*, vol. 602, p. 120603, 2021, doi: 10.1016/j.ijpharm.2021.120603.

[33] GEA Group, *Compact Feeder ™ Instruction Manual*. 2020.

[34] Coperion, “K-CL-SFS KT20 compact gravimetric twin screw feeder”, Accessed: Nov. 19, 2021. [Online]. Available: https://www.coperion.com/en/products-services/process-equipment/feeders/twin-screw-feeders

[35] K-TRON, “K-TRON Product Specification Volumetric Twin Screw Compact Feeder,” pp. 1–2, 2011, Accessed: Sep. 10, 2021. [Online]. Available: http://literature.puertoricosupplier.com/074/SC74018.pdf

[36] T. Li, “Predictive Performance of Loss-in-weight Feeders for Continuous Powder-Based Manufacturing,” 2020.

[37] C. for I. Rheology, “Protein Powder Rheology.” https://www.rheologylab.com/articles/food/protein-powder-rheology/ (accessed Nov. 21, 2021).

[38] H. Ramachandruni and S. W. Hoag, “Design and Validation of an Annular Shear Cell for Pharmaceutical Powder Testing,” *J. Pharm. Sci.*, vol. 90, no. 5, pp. 531–540, May 2001, doi: 10.1002/1520-6017(200105)90:5<531::AID-JPS1010>3.0.CO;2-U.

[39] D. Schulze, *Powders and Bulk Solids*. 1965.

[40] M. K. Taylor, J. Ginsburg, A. J. Hickey, and F. Gheyas, “Composite method to quantify powder flow as a screening method in early tablet or capsule formulation development,” *AAPS PharmSciTech*, vol. 1, no. 3, pp. 20–30, 2000, doi: 10.1208/pt010318.

[41] C. C. Sun, “Setting the bar for powder flow properties in successful high speed tableting,” *Powder Technol.*, vol. 201, no. 1, pp. 106–108, 2010, doi: 10.1016/j.powtec.2010.03.011.

[42] A. P. Gorle and S. S. Chopade, “Liquisolid Technology: Preparation, Characterization and Applications,” *J. Drug Deliv. Ther.*, vol. 10, no. 3-S, pp. 295–307, 2020, doi: 10.22270/jddt.v10i3-s.4067.

[43] S. Howard, “Solids: Flow Properties,” *Encycl. Pharm. Technol. Third Ed.*, pp. 3275–3296, 2013, doi: 10.1081/E-EPT3-100200005.

[44] Dupont, “Avicel Selection Guide,” pp. 1–2, 2020, Accessed: Aug. 18, 2021. [Online]. Available: https://www.pharma.dupont.com/content/dam/dupont/amer/us/en/nutrition-health/general/pharmaceuticals/documents/Download_Avicel Product Selection Guide.pdf

[45] Kerry, “Lactose Technical Manual,” pp. 14–18, 2019, Accessed: Aug. 28, 2021. [Online]. Available: https://azeliscanada.com/wp-content/uploads/2020/10/LACTOSE-Brochure-8.19-1.pdf

[46] Peter Greven, “Peter Greven - Your partner for pharmaceutical excipients,” pp. 1–8, 2018, Accessed: Aug. 12, 2021. [Online]. Available: https://www.peter-greven.de/fileadmin/user_upload/dweber/PG/PDFs/Broschueren/PG_Pharma_2018_GB.pdf

[47] JRS PHARMA, “PROSOLV SMCC ® High Functionality Excipient,” pp. 1–8, 2021, Accessed: Sep. 12, 2021. [Online]. Available: https://www.jrspharma.com/pharma-wAssets/docs/brochures/prosolv-smcc_gb_1809.pdf

[48] Dupont, “Why settle for super when you can have superior? High-quality Ac-Di-Sol ® offers all the advantages of a superior disintegrant,” pp. 1–8, 2020, Accessed: Aug. 23, 2021. [Online]. Available: https://www.pharma.dupont.com/content/dam/dupont/amer/us/en/nutrition-health/general/documents/AcDiSol brochure.pdf

[49] Pharma Excipients, “Filler.” https://www.pharmaexcipients.com/filler/ (accessed Nov. 17, 2021).

[50] D. Dietmar Schulze, “Ring Shear Tester RST-XS.s - smaller and more capabilites,” pp. 1–2, 2018, [Online]. Available: https://www.dietmar-schulze.de/flyer/rstxss_e.pdf

[51] Sympatec GmbH, “HELOS/BR RODOS/L ASPIROS.” https://www.sympatec.com/en/particle-measurement/sensors/laser-diffraction/helos/helos-br-rodos-l-aspiros/ (accessed Nov. 15, 2021).

[52] R. C. Rowe, P. J. Sheskey, and S. C. Owen, *Handbook of Pharmaceutical Excipients Fifth Edition*. 2006.

[53] P. Zarmpi, T. Flanagan, E. Meehan, J. Mann, and N. Fotaki, “Impact of Magnesium Stearate Presence and Variability on Drug Apparent Solubility Based on Drug Physicochemical Properties,” *AAPS J.*, vol. 22, no. 75, 2020, doi: 10.1208/s12248-020-00449-w.

[54] MKS Umetrics, *User Guide to SIMCA*, vol. 13. 2012.

[55] W. Engisch and F. Muzzio, “Using Residence Time Distributions (RTDs) to Address the Traceability of Raw Materials in Continuous Pharmaceutical Manufacturing,” *J. Pharm. Innov.*, vol. 11, pp. 64–81, 2016, doi: 10.1007/s12247-015-9238-1.

[56] W. Yu, K. Muteki, L. Zhang, and G. Kim, “Prediction of Bulk Powder Flow Performance Using Comprehensive Particle Size and Particle Shape Distributions,” *J. Pharm. Sci.*, vol. 100, no. 1, pp. 284–293, 2011, doi: 10.1002/jps.22254.

[57] A. M. Faqih, B. Chaudhuri, A. W. Alexander, C. Davies, F. J. Muzzio, and M. Silvina Tomassone, “An experimental/computational approach for examining unconfined cohesive powder flow,” *Int. J. Pharm.*, vol. 324, no. 2, pp. 116–127, 2006, doi: 10.1016/j.ijpharm.2006.05.067.

[58] J. Rojas, A. Lopez, S. Guisao, and C. Ortiz, “Evaluation of several microcrystalline celluloses obtained from agricultural by-products,” *J. Adv. Pharm. Technol. Res.*, vol. 2, no. 3, pp. 144–150, 2011, doi: 10.4103/2231-4040.85527.

[59] E. Doelker, D. Massuelle, F. Veuillez, and P. Humbert-Droz, “Morphological, Packing, Flow and Tableting Properties of New Avicel Types,” *Drug Dev. Ind. Pharm.*, vol. 21, no. 6, pp. 643–661, Jan. 1995, doi: 10.3109/03639049509048132.

[60] A. Yugatama, L. Maharani, H. Pratiwi, and L. Ikaditya, “Characteristics Testing of Microcrystalline Cellulose from Nata de Coco Compared to Avicel pH 101 and Avicel pH 102,” *Curr. Break. Pharm. Mater. Anal. Pharm. Technol.*, 2015, [Online]. Available: https://publikasiilmiah.ums.ac.id/bitstream/handle/11617/6204/A001.pdf?isAllowed=y&sequence=1

[61] Y. Bommireddy, A. Agarwal, V. Yettella, V. Tomar, and M. Gonzalez, “Loading-unloading contact law for micro-crystalline cellulose particles under large deformations,” *Mech. Res. Commun.*, vol. 99, pp. 22–31, 2019, doi: 10.1016/j.mechrescom.2019.06.004.

[62] W. Huang, Y. Shi, C. Wang, K. Yu, F. Sun, and Y. Li, “Using spray-dried lactose monohydrate in wet granulation method for a low-dose oral formulation of a paliperidone derivative,” *Powder Technol.*, vol. 246, pp. 379–394, 2013, doi: 10.1016/j.powtec.2013.05.042.

[63] J. Rojas, I. Buckner, and V. Kumar, “Co-proccessed excipients with enhanced direct compression functionality for improved tableting performance,” *Drug Dev. Ind. Pharm.*, vol. 38, no. 10, pp. 1159–1170, 2012, doi: 10.3109/03639045.2011.645833.

[64] I. Mitra, G. R. Biswas, and S. B. Majee, “Effect of Filler Hydrophilicity on Superdisintegrant Performance and Release Kinetics From Solid Dispersion Tablets of A Model BCS Class II Drug,” *Int. J. Pharm. Res. Technol.*, vol. 4, no. 2, pp. 28–33, 2014, [Online]. Available: http://www.ijccts.org/ijprt/fulltext/17-1543577470.pdf

[65] Y. A. Gueche *et al.*, “Selective Laser Sintering of Solid Oral Dosage Forms with Copovidone and Paracetamol Using a CO2 Laser,” *Pharmaceutics*, vol. 13, no. 2, pp. 1–21, 2021, doi: 10.3390/pharmaceutics13020160.

[66] H. Lieberman, L. Lachman, and J. Schwartz, *Pharmaceutical Dosage Forms: Tablets Volume 2, 2nd ed.* 1990.

[67] E. Azéma and F. Radjaï, “Stress-strain behavior and geometrical properties of packings of elongated particles,” *Phys. Rev. E*, vol. 81, no. 5, pp. 1–17, 2010, doi: 10.1103/PhysRevE.81.051304.

[68] K. Johanson, “Effect of particle shape on unconfined yield strength,” *Powder Technol.*, vol. 194, no. 3, pp. 246–251, 2009, doi: 10.1016/j.powtec.2009.05.004.

[69] C. Hildebrandt, S. R. Gopireddy, A. K. Fritsch, T. Profitlich, R. Scherließ, and N. A. Urbanetz, “Evaluation and prediction of powder flowability in pharmaceutical tableting,” *Pharm. Dev. Technol.*, vol. 24, no. 1, pp. 35–47, 2019, doi: 10.1080/10837450.2017.1412462.

[70] B. Suhr and K. Six, “Friction phenomena and their impact on the shear behaviour of granular material,” *Comput. Part. Mech.*, vol. 4, no. 1, pp. 23–34, 2017, doi: 10.1007/s40571-016-0119-2.

[71] K. C. Pingali, S. V. Hammond, F. J. Muzzio, and T. Shinbrot, “Use of a static eliminator to improve powder flow,” *Int. J. Pharm.*, vol. 369, no. 1–2, pp. 2–4, 2009, doi: 10.1016/j.ijpharm.2008.12.041.

[72] Ã. K. Rudolphi, E. Kassfeldt, and M. Torbacke, *Lubricants: Introduction to Properties and Performance*. 2014.

[73] M. S. Escotet-Espinoza, “Phenomenological and residence time distribution models for unit operations in a continuous pharmaceutical manufacturing process,” 2018.

6. Appendix

Appendix A – Materials' Dead Mass inside the Feeder

On Table A.1 it is represented the amount of each material's mass that covers the feeder (dead mass).

Table A.1 – Materials' dead mass inside the feeder.

Material	Dead mass (g)
Excipient A	13.0
Excipient B	10.6
Excipient C	22.6
Excipient D	26.4
Excipient E	13.0
Excipient F	16.6
Excipient G	30.0

Appendix B – Materials' Properties

In this appendix it is indicated the values of the materials' particle sizes (dv10, dv50, dv90) measured by Sympatec (Table B.1) as well as the materials' rheological properties measured by the Ring Shear Tester (Table B.2).

Table B.1 – Particle size properties measured on Sympatec.

Material	dv10 (µm)	dv50 (µm)	dv90 (µm)	VMD (µm)	SMD (µm)
Excipient A	37.9	113.5	215.6	73.81	121.33
Excipient B	79.2	196.0	290.7	126.62	190.70
Excipient C	63.1	124.0	201.7	104.54	128.51
Excipient D	1.5	6.2	41.7	4.65	33.72
Excipient E	33.5	121.9	222.8	65.47	126.01
Excipient F	18.0	43.1	111.1	33.98	55.38
Excipient G	13.3	37.7	73.5	22.87	41.21

Table B.2 – Parameters directly measured by the Ring Shear Tester at 2000 Pa.

Material	MPS (Pa)	UYS (Pa)	Tau,c (Pa)	phiE (º)	ρ_{tap} (kg/L)	ρ_{bulk} (kg/L)
Excipient A	3810	542	134.0	40.8	0.38	0.34
Excipient B	3731	355	92.2	38.2	0.37	0.35
Excipient C	3374	346	92.0	36.3	0.64	0.58
Excipient D	3671	1266	340.7	41.4	0.39	0.24
Excipient E	3805	428	109.7	38.8	0.47	0.45
Excipient F	4909	875	185.2	48.0	0.53	0.47
Excipient G	3189	761	228.3	34.1	0.55	0.36

However, through the parameters shown on Table B.2, it is possible to obtain more information about the materials and namely conclude about the powder's flow properties. With that purpose the HR and the CI were calculated (Equation 1.3 and Equation 1.4, respectively) as well as ffc (Equation 1.5) (Table B.3).

Table B.3 – Parameters obtained from Ring Shear Tester's usage.

Material	ffc	HR	CI (%)
Excipient A	7.03	1.10	9.40
Excipient B	10.51	1.05	4.91
Excipient C	9.75	1.11	10.02
Excipient D	2.90	1.65	39.47
Excipient E	8.89	1.04	3.94
Excipient F	5.61	1.13	11.79
Excipient G	4.19	1.53	33.76

Appendix C – Feeder's Parameters and Components

The following feeder's parameters were recorded during the stationary periods of the run.

MAX

On Table C.1 the feeder's parameters average values recorded from the feeder's runs where the maximum setpoint was considered are presented and on Table C.2 it is indicated the feeder's components used on those same runs.

Table C.1 – Feeder's parameters recorded from the maximum setpoint feeder's runs.

Material	Setpoint (g/s)	FF (g/rev)	RSD (%)	Massflow (kg/h)	Screw Velocity (rev/s)
Excipient A	6.250	1.25	1.41	6.193	300.3
Excipient B	6.250	1.22	1.18	6.245	307.7
Excipient C	4.167	1.98	0.20	4.165	126.5
Excipient D	0.104	0.18	1.28	0.104	34.3
Excipient E	3.472	1.68	0.22	3.434	126.0
Excipient F	0.347	1.01	0.89	0.350	20.7
Excipient G	4.167	1.37	0.37	4.159	182.2

Table C.2 – Feeder's components utilized during maximum setpoint feeder's runs.

Material	Topup (L)	Screw (mm/rev)	Gearbox
Excipient A	1.6	20	63:1
Excipient B	1.6	20	63:1
Excipient C	1.6	20	63:1
Excipient D	0.4	10	455:1
Excipient E	1.6	20	63:1
Excipient F	1.6	10	455:1
Excipient G	1.6	20	63:1

MIN

On Table C.3 the feeder's parameters recorded from the feeder's runs where the minimum setpoint was considered are presented and on Table C.4 it is indicated the feeder's components used on those same runs.

Table C.3 – Feeder's parameters recorded from the minimum setpoint feeder's runs.

Material	Setpoint (g/s)	FF (g/rev)	RSD (%)	Massflow (kg/h)	Screw Velocity (rev/s)
Excipient A	0.056	0.36	0.95	0.056	9.38
Excipient B	0.080	0.28	1.36	0.079	17.63
Excipient C	0.120	0.49	3.69	0.119	14.91
Excipient D	0.017	0.14	3.18	0.017	7.65
Excipient E	0.140	1.47	3.75	0.140	5.75
Excipient F	0.050	0.90	2.69	0.050	3.36
Excipient G	0.020	0.14	3.10	0.020	8.79

Table C.4 – Feeder's components utilized during minimum setpoint feeder's runs.

Material	Topup (L)	Screw (mm/rev)	Gearbox
Excipient A	1.6	10	455:1
Excipient B	1.6	10	455:1
Excipient C	1.6	10	455:1
Excipient D	0.4	10	455:1
Excipient E	1.6	10	455:1
Excipient F	1.6	10	455:1
Excipient G	1.6	10	455:1

Appendix D – Data obtained from Digital Twin Program

After uploading the Excel files with the feeder's parameters (massflow, screw speed and weight) obtained from the maximum setpoint feeder's runs, the Digital Twin program automatically defines a ff_min, a ff_max and a beta for each material as indicated on Table D.1. The same procedure is applied for the minimum setpoint feeder's runs.

Table D.1 – Digital Twin feeder's runs representative variables considering the uploaded data.

	MAX			**MIN**		
Material	**ff_min (g/rev)**	**ff_max (g/rev)**	**beta (g^{-1})**	**ff_min (g/rev)**	**ff_max (g/rev)**	**beta (g^{-1})**
Excipient A	1.50	1.60	2.00	0.36	0.36	1.02
Excipient B	1.50	1.60	2.00	0.00	0.27	1.00
Excipient C	0.48	2.01	1.00	0.50	0.50	1.00
Excipient D	0.00	0.18	1.00	0.01	0.14	0.99
Excipient E	0.50	1.69	1.03	0.44	1.45	1.00
Excipient F	0.50	1.40	1.00	0.00	0.13	1.00
Excipient G	0.72	1.02	1.00	0.70	0.90	1.00

From all these runs, the data, from the feeder's runs that had the 20C screw assembled, was used for the development of the ff_min 20C, ff_max 20C, beta 20C models and the data correspondent to the feeder's runs that used the 10C screw was utilized for ff_min 10C, ff_max 10C, beta 10C models' development (Appendix E).

Appendix E – PLS Models Information (Confidential)

On the following tables the information relatively to the confidential models is indicated.

Table E.1 – Information to calculate the $FF_{predicted}$ for the FF 20 C model.

Var ID	Model Coefficients FF 20C
Constant	0.195
Bulk	3.137
Equation	$FF_{predicted}$ 20C = 0.195 + 3.137×Bulk
Error	($FF_{predicted}$ 20C) +/- 0.05

Table E.2 – Information to calculate the $FF_{predicted}$ for the FF 10 C model.

Var ID	Model Coefficients FF 10C
Constant	– 1.134
dv10	– 0.046
ffc	0.469
Equation	$FF_{predicted}$ MIN= – 1.134 – 0.046×dv10 + 0.469×ffc
Error	($FF_{predicted}$ 10C) +/- 0.09

Table E.3 – Information to calculate the ff_min 20C parameter.

Var ID	Model Coefficients ff_min 20C
Constant	4.587
dv50	0.022
ffc	– 0.633
Tau,c	– 0.009
Equation	**ff_min 20C$_{predicted}$** = 4.587+ 0.022×dv50 – 0.633×ffc – 0.009×Tau,c

Table E.4 – Information to calculate the ff_max 20C parameter.

Var ID	Model Coefficients ff_max 20C
Constant	3.478
dv50	– 0.005
Tau,c	– 0.010
Equation	**ff_max 20C$_{predicted}$** = 3.478 – 0.005×dv50 – 0.010×Tau,c

Table E.5 – Information to calculate the beta 20C parameter.

Var ID	Model Coefficients beta 20C
Constant	1.928
dv50	0.021
ffc	– 0.378
Equation	**beta 20C$_{predicted}$** = 1.928 + 0.021×dv50 – 0.378×ffc

Table E.6 – Information to calculate the ff_min 10C parameter.

Var ID	Model Coefficients ff_min 10C
Constant	3.762
dv50	– 0.006
Tau,c	– 0.004
phiE	– 0.057
Equation	**ff_min 10C$_{predicted}$** = 3.762 – 0.006×dv50 – 0.004×Tau,c – 0.057×phiE

Table E.7 – Information to calculate the ff_max 10C parameter.

Var ID	Model Coefficients ff_max 10C
Constant	2.331
dv10	– 0.042
ffc	0.390
phiE	– 0.076
Equation	**ff_max 10C$_{predicted}$** = 2.331 – 0.042×dv10 + 0.390×ffc – 0.076×phiE

2021

BEATRIZ FILIPA CABRAL DIAS

OPTIMIZATION OF LOSS IN WEIGHT FEEDING OF PHARMACEUTICAL POWDERS TO ENABLE CONTINUOUS DIRECT COMPRESSION

NOVA SCHOOL OF SCIENCE & TECHNOLOGY